THE FUNCTIONAL ROLE OF SUPPLEMENTARY EYE FIELD UNDERLYING VALUE-BASED DECISION MAKING

by
Xiaomo Chen

A dissertation submitted to Johns Hopkins University in conformity with the requirements for the degree of Doctor of Philosophy

Baltimore, Maryland
September, 2013

Abstract

In nearly every moment of our lives, we make decisions. However, the neuronal mechanism underlying decision-making is still not clear. Currently, there is a debate on whether value-based decisions are based on the selection of goals or the selection of actions. We investigated this question by recording from the supplementary eye field (SEF) of monkeys during an oculomotor gambling task. We found that SEF neurons initially encode the option and action values associated with both task options. Later on, the competitive interactions between the different options result in their selection. Specifically, competition occurred in both action space and value space as represented in SEF. However, SEF encodes the chosen option 60~100 ms before the chosen action. When neuronal activity in SEF was reversibly inactivated, the monkeys' selection of the less valuable option was significantly increased. These results suggest that SEF is actively engaged in value based decision-making by forming a map of the competing saccade targets. Activity within this map reflects the chosen option first, and then later the corresponding necessary action . This SEF population activity is causally related to the selection of a saccade based on subjective value, and reflects both the selection of goals and of actions. Moreover, in contrary to the two major decision hypothesis under the debate, our results suggest value based decision rely on the selection of both goals and actions. This study therefore supports a new cascade choice theory of value-based decision making in which the competition is present for both goals and actions. The early competition between goals (value) can further bias the competitive process between actions.

Advisor: Dr. Veit Stuphorn

Readers: Drs. Veit Stuphorn and Peter Holland

Acknowledgements

I would never be able to finish my dissertation without the guidance of my advisor, support from committee members, help from friends, and love from my family. During these five years, the thought of writing these acknowledgements was always on my mind, because of the constant help and encouragement I have been blessed with. Now that I have finally reached this point, I would like to express my sincerest appreciation to everyone who have supported and helped me during my Ph.D. study.

I would like to express my deepest gratitude to my advisor, Dr. Veit Stuphorn, for his superlative guidance, immense understanding, generous support, and considerate care in every little aspect. As an international student coming from an interdisciplinary background, it is really hard to imagine how I could have survived these years and completed my Ph.D. work without Veit's help. Whenever I was stuck with any kind of difficulties, Veit always had a brilliant solution waiting there to help me out. Whenever I was reading his comments on my work, I always had a strange mixture of feeling of gratitude (for the detailed attention to every sentence and point), exhilaration (for the always insightful ways to dramatically improve the argument to a new level) and regret (for not thinking about it beforehand). I am very lucky to have Veit as my mentor in my academic life. I've learned a lot from Veit, not only about how to be a good scientist, but also about how to be a good adviser to others (eventually). Wherever I go, I would always be proud of my "Stuphorn lab" badge.

I've been especially fortunate to have Dr. Susan Courtney, Dr. Peter Holland, and Dr. Steven Yantis on my thesis proposal/advance-examination committee. In the committee meeting, their challenging but always insightful questions inspired me to think from different angles and reminded me of the importance of the big picture. Outside the meetings, they have always been there for me whenever I needed assistance. I still vividly remember Peter's extra guidance which had helped me immensely in my study about the reinforcement theory during my first year. It was Steve's advanced exam reading list that furthered my reading into the theories on attention, and led to my first encounter with my future advisor, Dr. Tirin Moore's work. It was Susan's timely help which allowed me to be better prepared my post-doc interview. Without her thoughtful suggestions, there would be no section 4.2.5 in this dissertation and other relevant discussions. Besides my committee members, I would also like to thank the wonderful faculty members in my department, especially Dr. Howard Egeth for his helpful suggestions during the human psychophysics work.

I was also very lucky to become part of the Mind and Brain institute (MBI) in addition to the department of psychology and brain sciences (PBS). Because of this, I could always have double the happy hours, double the parties, and double the seminar dessert from both places. More importantly, I was extremely grateful that I could receive twice the help and support from both PBS and MBI. The faculty members from MBI are like my friends. I would like to express my sincere appreciation to Dr. Steve Hsiao, Dr. Ed Corner, Dr. Ernst Niebur, Dr. Rudiger von der Heydt, Dr. James Kenierim, Dr. Steward Hendry, and Dr. Kristina Nielsen in so many different aspects. Especially, I would like to express my gratitude to Steve (Hsiao) who interviewed me with Veit before

I came here, and helped me getting into the program allowing me to pursue my scientific dream here. There are not enough words in my English language to describe the people and their help which I want to thank here. 谁言寸草心，报得三春晖 (the little grass can hardly repay the kindness of the warm sun). All in all, I could not have achieved what I have now without the help from any one of them.

I would also like to thank my friends from the lab, Dennis Sasikumar, Katie Scangos, Nayoung So, Eric Emeric, Jaewon Hwang, Kitty Xu, William Vinje and Xinjian Li. Besides the tremendous help to my researches, they are also kind friends whom I can always count on to join me in our breaks from the long work. As Dennis said, "No one gets to select who their co-workers are going to be, but I don't think it would worked better that had I picked all of you myself." I would also like to acknowledge the cooperation of my non-human friends from the lab, Aragorn and Isildur. Without their high intelligence and devotedness to the work, I could not have completed this dissertation work.

I could not have enjoyed my graduate study here without my dearest friends. I am so grateful to my great friends Yi-shin Sheu, Zheng Ma, Jenny Wang, Heeyeon Im, Steven Chang, et al from PBS and Stefan Mihalas, Eric Carlson, Ann Martin, Jonathan Williford, Sachin Deshmukh, Fancesco Savelli, et al from MBI for accompanying me during these wonderful five years here at Hopkins. We had a lot of fun memories together such as going to class, suffering from exams, partying, eating out, hiking, et al. People always say "your friend define you". I am really glad we could know each other here and be friends. I also thank many members of the MBI family, Bill Quinlan, Bill Nash, Susan Soohoo, Eric Potter, Charles Meyer, Debbie Kelly, Brance Amussen, Lei Hao. Besides

their technical supports, their warm-hearted friendliness always made me feel not far away from home. In addition, I would like to take this opportunity to thank some of my friends outside my work, such as my loyal roommate (Alyssa Toda), my dearest cello tutor (Bai-Chi Chen) and cello mates (Carla Harrision, Susan Tobias and Lydia Zieglar) and my tennis partners.

At last, but not least, I would like to thank my family members. I am forever in debt and gratitude to my beloved mother (Jianhua Yuan) and father (Jiansheng Chen), who instilled the love of science and knowledge in me from early on; who always give me their shoulder whenever I feel tired or frustrated; and who devote all their love and wisdoms to raise me up to more than I could be. I'd like to thank my cousin, Cheng Wang, who always feels like a little brother to me. Finally, I should thank my husband, Kunlun Bai, who is always there cheering me up and stands by me through bad and good times.

Table of Contents

List of Figures

List of Tables

Chapter 1

Introduction

In nearly every moment of our lives, we make decisions. However only till very recently, have we begun to investigate the neuronal mechanism of decision-making (Gold and Shadlen, 2007). Value based decision- making requires the ability to select both the reward option with the highest available value and the appropriate action necessary to obtain the desired option. The neuronal mechanisms underlying these processes are still not well understood.

1.1 Value based decision-making

Neurophysiological understanding of decision- making was pioneered by studies on perceptual decision- making (Britten et al., 1992; Shadlen and Newsome, 1996, 2001; Pastor-Bernier and Cisek, 2011) . Recently, value based decision-making, in which the decisions are based primarily on the subjective value associated with each of the possible alternatives, has become the focus of the nascent field of neuroeconomics (Glimcher, 2005; Kable and Glimcher, 2009). While perceptual decision- making depends more on the representation of the external state such as the visual stimuli, value based decision-

making is more driven by the desirability of the object which depends on the internal state.

A network of cortical areas has been identified participating in value based decision- making (Sugrue et al., 2005; Gold and Shadlen, 2007; Rangel et al., 2008; Kable and Glimcher, 2009; Padoa-Schioppa, 2011). Neurobiological correlates of value have been described in orbitofrontal cortex (Padoa-Schioppa and Assad, 2006), amygdala (Nishijo et al., 1988a, b; Paton et al., 2006), as well as other cortical areas traditionally associated with reward-seeking behavior. The value signals from those areas have been found in relation to the obtained reward option itself, but do not reflect the motor actions required to obtain it. On the other hand, the motor related cortical areas have been identified decades ago (Tehovnik et al., 2000; Lynch and Tian, 2006), which include superior colliculus (SC), lateral inferior parietal cortex (LIP), and frontal eye field (FEF) (Bizzi, 1967; Bizzi and Schiller, 1970; Goldberg and Bushnell, 1981; Bruce and Goldberg, 1985). These cortical areas are dominated by movement information (Leon and Shadlen, 1999). Where the decision is made and how value representations participate in action selection are still under debate. Currently, there are two major hypotheses for this process.

1.1.1 Good-based hypothesis

The good-based hypothesis (Padoa-Schioppa, 2011) suggests that the decision is made in a goods space. It is consistent with the economic theories arguing that human make decisions between options regarding different goods by integrating all relevant factors (gains, risk, cost, et al) into a single variable capturing the subjective value of each option. Neurophysiological studies have found such subjective value activity in the

obitofrontal (OFC) (Padoa-Schioppa and Assad, 2006, 2008; Padoa-Schioppa, 2009) and ventromedial prefrontal cortex (vmPFC) (Wallis, 2007; Kennerley and Walton, 2011; Padoa-Schioppa, 2011). In particular, neural activity in OFC correlates with the value of each single option independent of other options (Padoa-Schioppa and Assad, 2008), and adjusts its gain to reflect the full range of values presented in a given block of trials (Padoa-Schioppa, 2009). This hypothesis satisfies the normal intuition about decision-making. For example, when choosing between an apple and a banana, we would think about the apple rather than how to move our hands when making the decisions. This hypothesis also follows the classic tradition of cognitive psychology, in which the cognitive system responsible for decisions is separate from the sensorimotor systems that implement its commands (Pylyshyn, 1984). This theory in its purest form would predict that motor areas should only represent the motor plan of the chosen option.

1.1.2 Action-based hypothesis

Action-based hypothesis (Cisek, 2006, 2007; Cisek and Kalaska, 2010) suggests that decisions are made through a biased competition between action representations. In this hypothesis, the subjective value is still important, but these signals are not directly compared in the abstract space of goods. Instead, they together with other factors such as action costs cause bias influence on a competition that take place within a representation of potential actions. Current findings in perceptual decision- making have supported this hypothesis (Shadlen and Newsome, 2001; Gold and Shadlen, 2007). The neuronal activity in LIP (Shadlen and Newsome, 1996, 2001), SC (Horwitz and Newsome, 1999, 2001), FEF (Hanes and Schall, 1996), dLPFC (Kim and Shadlen, 1999), and basal ganglia (Ding and Gold, 2013) act as accumulators, in which different actions competes

with each other by accumulating evidence supporting certain action as described in the accumulator model. This hypothesis can also be supported by the perturbation experiment in which inactivation of deeper layer of SC (McPeek and Keller, 2004) or sub-threshold SC micro-stimulation (Carello and Krauzlis, 2004) influence monkeys choice behavior rather than simple motor control. This theory in its purest form predicts that chosen value should not exist before an action is chosen, since the competition in the action space is the only precursor to the decision.

Both good-based hypothesis and action-based hypothesis are based on the neurophysiology recordings in different cortical areas where either value or action is coded. But none of them have taken into account of the recording in the association areas where action value has been founded. In order to investigate the "elephant" from a different angle, we decided to record in one of the association areas (supplementary eye field, SEF) to see how value can participate or help with action selection in value based decision-making.

1.2 Supplementary eye field

We used an ocular motor task in the study of this decision-making problem. The first work on saccadic cortical region can be traced back to Ferrier (Ferrier, 1875, 1886). The experiments were done by electrically stimulating exposed cortex of anesthetized monkeys. Nowadays, the cortical regions identified contributing to the eye movement include the frontal eye field (FEF), the parietal eye field (PEF) which is located in the lateral bank of the intraparietal sulcus (LIP), the supplementary eye field (SEF) which is part of the dorsal medial frontal cortex (DMFC), the medial superior temporal area (MST), the prefrontal eye field region (PFEF or dorsal lateral prefrontal cortex, DLPFC),

and a region on the medial surface of the parietal lobe called the precuneus region in human imaging studies and area *7m* in monkey studies (Tehovnik et al., 2000; Lynch and Tian, 2006).

SEF was first described by Schlag and Schlag-Ray (Schlag and Schlag-Rey, 1985, 1987) as a region in the dorsomedial frontal cortex in which neurons discharge before saccadic eye movements. The identification of this area was motivated by the observation of eye movement-representing area in the dorsal bank of the cingulate sulcus, which was found while mapping the supplementary motor areas (SMA) (Woolsey et al., 1952). This area is located rostral to the SMA and lateral to the pre-SMA. Previous studies showed that the neurons in SEF discharge during saccadic movement (Bruce et al., 1985; Mann et al., 1988; Schall, 1991; Bon and Lucchetti, 1992), active fixation (Bon and Lucchetti, 1990; Lee and Tehovnik, 1995), onset of visual stimuli (Schlag and Schlag-Rey, 1987; Schall, 1991; Russo and Bruce, 1996), smooth pursuit eye movement (Heinen, 1995; Heinen and Liu, 1997), and hand-eye coordination (Mushiake et al., 1996).

Despite its similarity to other oculomotor areas, SEF also demonstrates many differences especially in regard to its contribution to internal guided saccades. In the first study of SEF, Schlag and Schlag-Rey (Schlag and Schlag-Rey, 1987) noted that unlike FEF, SEF showed activity prior to spontaneous exploratory saccades. In addition, SEF showed longer latency in response to electrical stimulation, suggesting that SEF is more remote along the final common pathway compared to FEF. Based on those observations, the authors suggested that the two eye fields have different roles of visually guided (FEF) and internally guided (SEF) saccades. Chen and Wise (Chen and Wise, 1995) found that SEF is involved in oculomotor learning where the neurons were most active during the

learning of new and arbitrary stimulus-saccade associations. In addition, in anti-saccade experiment, the pre-saccadic activity of SEF neurons was highly predictive of successful anti-saccades, showing higher activity in anti-saccade trials than in pro-saccade trials with the same saccade metric (Schlag-Rey et al., 1997; Amador et al., 1998, 2004). It was also reported that SEF neurons detect and predict reinforcements (Amador et al., 2000; Stuphorn et al., 2000a; Coe et al., 2002; So and Stuphorn, 2012). In the countermanding task, SEF neurons showed error- and conflict- monitoring activity (Stuphorn et al., 2000b). However, unlike neurons in FEF and SC, the neurons in SEF were not sufficient to initiate eye movement in visually guided saccades (Stuphorn et al., 2000b; Stuphorn et al., 2010).

The idea of SEF involved in the control of internally guided saccades can be also supported by perturbation experiments which test the causal relation between the neuronal activity and the behavior. Electrical stimulation of the SEF produced saccades that take the eyes to a particular orbital position ("goal-directed saccades"), and prolonged stimulation kept the eyes at that positions. While stimulation of the FEF elicited saccades that had specific direction and amplitudes, prolonged electrical stimulation yielded a staircase of identical saccades with intervening fixation (Tehovnik and Lee, 1993; Tehovnik, 1995). Moreover, the behavioral state of animals has a much greater effect on saccadic eye movements evoked electrically from SEF than from FEF (Tehovnik et al., 1999). In the experiment, monkeys were required to fixate the visual target for 600 ms after which a juice reward was given. When stimulating the SEF early during the fixation period, 16 times as much current was required to evoke saccades than when current was delivered after termination of the fixation spot. During countermanding

task in which SEF showed error and monitor signal (Stuphorn et al., 2000a), electrical micro-stimulation to SEF neurons improved the monkeys' performances (Stuphorn and Schall, 2006). Lesion and reversible inactivation study on SEF showed mild but significant deficits in temporal discrimination task. In the visual guided task, DMFC lesion produced a mild impairment on the contralateral side which recovered within weeks. FEF lesions produced a much more dramatic deficit on the task that lasted for 2 years of continued testing (Schiller and Chou, 1998). Human patients with SEF lesions showed impairment in sequence of memory-guided saccades, while there were no impairment in visually guided or single memory-guided saccades (Gaymard et al., 1990).

Consistent with the idea that SEF is involved in internal guided saccade, the design of this dissertation study was based on the hypothesis of SEF's participation in the process of value based decision-making in the case of eye movements. As discussed above, value based decision depends on the internal representation of desirability as well as selectivity, and is an internal guided process. SEF has appropriate anatomical connection for such a role because it sits in the association area linking the option value coding cortical areas to the motor related areas. It receives input from orbitofrontal cortex and the amygdala (Huerta and Kaas, 1990; Ghashghaei et al., 2007). In addition, SEF also forms a cortico-basal ganglia loop with the caudate nucleus, superior temporal polysensory (STP) area and the nuclei in the central thalamus that are innervated by superior colliculus (SC) and substantia nigra pars reticulata (SNpr). Caudate nucleus, as part of this cortico-basal ganglia loop, has already been known to contain saccadic action-value signals (Lau and Glimcher, 2008). Moreover, SEF has reciprocal connections with oculomotor cortical areas, such as FEF, LIP, and 7A (Huerta and Kaas, 1990), which can

modulate the neuronal activity in the motor area. Previous recording found that neurons in SEF became active before value based saccades much earlier than neurons in FEF and LIP (Coe et al., 2002). A previous research in the lab has found reward options and of saccadic actions in stimulus driven saccades (So and Stuphorn, 2011). However, whether this neuronal activity participates in the ongoing value based decision process is still unknown. It could either represent the decision variables used in the decision process itself, or merely reflect the downstream outcome of the decision.

1.3 Thesis overview

We investigated whether and how SEF participate in value based decision-making through an integrated application of physiological recording, and perturbation techniques. In addition to non-primate neurophysiology recording, we also carried out a human psychophysics pilot study to test the experiment paradigm before the physiological recording (Chapter2). Although the human psychophysics experiment design is not identical to the one used in the monkey study, it advanced our understanding of how visual salience can influence value-based choice behavior through modifying value representation. In the main experiment, we designed a gamble task in which monkeys had to choose between two options by making an eye movement to the desired option (Chapter 3). This decision task allowed us to investigate the neuronal activity in terms of both value representation and direction representation. We found that population neuronal activity in SEF represented both chosen and non-chosen option in a competitive way (Chapter 4), which argues against the value based hypothesis in its pure form. Moreover, our results support a sequential process between value and direction representation, whereby the chosen option is selected first, and then biases the action

selection process (Chapter 5). This result argues against action-based hypothesis in its pure form. Our neurophysiologic results therefore support a new cascade hypothesis of decision- making which will be discussed in detail in Chapter 5 and Chapter 7. Consistent with these neural recording results, reversible inactivation of SEF produced a larger error rate and noisier choice behavior (Chapter 6). These results further suggest that SEF causally contributes to the value based decision process. The dissertation will close with a conclusion, proposing a possible parallel decision- making process in both value and direction space, and the possible role of SEF in value based decision- making (Chapter 7).

Chapter 2

A human pilot study ---mechanisms underlying the influence of saliency on value-based decisions

This chapter will describe a behavioral study in humans, which was conducted before the physiological recording as a pilot study. Though the human psychophysics experiment design was not eventually used in the monkey study because of technical issues, the result suggest an interesting way of how visual salience can influence value-based choice behavior through modulating value representation and motor competition.

Value-based decision- making is the selection of an action among several alternatives based on the subjective value of their outcomes. While ideally this choice should be independent of irrelevant target properties, it is well-known that low level physical properties can profoundly influence decision-making. During free viewing of natural scenes and video sequences, saccades are drawn to more salient parts of an image (Parkhurst et al., 2002; Parkhurst and Niebur, 2003; Berg et al., 2009), observers find

these parts more interesting (Masciocchi et al., 2009), and high salience targets are detected faster and more accurately (Egeth and Yantis, 1997; Wolfe, 1998). The question thus arises whether visual salience influences not only simple perceptual but also value-based decisions.

A number of recent studies demonstrated that both visual salience and subjective value can affect decision- making (Navalpakkam et al., 2010; Markowitz et al., 2011; Schutz et al., 2012). Nevertheless, the mechanisms underlying this behavioral phenomenon might differ depending on the specific influence of salience in the task. Sensory stimuli can vary in many different feature dimensions and any of these feature domains can influence the overall salience of the target. However, value information is typically carried only by some of the features of a visual target. It is therefore of importance, whether salience is manipulated on the same or a different feature dimension as value.

In a situation, in which salience is manipulated on a different feature dimension than the one indicating value, the main effect of salience manipulations will be to influence the overall contrast of the target relative to the background and other targets. In other words, low salience will lead to a lower probability that the target will be detected to be present. However, once detected a low salience target will provide as much information about its value as a high salience target. Such salience manipulations were often employed in previous research, either by modulating detectability of targets (Markowitz et al., 2011) or of distractors (Navalpakkam et al., 2010). This generates a 'neglect' situation, in which high value targets can be overlooked, if they are of lower salience than the background or alternatives.

The situation is different when the salience of the feature dimension is manipulated that carries value information, but other feature dimensions of the target are still highly salient. In this situation, the perception of the value information is selectively influenced by the salience manipulation, while all the other perceptual dimensions are the same. The influence of the salience manipulation on choice behavior is therefore not simply to make the agent unaware of a low salience target, but rather to create targets whose value is harder to perceive. There are fewer studies of this type (Schutz et al., 2012) and as a result we know much less about the influence of salience on value-related information.

In this study, we designed therefore a two alternative forced choice task, in which items in a visual display were endowed with different values (rewards). Human participants rapidly chose between items, attempting to maximize the reward amount. We manipulated visual salience and value of the targets simultaneously and independently across trials, while keeping the detectability of all targets constant. That is, we designed visual stimuli, for which one visual feature (luminance contrast with the background) was large enough to ensure that their location could be detected rapidly. Another visual feature (color saturation) was manipulated so that the visual feature carrying value information (color hue) was more or less perceptually salient. Therefore, the manipulation of salience influences the perception of value. The salience is with respect to behaviorally relevant information (i.e. target value), but not with respect to the ability of the subject to localize the targets on the screen. In this way we could manipulate the visual salience of value information without directly affecting motor processes used to report the choice. We also mixed no-choice trials in with the choice

trials, in which subjects could only select the single target on the screen. The no-choice trials were controls to test the effect of visual salience and value on behavior without any interference by the choice process.

We found that both value and salience have strong effects on the decision process by themselves, as has congruency between value and salience. Specifically, reaction times were significantly correlated with both value and salience of the chosen target, and with value difference and salience difference between the chosen target and the non-chosen target. In addition, the error rate, defined as the rate of choosing the lower valued target, was significantly higher in incongruent trials than in any other type of trials.

After characterizing behavior in a descriptive regression model, we analyzed the neuronal mechanisms underlying our behavioral data using a series of four stochastic accumulator models based on different functional assumptions (Bogacz et al., 2006; Cisek et al., 2009; Purcell et al., 2010; Hanks et al., 2011; Krajbich and Rangel, 2011). All models consist of two accumulators, each adding up value information in support of one of the two possible choices. For the "independent model", we assumed that the two accumulators did not interact, while the other accumulator models implemented mutual inhibition between them. The "speed model" assumed that salience influenced the rate with which value information was accumulated by modulating the strength of the incoming value information. The "onset model" was motivated by the observation that salience can reduce visual processing time (Ratcliff and Smith, 2011; White and Munoz, 2011) and assumed an earlier accumulation onset time rather than an increased accumulation rate. The full model combined both ways for salience to affect the accumulation process. Comparison between model predictions and behavior suggested

that mutual inhibition and salience-induced differences in accumulation onset time, but not accumulation rate, are necessary to explain the behavior of the human participants.

2.1 Method

2.1.1 Subjects

Fifteen participants (Age: 18-30, eight female) undergraduate and graduate students naïve to the purpose of the study, were recruited from the Johns Hopkins University community and participated in the experiment after providing informed consent. All participants reported normal or corrected-to normal vision and no history of color blindness. Among these 15 participants, 9 (Age: 26-30, five females) participated in the two pilot experiments, 9 (Age: 18-30, five females) participated in the main experiment, and 3 participated in all three experiments. All procedures were approved by the Johns Hopkins University Homewood Institutional Review Board.

2.1.2 Pilot Experiments

In the first pilot experiment, we determined saturation levels to be used in the main experiment based on simple color detection. Four targets with equal brightness appeared on the screen, of which one was colored and the others were gray. The participants were required to localize the colored target and to indicate its position by pressing the corresponding key on a keyboard. In order to encourage accuracy, we did not set a response deadline. We tested all five colors (cyan, brown, green, blue, yellow) used in the main experiment (Figure 2.1) in a range (1%-16%) of saturation levels. In the pilot experiment, the color of the targets in the detection experiment did not carry any value information and we did not observe systematic behavioral differences across colors

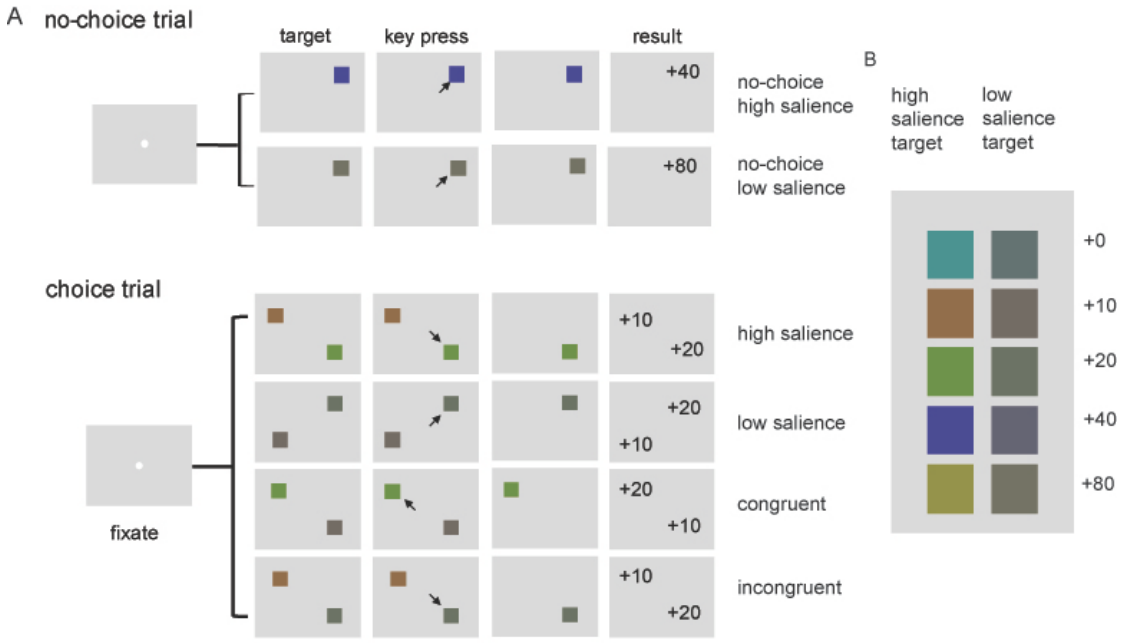

Figure 2.1 Behavioral paradigm. A: Sequence of events during no-choice trials (top) and choice trials (bottom). The type of stimulus is listed to the right. The black arrow is not part of the stimuli; it symbolizes the participants' choices which then lead to the next stimulus shown. In all cases shown, the arrow corresponds to the optimal choice. B: Visual cues used. High and low salience targets are left and right, respectively. Rows correspond to values, as shown to the right.

(Figure 2.2). In contrast, mean reaction time varied systematically with the saturation level, which for our purposes served as a measure for the salience of a target. Low saturation levels were defined as in the 3-5% range because the reaction times in response to these targets were around 50 ms longer than those in response to high saturation targets, defined as 16% where performance plateaued. Accuracy was nearly perfect for all values above 6% (with one outlier). Thus, low saturation level was chosen for each color (5% for yellow, 4% for cyan, brown and green, and 3% for blue), so that the salience of the color information was substantially reduced from high saturation level (16% for all colors), but still strong enough to be detectable.

In order to test, whether the manipulation of the color saturation by itself had an effect on the speed with which the targets could be detected, we performed a second pilot experiment (the singleton task) with nine participants (results shown in Figures 2.4 and 2.7). In this task, 10 targets with different color or saturation as selected in the pilot experiment were used. There was no difference in value associated with the targets.

In each trial, only one target appeared on the screen and the participants were asked to indicate its location by pressing the corresponding key. They were encouraged to do so as fast as possible while maintaining accuracy. The task made sure the detectability of all the targets was the same.

2.1.3 Stimuli

In the main experiment, the value associated with a particular target was indicated by its color. The color properties of the targets were derived from the hue ($H \in [0°,360°)$), saturation ($S \in [0,1]$) and brightness ($V \in [0,1]$) color space. In this space, hue is the attribute of a visual sensation according to which an area appear to be one of the

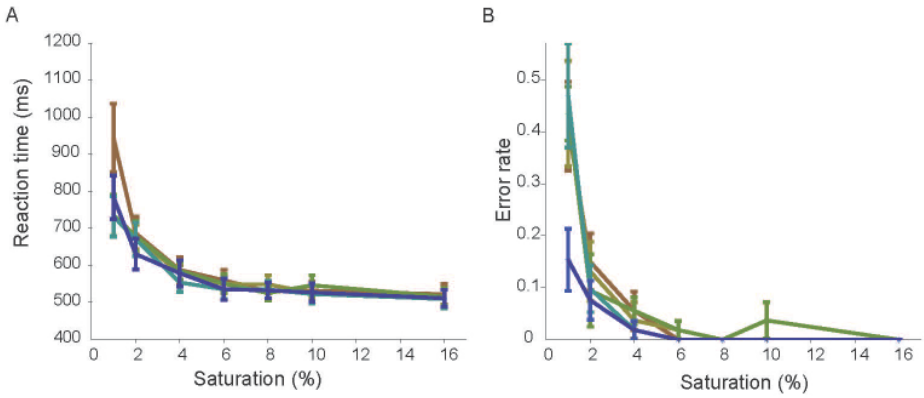

Figure 2.2 Effect of saturation level on reaction time and error rate for different color targets. The mean reaction times and error rates for nine subjects are plotted. The colors of the lines in the plots correspond to the colors of the targets used in the task. A: Mean reaction times plotted as a function of the saturation level. Error bars represent standard error of the mean reaction time. B: Error rates plotted as a function of the saturation level. Error bars represent standard error of error rate.

perceived colors; saturation is the colorfulness of a stimulus relative to its own brightness; and brightness is the attribute of a visual sensation according to which an area appears to emit more or less light. Five different colors indicated five different values that could be earned (“cyan”, hue 180°: 0 points;“brown”, 30°: 10 points; “green”, 90°: 20 points; “blue”, 240°: 40 points; “yellow”, 60°: 80 points) (Figure 2.1B). The targets were approximately 1.5×1.5° in size and were always presented approximately 20° away from the central fixation point at angles 45°, 135°, 225° or 315° relative to the horizontal. The background was approximately 16×22cm in size and was uniformly gray and the brightness of each target exceeded that of the background by 4%. Since the targets had all the same brightness, the participants had to rely on color information alone to determine the relative value of each target. We manipulated the salience of this reward-related information by modulating color saturation independently of target value, as determined in the first pilot experiment. As discussed, the selection of high and low saturation levels for each hue was guided by the psychophysical data in the second pilot study.

2.1.4 Main experiment

At the start of the main experiment, participants received instructions on the nature of the task. They were informed that they would have the opportunity to earn “points” which accumulated over trials, and they were encouraged to maximize the number of points earned.

Participants then were presented with targets on a computer monitor (Figure 2.1A) in front of them that varied in value and salience. The task consisted of two types of trials: choice and no-choice trials. At the beginning of each trial, the participants were required to fixate the fixation point for 1500 ms. In choice trials, after the fixation point

disappeared, two targets appeared in diagonally opposite locations on the screen. Participants chose a target by pressing a key on the keypad (Insert: left up; Delete: left down; Home: right up; End: right down; the relative locations of these keys on the keypad agree with the locations of the corresponding stimuli on the screen) that corresponded to the location of the desired option. Pressing any key other than these four was considered an invalid choice. No-choice trials were used as controls to test the influence of both salience and value without interference by choice. In no-choice trials, only one target appeared on the screen and participants had to press the key that corresponded to the target location. Pressing one of the other three keys was considered an error. The response deadline (2000 ms) was chosen generously to encourage participants to take as much time as necessary to choose the appropriate target. Following a valid key press, the amount of points associated with the chosen target and the non-chosen target were revealed on the monitor. Otherwise, no points were revealed, the next trial started after an inter-trial interval whose length was selected randomly (uniform distribution) from the range 1000-1500ms.

Six comparisons were selected from the set of possible value differences between the two stimuli: 0 *vs.* 10 points, 0 *vs.* 20 points, 10 *vs.* 20 points, 20 *vs.* 40 points, 20 *vs.* 80 points, and 40 *vs.* 80 points. Each of these pairs was presented with equal frequency. These comparisons were selected so that across different trial types targets with medium values (10, 20, 40 points) had equal probability to be either larger or smaller in value than the alternative target. In addition, this set included comparisons with smaller and larger value differences. For each value comparison, there were four different salience-value combinations (Figure 2.1A): In low salience trials, both targets were of low salience. In

high salience trials, both targets were of high salience. In congruent trials, the high value target was of high salience, while the low value target was of low salience. Finally, in incongruent trials, the high value target was of low salience and the low value was of high salience. This resulted in 24 different combinations of choice trials (6 value comparisons × 4 value-salience combinations). Together with 10 different types of no-choice trials (5 values x 2 salience levels), there were 34 different trial types that formed one block of trials. The trials were presented in blocks, so that a trial of a particular type was not presented again until the next block. Within a block, the order of trials was randomized.

Participants were initially trained with high salience (32% saturation level) no-choice and choice trials. After they achieved an accuracy of 90%, the main experiment began. Each participant performed the same number of trials, 11 blocks with 34 trials each, 374 trials total.

2.2 Results

2.2.1 Influence of value on reaction time

Our behavioral results showed a significant effect of the chosen target value on reaction times in correct trials. The mean reaction time during both no-choice and choice trials reflected the value of the chosen target. For all types of choice trials, reaction time was significantly correlated with the chosen target value; high salience (t-test, df=34, $p<10^{-9}$), low salience (t-test, df=34, $p<10^{-10}$), congruent (t-test, df=34, $p<10^{-8}$), and incongruent (t-test, df=34, $p<10^{-6}$) (Figure 2.3). The correlation coefficients were significantly smaller than zero as tested by the t-test in all cases; the larger the chosen value, the shorter the reaction time. This result reflected most likely the motivational

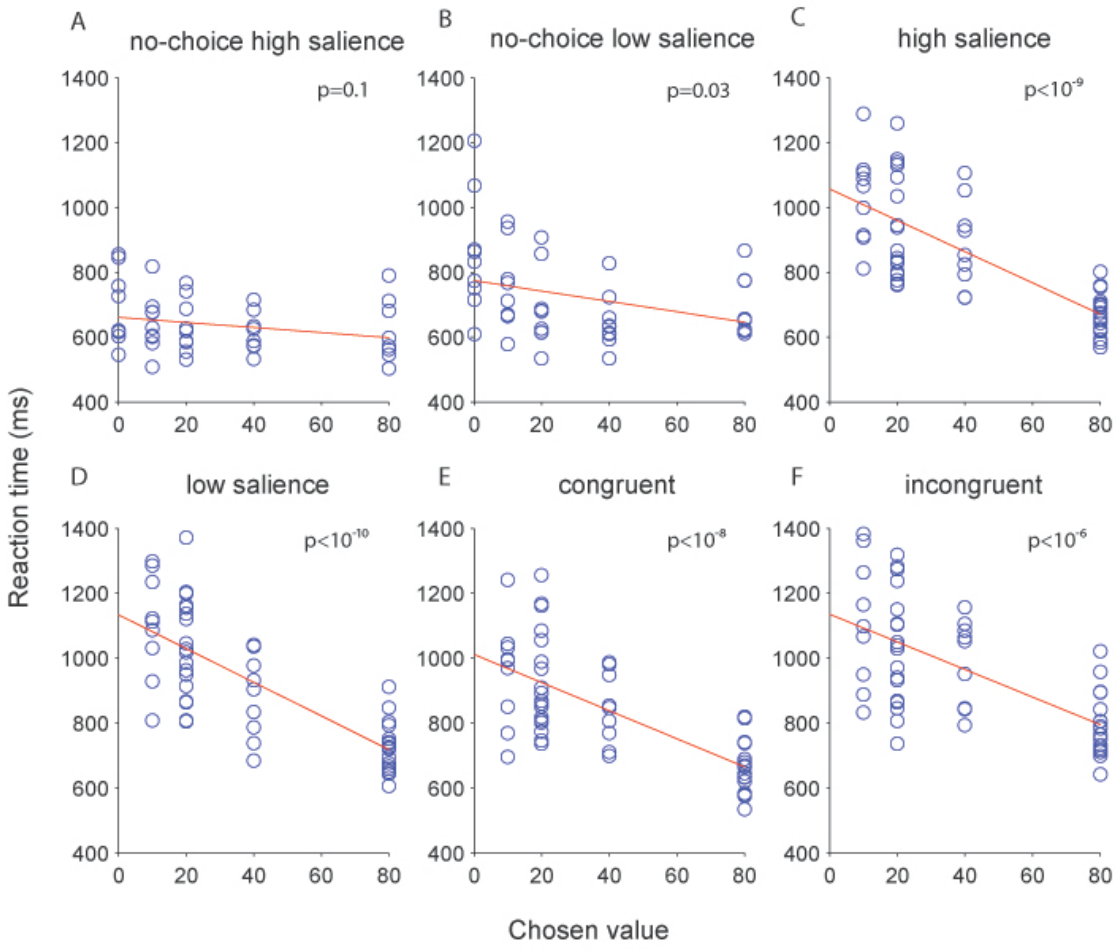

Figure 2.3 Effect of chosen value on reaction time. The mean reaction times for all participants are plotted against the value of the chosen targets in (A) no-choice high salience trials, (B) no-choice low salience trials, (C) high salience trials, (D) low salience trials, (E) congruent trials and (F) incongruent trials. Each circle shows the mean reaction time of one participant in the respective condition. The red line shows the result of linear regression.

drive of the chosen target value on the speed of decision- making and response execution processes. Interestingly, the relative importance of this motivational drive was weaker on no-choice trials than on choice trials (slope of no-choice trials: high salience: -0.78 ms/point, low salience: -1.6 ms/point; slope of choice trials: high salience: -4.82 ms/point, low salience: -5.19 ms/point, congruent: -4.33 ms/point, incongruent: -4.25 ms/point), and in no-choice trials, the correlation between value and reaction time was significant only for low salience (t-test, df=43, p=0.03), but not high salience trials (t-test, df=43, p = 0.1) (Figure 2.3).

Not only had the absolute value of the chosen target a significant effect on reaction time, but also the difference between chosen and non-chosen target. In our experimental design, we used only six out of the full set of all possible value combinations. Within this subset of choices, the value of the chosen target (i.e. the target with the higher value) was positively correlated with the value difference between chosen and non-chosen target. Therefore, we could not use a simple regression analysis to test whether the reaction time were correlated with value differences independent of chosen value. Nevertheless, a partial correlation analysis showed that, when we controlled for the contribution of the chosen value, the reaction time was still significantly correlated with the value difference between the chosen and the non-chosen target in all choice trials (Spearman partial correlations; high salience trials: df=42, $p<10^{-4}$, low salience trials: df=42, p=0.015, congruent trials: df=42, p=0.016, incongruent trials: df=42, p=0.002). This relationship was also negative (slope high salience trials: -0.57 ms/point, low salience trials: -0.33 ms/point, congruent: -0.33 ms/point, incongruent: -0.42 ms/point): the larger the value difference, the shorter the reaction time. This finding supports the

view that participants compared the values of both targets before making a choice. Larger value differences made it easier to discriminate the more valuable target and resulted in faster responses, while smaller differences decreased the discriminability and required more time to select the correct response.

2.2.2 Influence of salience on reaction time

The salience of the reward information, i.e., the color saturation level of the targets, had a significant influence on reaction times when compared to the singleton task, the second pilot experiment (Figure 2.4). In the singleton task, the reaction time for high salience targets (high salience singleton, mean: 467 ms) was identical to that for low salience targets (low salience singleton, mean: 467 ms) and much faster than the reaction time in no-choice trials. On the other hand, in no-choice trials when there was no interference between salience and value, the reaction time for high salience trials (mean: 638 ms) was significantly faster (Kolmogorov–Smirnov (K-S) test, $p < 10^{-10}$) than for low salience trials (mean: 726 ms).

At first sight, the large latency difference between singleton and no-choice trials is surprising, since the only difference between the two trial types is that color is behaviorally meaningful in one (no-choice), but not the other (singleton). However, this difference likely reflects a simple speed-accuracy trade-off caused by contextual differences in task demands. In the singleton task, the subjects could be sure that on any given trial there was only one target on the screen. The task was in essence to detect the changing location of the target as fast as possible. For this purpose, luminance contrast provided sufficient information, while target color could be safely ignored. In this situation, the subject's threshold for selecting a target could be lower than in the choice

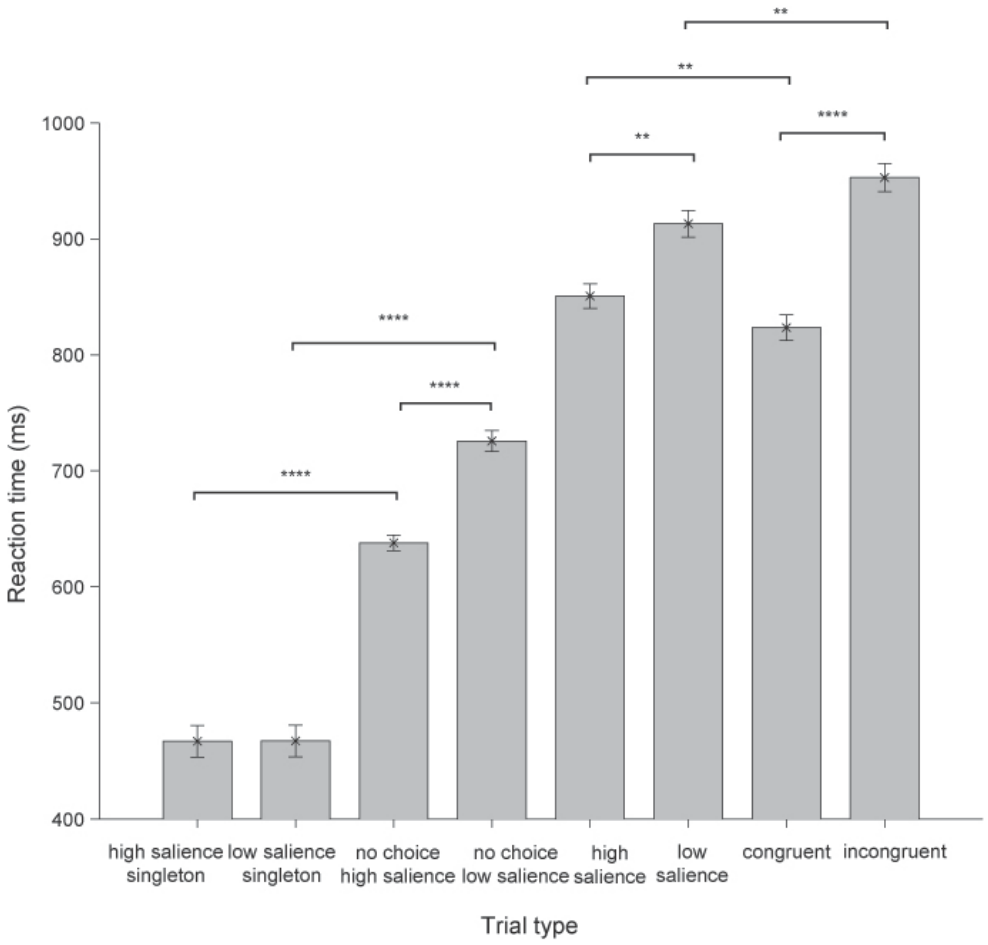

Figure 2.4 Mean reaction time modulated by both salience and value. Mean reaction time across all participants on high salience singleton trials (the singleton task), low salience singleton trials (the singleton task), no choice high salience trials, no choice low salience trials, high salience trial, low salience trial, congruent trials and incongruent trials. Asterisks indicate statistical significance of difference between conditions, * means $p \leq 0.05$, **means $p \leq 0.01$, *** means $p \leq 0.001$, ****means $p \leq 0.001$; in all cases from t-tests. Sample size is nine. Error bars represent standard error of the mean.

condition without affecting accuracy, due to the absence of distractors. In contrast, during our main experiment the no-choice trials were embedded in a larger number of choice trials. In this situation the subject's threshold for selecting a target had to be higher than in the choice condition, because in the majority of trials there were two competing targets, whose value needed to be compared. In principle, there was an absence of distractors in the no-choice trials that was similar to the singleton trials. However, since the two trial types were randomized, the subjects could not be sure when a no-choice would occur and therefore could not adjust their response criteria selectively.

In choice trials, the reaction time in high salience trials (mean: 851 ms) was significantly faster (K-S test, $p=0.032$) than in low salience trials (mean: 913 ms). Moreover, the congruency between differences in value and reward salience had a strong effect on the target selection process. In congruent as well as in incongruent trials, the two targets varied both in value and in salience. In congruent trials, the more valuable target had also more salient reward information. Thus, both the difference in value and in salience supported the same target. In contrast, in incongruent trials the more valuable target had less salient reward information. Here, the difference in value and in salience supported different targets. Accordingly, across all value levels, the reaction time on congruent trials (mean: 822 ms) was significantly faster (K-S test, $p<10^{-13}$) than on incongruent trials (mean: 953 ms; Figure 4). This difference could not be explained merely by the fact that the chosen targets differed in salience. The reaction time on congruent trials was still significantly faster (K-S test, $p=0.01$) than that on high salience trials (Figure 2.4), even though the salience of the chosen targets were the same.

Likewise, the reaction time on incongruent trials was also significantly slower (K-S test, $p<0.01$) than that on low salience trials (Figure 2.4).

2.2.3 Error trials

In the experiment, we did not set a very stringent time-limit on the decision process. Therefore, the error rates, defined as the rate of choosing the lower valued target, were low in general. Nevertheless, we also saw an effect of congruency on error rate (Figure 2.5A). The error rates for high salience, low salience, and congruent trials was low (high: 4.3%; low: 5.8%; congruent: 4.4%). Specifically, the error rate for low salience trials was not significantly higher (K-S test, $p=0.25$) than the one for high salience trials. This indicated that the participants were still able to identify the color of the low salience targets, although those targets were harder to identify. In contrast, the error rate for incongruent trials was much higher (13.1%). This is higher than the error rates for high salience (K-S test, $p=0.01$), and congruent trials (K-S test, $p=0.01$) as well as for low salience trials although the latter difference was not significant (K-S test, $p=0.07$).

Furthermore, we compared the reaction time distribution of the error and correct trials during choice trials. To quantify the differences, we plotted the cumulative distribution for both error trials and correct trials in all four trial conditions. As shown in Figures 2.5C and 2.6, in low and high salience trials, the reaction time on error trials (mean RT: low salience trial: 959 ms, high salience trial: 924 ms) tended to be longer than on correct trials (mean RT: low salience trial: 913 ms, high salience trial: 851 ms). Though the differences did not reach significance (K-S test, $p=0.28$ and $p=0.25$, respectively), the difference is significant (K-S test, $p=0.048$) for the combined

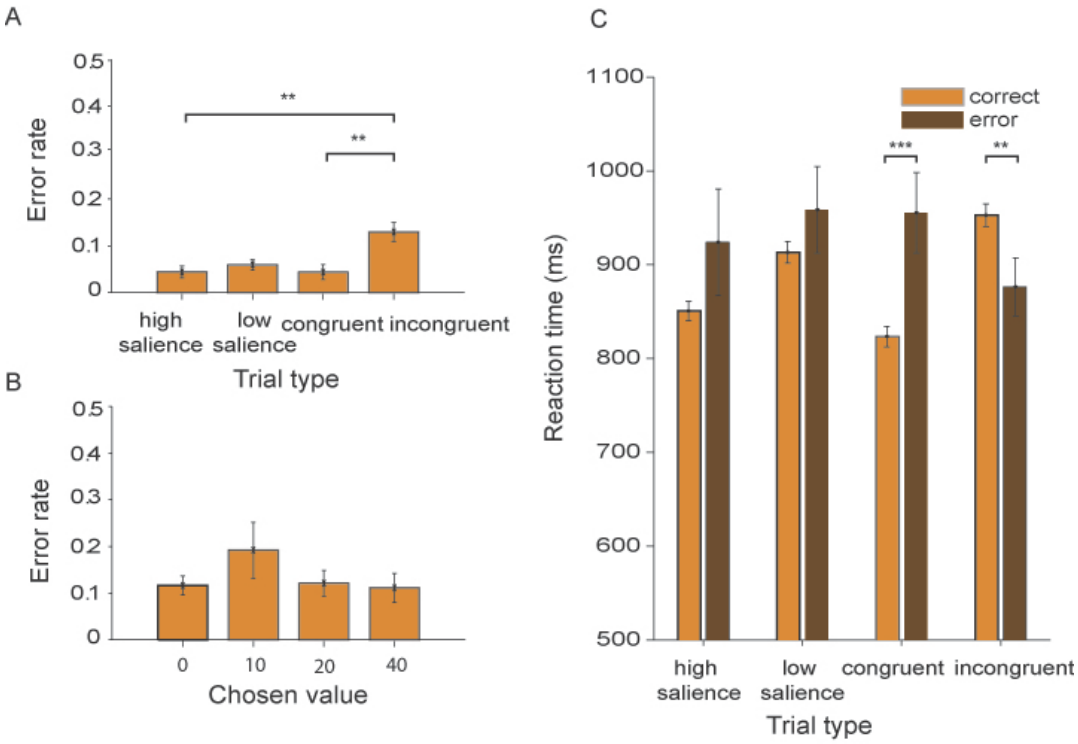

Figure 2.5 Error rates and mean reaction times on different trial types. A: Mean error rate for all participants for different trial types. B: Mean error rate in incongruent trial for all participants as a function of chosen value. C: Mean reaction time for both correct (light orange) and wrong (dark orange) choice on different trial types. See Fig. 5 for the meaning of the asterisks. Sample size is nine. Error bars represent standard error of the mean reaction time.

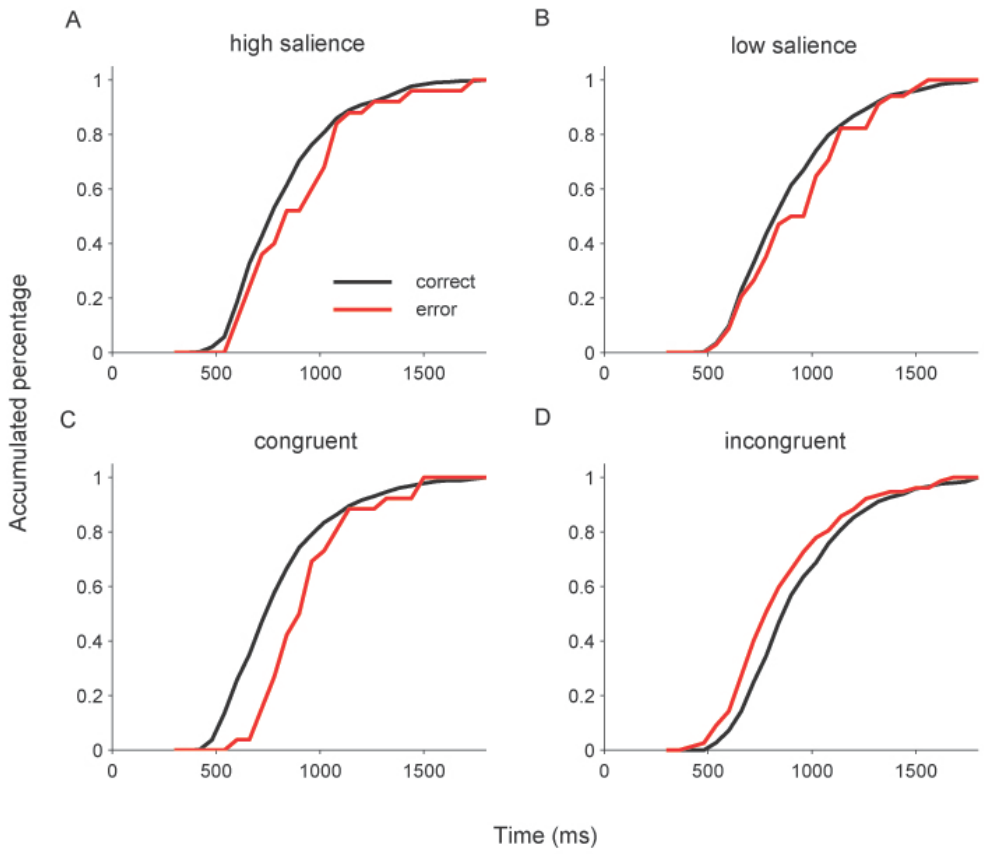

Figure 2.6 Cumulative reaction time distributions. Cumulative distributions of reaction time are plotted for correct (black) and error (red) trials on high salience trials (K-S test, p=0.28), low salience trials (K-S test, p=0.25), congruent trials (K-S test, p=0.001), and incongruent trials (K-S test, p=0.01).

population. In congruent trials, this difference became larger. The reaction time for error trials (mean RT: 955 ms) was significantly longer (K-S test, p=0.001) than for correct trials (mean RT: 823 ms). In contrast to all other trial types, in incongruent trials the reaction time for error trials (RT: 876 ms) was significantly shorter (K-S test, p=0.01) than for correct trials (mean RT: 953 ms). Note that this shorter reaction time on error trials was not confounded by the chosen value on those trials. First, on error trials (by definition) a smaller value was chosen than on correct trials. Second, the error rate did not increase as the chosen value increase (Figure 2.5B). The chosen value on error trials was therefore on average not larger than the chosen value on correct trials. This specific difference in the reaction time distributions between congruent and incongruent trials turned out to be important, because, as we shall see below, it allowed us to distinguish between different types of accumulator models of the decision process.

2.2.4 Descriptive model of behavior

To summarize, in the main experiment, the reaction time across the six different trial types was correlated with the value of the chosen target, the salience of the reward information, and the contingency between value and salience (Figure 2.7). Across all chosen values in the main experiment, the reaction time was shortest for no-choice high salience trials, increased successively for no-choice low salience, congruent, high salience, low salience trials, and was longest for incongruent trials. This was very different from the results in the second pilot experiment (singleton task), in which the results showed no difference between reactions to high and low salience targets (Figures 2.4 and 2.7).

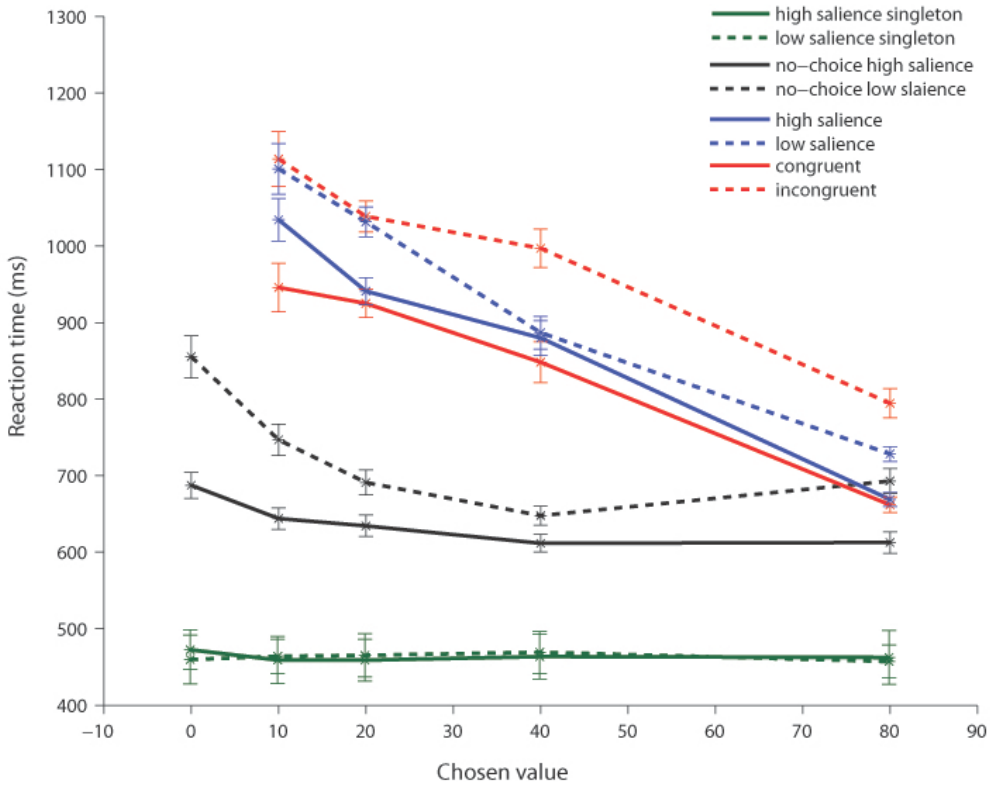

Figure 2.7 Mean reaction times for both second pilot and main experiment. Mean reaction time in the second pilot experiment are plotted against different targets with corresponding colors without value information on high salience singleton trials (green solid line), low salience singleton trials (green dotted line) in the singleton task (second pilot experiment). The reaction time in the main experiment are plotted against value of the chosen targets on no-choice high salience trials (black solid line), no-choice low salience trials (black dotted line), high salience trials (blue solid line), low salience trials (blue dotted line), congruent trials (red solid line), and incongruent trials (red dotted line). Sample size is nine. Error bars represent standard error of the mean reaction time.

We further used a descriptive model to quantify the trends we had observed in the behavior data. There were a number of factors that could contribute to the decision-making process, including 1) the value of the chosen target, 2) the salience of the chosen target, 3) the value of the non-chosen target, 4) the salience of the non-chosen target, 5) the value difference between chosen and non-chosen target, 6) the salience difference between chosen and non-chosen target, as well as the multiplicative interaction between salience and value for both 7) chosen and 8) non-chosen target. In order to quantify the effect of each of these possible factors, we fitted a family of nested regression models to the reaction times in correct choice trials that included all possible iterations of the seven factors plus a baseline term. In order to combine the reaction time data across all participants, we normalized reaction times within each participant between 0 to 1 (thus, the normalized RTs computed in eq. 11 cannot be directly compared with the actual RTs in Fig. 4). By comparing the Bayesian information criterion value (BIC), and Akaike value (Burnham and Anderson, 2002; Busemeyer and Diederich, 2010) of each model (Table 1), we identified the best fitting model. Of all linear models tested, the lowest BIC value and lowest Akaike value occurred for the same model:

$$\begin{aligned} RT_{normalized} = {} & 0.5209 - 0.0015 * v_{chosen} - 0.0373 * s_{chosen} \\ & - 0.0018 * (v_{chosen} - v_{nonchosen}) - 0.0188 * (s_{chosen} - s_{nonchosen}) \end{aligned} \quad (2.1)$$

where v_{chosen} and $v_{non\text{-}chosen}$ are the point values of the chosen and non-chosen target ($v_i \in (0, 0.1, 0.2, 0.4, 0.8)$), and S_{chosen} and $S_{nonc\ hosen}$ are the salience values of the chosen and non-chosen targets ($S_i \in (0,1)$), respectively. All four parameters (but none of the other four possibilities listed above) contributed significantly to the regression, including: 1) value of the chosen target (t-test: $p<10^{-7}$), 2) salience of the chosen target (t-test:

Rank	Variables resulting in model	BIC	AIC	Evidence ratio
1	$v_{chosen}, s_{chosen}, dv, ds$	-8711	8734	1
2	$v_{chosen}, s_{nonc\ hosen}, ds, v_{nonc\ hosen}$	-8711	-8734	1
10	$v_{chosen}, s_{chosen}, dv, v_{nonc\ hosen}$	-8710	-8733	1.23
13	$v_{chosen}, s_{chosen}, dv$	-8708	-8726	3.90
17	$v_{chosen}, s_{chosen}, dv, ds, v_{nonc\ hosen} \times s_{nonc\ hosen}$	-8705	-8732	23.90

Table 2.1 BIC table for descriptive behavior regression model. All possible combinations of eight independent variables: v_{chosen}, s_{chosen}, $v_{nonc\ hosen}$, $s_{nonc\ hosen}$, $v_{chosen} - v_{chosen}$ (dv), $s_{chosen} - s_{nonc\ hosen}$ (ds), interaction between chosen value and salience ($v_{chosen} \times s_{chosen}$), interaction between non-chosen value and non-chosen salience ($v_{nonc\ hsen} \times s_{nonc\ hosen}$) were tested against the behavioral data. The first column shows the BIC rank of the model among all other 255 models. The second column shows the selected variables with the corresponding rank. The third column shows the BIC value, the forth column shows the AIC value, and the fifth column shows the BIC evidence ratio for each model compared with the best fitting model.

$p<10^{-5}$), 3) value difference between chosen and non-chosen target (t-test: p<10-4), and 4)salience difference between chosen and non-chosen target (t-test: p=0.001). Table 1 shows the BIC values, Akaike value and evidence ratio (relative to the best-fitting model) for different models ranked by their fit to the behavioral data. From the evidence ratios it is clear that there were actually approximately 12 different regression models all containing 4 variables that all fitted the data almost as well as the best-fitting model. This phenomenon is likely related to the fact that the variables we chose were most likely not completely independent of each other such as the equation containing S_{chosen} and $S_{nonchosen}$ can be equally expressed as an equation containing S_{chosen} and dS. However, there was a clear drop in evidence for alternative 3- or 5-variable models.

2.2.5 Accumulator models

The behavioral results, confirmed by a linear regression model, showed that both value and salience of the targets as well as the congruency between them influence the decision- making process. To make progress towards understanding the underlying mechanisms, we modeled the decision process using accumulator models with four functionally related architectures (Figure 2.8). In addition to suggesting a functional mechanistic explanation of the underlying mechanisms, accumulator models have the additional advantage over descriptive regression models (like the one developed in the previous section) that they describe the entire distribution of behavioral data, rather than only their mean values. This modeling approach allowed us to address several questions beyond the identification of the behaviorally relevant factors. Most importantly, it allowed us to ask questions regarding the functional architecture of the decision-making mechanism that implements the value-based decisions. In the following simulation-based

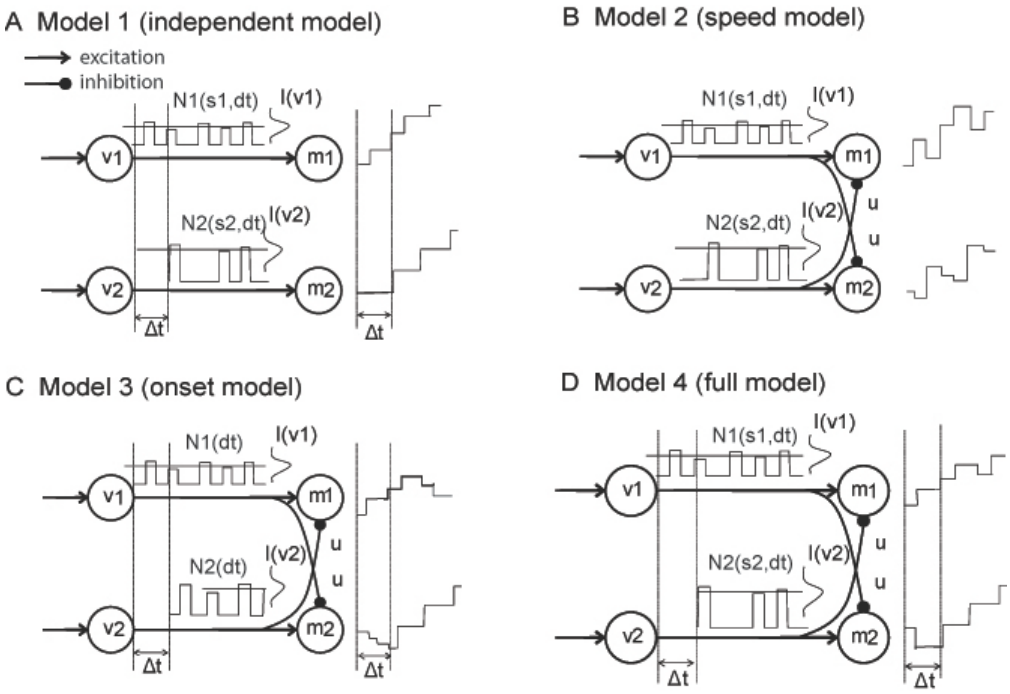

Figure 2.8 Architecture of the four accumulator models. A: Model 1: Independent model, without mutual inhibition between the targets. B: Model 2: Speed model. Salience influences the rate of accumulation but not its the onset. C: Model 3: Onset model. Salience influences the onset of accumulation but not its rate. D: Model 4: Full model with feed forward inhibition model salience influencing both the onset of accumulation and its rate. v_i are the units that transfer sensory input into value. m_i are the accumulators that integrate the input and trigger a motor response. Consistent with appendix equation 2, $\Delta t=t_1-t_2$ is the onset difference generated by salience differences, N_i is the number of accumulations that occur in each accumulator mi, $I(v_i)$ is the rate of accumulation for each accumulator mi, and u is the mutual inhibition parameter between two accumulators

analysis, we focused specifically on two of these mechanistic questions. First, is there a role for inhibitory interactions between the processes representing the two targets? Second, how does the salience of the reward information influence the decision- making process? In addition, accumulator models incorporated in a natural fashion non-linearity in the decision-making process, such as the threshold, which is not easy to be captured in a linear regression model.

Models 1-3 have the same complexity (6 parameters). As described below, they are special cases of the general functional Model 4 which is slightly more complex with 7 parameters. In order to determine the importance of particular factors, for Model 1-3, we systematically constrained one factor of the general model (Model 4), while allowing the other factors to change freely to achieve the best possible fit with the behavioral data. All other aspects of the functional architecture were held constant across the four different variants (mutual inhibition for model 1, onset difference for model 1, accumulation speed for model 3, none for model 4) .All models have two accumulator units, each of which integrates the input from the target whose choice they would trigger until it reaches the response threshold. The quanta size of the input for accumulation is determined by the target value. The rational for this design choice follows immediately from the idea that what is accumulated during the decision process is support for a particular choice (here the value that is associated with selecting a particular target). In Model 1 (independent model), salience influences both the onset and the rate of accumulation but the two accumulators are independent, with no inhibitory interaction between them (Figure 2.9A). In contrast, Models 2 (speed model) and 3 (onset model) are feed-forward inhibition models. Here, the two accumulator units also integrate the input from the target

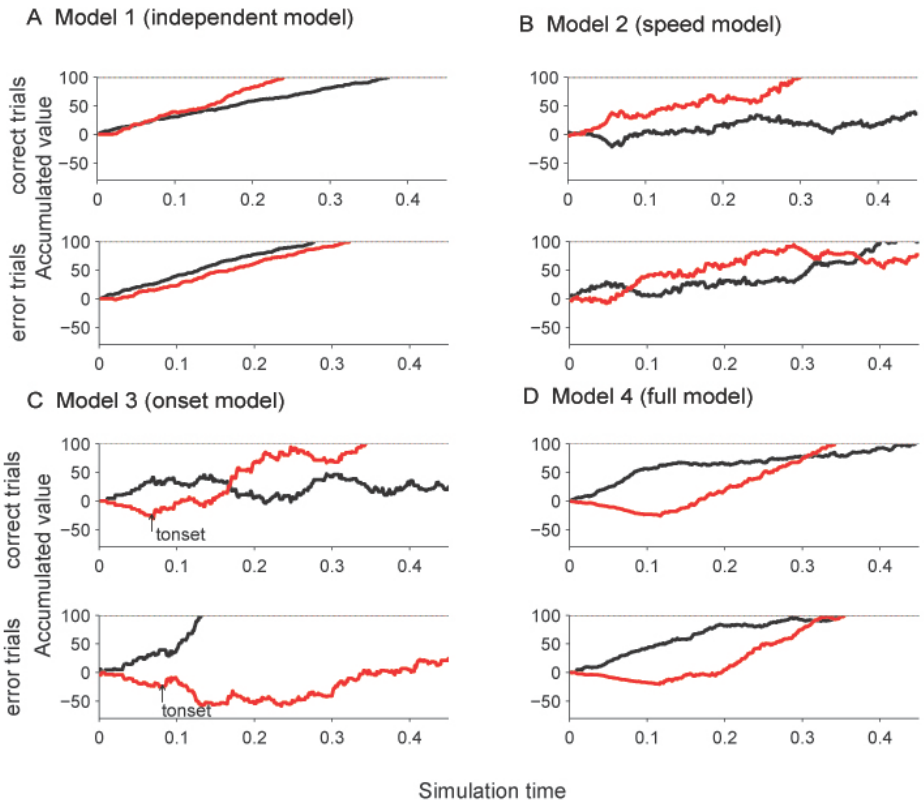

Figure 2.9 Examples of the time evolution of variables in independent models in incongruent trials. Within each plot, the upper panels are examples for correct trials, the lower panels for error trials. The paths for high value low salience targets are shown in red, and for low value high salience targets are in black. All competitions start at 0 and threshold is always 100. A: Model 1: independent model, no mutual inhibition between targets. B: Model 2: speed model, salience influences the rate of accumulation. C: Model 3: onset model, salience influences the onset of accumulation. D: Model 4: the free model.

whose choice they would trigger, but in addition they receive inhibitory input from the alternative target, with the inhibitory strength determined by the behavioral fit. The strength can therefore approach zero, which includes the condition enforced in model 1. The key difference between Models 2 and 3 is the mechanism by which salience influences the integration process. Model 2 assumes that salience influences the quality of the perceptual process output, and thus the probability of accumulation, which is independent of the input strength which is determined by value (Figure 2.9B). This results in a modulation of the mean drift rate, which is orthogonal to the effect of value, as supported by our behavioral analysis. In Model 3, on the other hand, salience is assumed to influence the onset time of the accumulation process (Figure 2.9C), but not the probability of accumulation (i.e., mean drift rate). Finally, salience is free to modify both onset and drift rate in Model 4 (Figure 2.9 D).

We optimized the parameters in all four models using the observed reaction times in correct choice trials, which were used as the training set for parameter tuning. We then compared the simulated reaction time distribution with the training set reaction distribution using person chi-square statistics (Van Zandt et al., 2000; Purcell et al., 2010) . This method maximized the proportion of correct responses in addition to matching the distribution of observed RTs. In order to avoid over fitting of the training data and to test the models' capability of prediction, in addition, we compared the predicted behavioral performance with two test sets, neither of which was used during training. One was the observed behavior in no-choice trials, the other was the behavior in erroneous choice trials (the trials in which the participant chose the lower valued target). In addition, we

also used the BIC to test both fitness and prediction of the models. The results of this analysis are consistent with the results using the chi-square criterion (table 2).

2.2.6 Mutual inhibition is necessary to explain behavior

The independent model (Model 1) did not explain the reaction times well. Its mean χ^2 fit (7.08) was significantly larger than that for the other two constrained models (Model 2: mean χ^2 fit, 2.44; t-test, df=29, $p<10^{-8}$, Model 3: mean χ^2 fit, 2.24; t-test, df=29, $p<10^{-10}$). More importantly, the predicted reaction times in no-choice trials did not fit the observed reaction times (Figure 2.10 A,B). Specifically, a very general characteristic of the observed reaction time data was the increased reaction time latency on choice trials as opposed to no-choice trials (Figure 2.7). In contrast, the independent model predicted that the reaction times for choice trials were as fast as those in no- choice trials, due to the lack of inhibition from the non-chosen target. In addition, Model 1 overestimated the error rate on incongruent trials (Figure 2.10C) and it failed to predict the observation that on incongruent trials the reaction times on error trials were shorter than those on correct trials (Figure 2.10D). For no-choice trials, the mean χ^2 value (12.84) of Model 1 was significantly larger than that of the other two models (Model 2: χ^2: 8.38, t-test, df=29, $p<10^{-15}$, Model 3: χ^2: 3.61, t-test, df=29, $p<10^{-34}$). In sum, the analysis of Model 1 showed very clearly that mutual inhibition between two choices is important for target selection. Model 2, in which salience modulates the accumulation rate, reaction time differences caused by salience differences were positively correlated with the time it took the accumulated activity to reach the threshold. Therefore, this model predicted that the reaction time difference caused by salience will be larger for choice trials than for no-

	choice trial		no-choice trial	
	BIC_{fit}	χ^2_{fit}	BIC_{test}	χ^2_{test}
Independent model	-111.86	7.08	-15.76	12.87
Speed model	-114.68	2.44	-39.30	8.38
Onset model	-115.51	2.44	-44.27	3.61
Full model	-114.37	3.50	-37.89	8,20

Table 2.2 Fitness of four different models in fitting reaction time on choice trials and predicting reaction time on no-choice trials. The first column shows the type of the model under testing. The second and third columns show the *BIC* value and χ^2 for the choice trials when optimizing model parameters during the training section. The fourth and fifth rows show the *BIC* value and χ^2 for the no-choice trials when testing the models' capability of prediction.

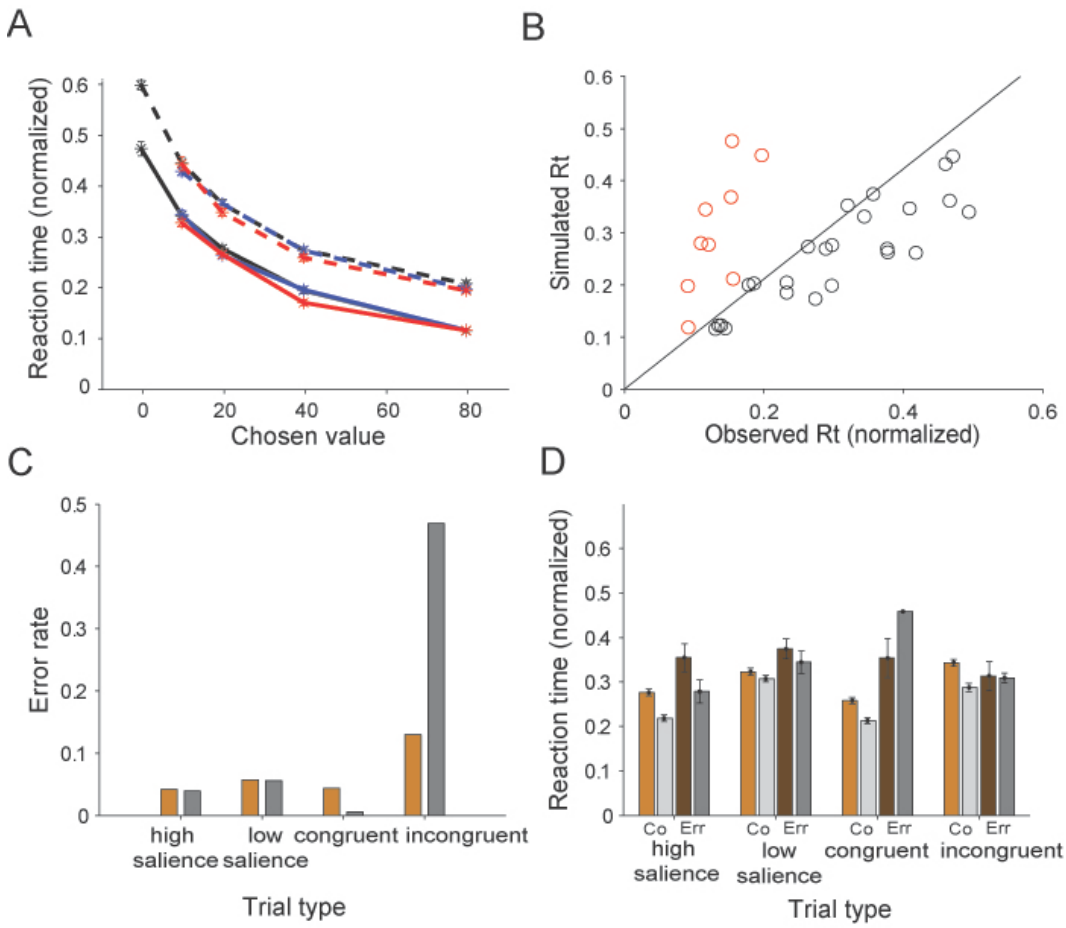

Figure 2.10 Predictions of Model 1 (independent model). A: Predicted mean reaction times are plotted against the value of the chosen targets on different trial types. Each sample size is a 100 simulations. Error bars represent standard error of the mean reaction time. Symbols are as in Figure 7. B: Predicted mean reaction times are plotted against observed mean reaction time for 24 different choice trial types (black circle) and 10 different no-choice trial types (red circle). C: Comparison between observed (light orange) and predicted error rate (grey) on different trial types. D: Comparison between observed (correct trial: light orange; error trial: dark orange) and predicted (correct trial: light grey; error trial: dark grey) mean reaction times on different trials types. Symbols are as in Figure 5.

choice trials (Figure 2.11A). On the other hand, in Model 3, in which salience modulates the accumulation onset, reaction time differences caused by salience were independent of how long it takes the activity to reach threshold. Therefore, this model predicted that the reaction time difference caused by salience will be similar for choice and no-choice trials (Figure 2.12A). Consequently, when the parameters of both models were adjusted so that they fit the reaction time differences in choice trials, the salience-induced reaction time differences in no-choice trials predicted by Model 2 should be smaller than the ones predicted by Model 3. This is exactly what the simulations showed (Figures 2.11A, 2.12A). Specifically, Model 2 predicted that reaction times in no-choice trials should not be significantly influenced by salience, as can be seen by comparing the solid and dotted black lines in Figure 2.11B. This prediction is not unreasonable. The luminance contrast of high salience targets was similar to that of low salience targets. This allowed the single targets to be equally localized. Furthermore, value information was not behaviorally relevant, since no choice was required. Therefore, one might expected that differences in salience do not necessarily influence reaction time similar as in the singleton task (Figure 2.7). In contrast, Model 3 predicted that reaction times to targets with high salience of the reward information should be faster than the ones to targets with low salience, as indicated in the corresponding plot in Figure 2.12A.

This difference in the predictions of the two models allowed us to compare how well they fit the observed behavioral data. A comparison of the actual (Figure 2.7) with the predicted reaction times (Figure 2.11A, 2.12A) showed that, overall, Model 3 agreed much better with observations than Model 2. The behavioral fit of Model 3 (mean χ^2_{test} =3.61) in no-choice trials was significantly (t-test, df=29, $p<10^{-15}$) better than that of

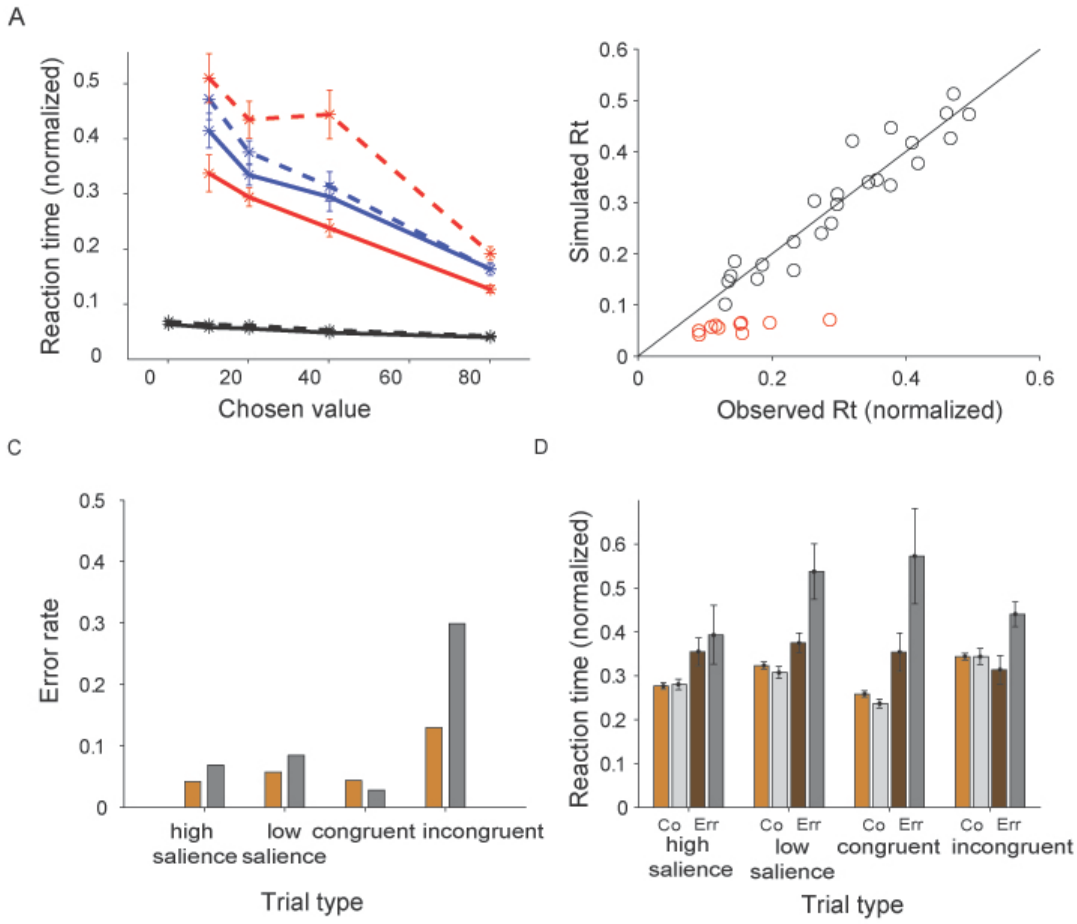

Figure 2.11 Predictions of Model 2 (speed model). Symbols are as in Figure 2.10.

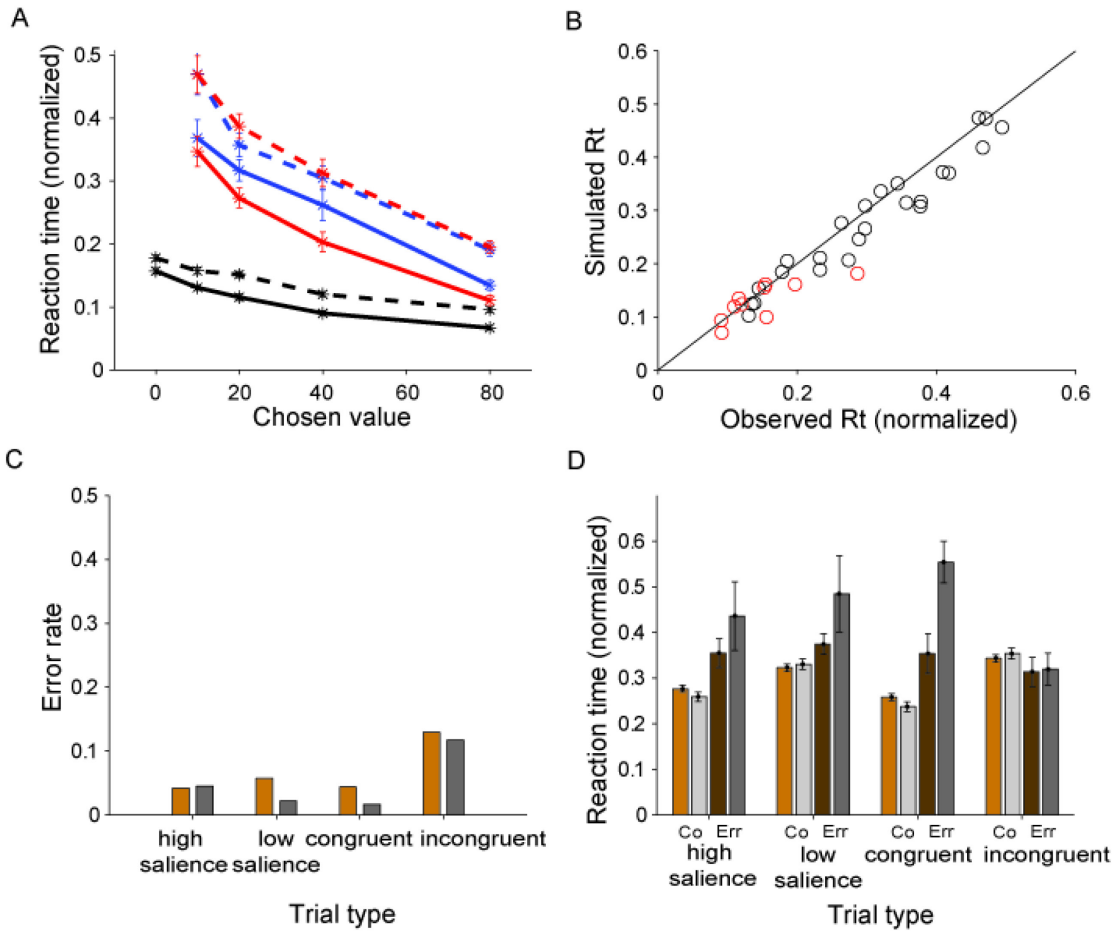

Figure 2.12 Predictions of Model 3 (onset model). Symbols are as in Figure 2.10.

Model 2 (mean χ^2_{test} =8.38). In particular, the human participants showed consistently longer reaction times in no-choice trials with low salience targets compared to trials with high salience targets. Consequently, the comparison of predicted to observed reaction times in Figures 2.11B and 2.12B showed that for most no-choice trials (indicated by the red circles) the predicted RTs of Model 2 are too short, while the predictions of Model 3 for no-choice trials were as accurate as for choice trials.

Secondly, the two models also made different predictions with regards to the reaction times in error trials, providing another opportunity to determine which model provided a better description of behavior. The behavioral data showed that the reaction time in all trial types was significantly longer for erroneous than for correct responses, except for incongruent trials for which the pattern was incongruent trials for which the pattern was the opposite (Figure 2.5C). Thus, there was an inversion of reaction time for congruent and incongruent trials with respect to correct and erroneous responses. Both models predicted correctly that in congruent trials the reaction time was significantly longer on error trials than on correct trials (Model 2: K-S test, p=0.004; Model 3: K-S test, p=0.003). On incongruent trials, however, Model 2 predicted that the reaction time on erroneous trials was also significantly longer (K-S test, p=0.002) than on correct trials (Figure 2.11D). This is because an error can only occur when the accumulator associated with the low value target happened to reach the threshold earlier than the one associated with the high value target. Since in Model 2 the low value accumulator tended to rise slowly, this can only happen if the competing high value accumulator also rose slowly. Thus, in this model the reaction time on error trials had to be longer than on correct trials (Figure 9B).

In contrast, Model 3 accurately predicted shorter reaction times on erroneous than on correct incongruent trials (Figure 12D). Sensitivity analysis showed that the difference in onset time of the accumulation between high and low salience targets was significantly linearly correlated (t-test, df=47, $p<10\text{-}8$, Sobol Index: 0.43) with the reaction time differences between error and correct trials on incongruent trials (Figure 13). In Model 3, errors were due to the earlier onset of accumulation for the low value targets. This onset time difference, especially when it is large, created a window of opportunity for the low value accumulation process during which it experienced no competition from the high value accumulation process. Therefore, in this model the reaction times on error trials tended to be shorter than on correct trials (Figure 2.9C). The fact that this prediction, which was specific for Model 3, was confirmed by the behavioral data gives further support for the hypothesis that differences in the onset latency of accumulation (as in Model 3) rather than in the rate of accumulation (as in Model 2) explains the salience effect in our behavioral choice task.

Finally, we also optimized the full model, where salience could influence both onset and rate of the accumulation (Figure 2.14). This model has one parameter more than Models 2 and 3. We would therefore expect at least as good a fit to the training data as the best of the less complex models. However, Model 4 does not necessarily have better predictive power for the test data since it might still contains terms based on incorrect assumptions. Indeed, the full model did not significantly improve the accuracy of the reaction time fits in the training set (correct choice trial, mean $\chi 2$ fit =3.50), and it resulted in decreased accuracy when predicting the reaction time in the testing set (no-

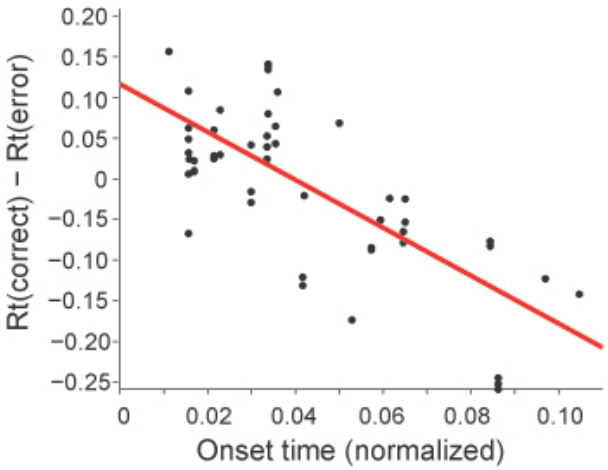

Figure 2.13 Effect of difference in the onset time of accumulation in Model 3 (onset model). The predicted mean reaction time difference between error and correct trials on incongruent trials is correlated with the simulated time of accumulation onset, shown in 50 different simulations (black circles), together with the regression line (red).

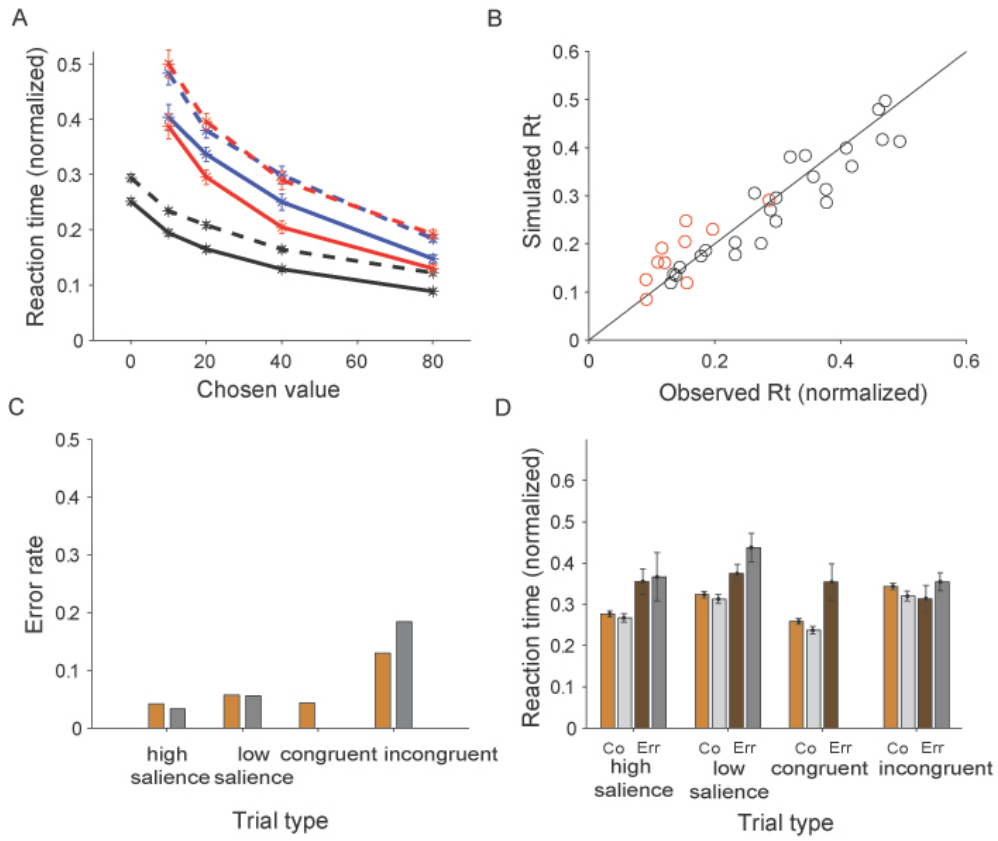

Figure 2.14 Predictions of Model 4 (full model). Symbols are as in Figure 2.10.

choice trials, mean $\chi 2$ test =8.20) over Model 3. This provided additional support for Model 3.

2.3 Discussion

We studied the influence of visual salience on value-based decision processes of human observers performing a two-alternatives-forced-choice task. Most previous studies examined the effect of visual saliency (Berg et al., 2009) and value (Platt and Glimcher, 1999; Bendiksby and Platt, 2006; Milstein and Dorris, 2007; Milosavljevic et al., 2010) on saccades and decisions in isolation. In contrast, we manipulated saliency and value of targets simultaneously, in order to investigate how these two factors interact and how they influence the decision process.

Our behavioral results showed that not only value, but also visual salience as well as congruency between value and visual salience influence the decision process. Specifically, we found that reaction time across all trial types is correlated with all three of these variables. Furthermore, congruency had an effect on error rates as well as on reaction times in error trials. These findings are in broad agreement with recent behavioral studies of eye movements in macaque monkeys and humans which also manipulated salience and value information simultaneously (Navalpakkam et al., 2010; Markowitz et al., 2011; Schutz et al., 2012). This convergence of findings across species and effector systems indicates that these behavioral trends are robust and reflect basic selection mechanisms in the primate brain. However, despite the similarity of the behavioral findings, the mechanism underlying these phenomena can differ depending on whether salience and value information share the same feature dimension as will be discussed later.

2.3.1 Onset time differences

The speed and the onset model are based on different hypotheses how salience modulates the decision process. In the speed model, salience influences accumulation speed by modulating the probability of an increase in activity, which influences how likely the accumulator responds to the input independent of its strength. A possible neurophysiological interpretation could be that salience modulates the likelihood that an individual neuron responds to synaptic input, or how many neurons out of the entire pool of 'decision' neurons respond to the input in a given time interval and for a given stimulation. This interpretation does not seem to be unreasonable, given our current understanding of primate decision-making mechanisms. It is therefore quite noteworthy that our analysis ruled out this model so convincingly. Instead another model, namely the onset model, explained the observed reaction time distribution of error trials and no-choice trials much better.

In the onset model, salience influences the onset time of accumulators to accumulate value information instead of influencing accumulation speed. Specifically, this stochastic model suggests an earlier accumulation onset time when processing high compared to low salience targets. What might be the sources of this earlier onset? One possibility is that the difference is due to an attentional shift. Specifically, high salience targets might attract attention first, as predicted by bottom-up attentional guidance models (Itti et al., 1998). Focus on one of the targets might in turn result in an advantage for the accumulation process associated with this target, similar to the logic underlying a recent model of how value-based decisions are guided by visual attention (Krajbich and Rangel, 2011; Lim et al., 2011). However, in our paradigm, attentional guidance can only

explain the behavioral results on choice trials but not on no-choice trials. In the latter, attention should always be focused on the only target present, but we found that reaction times still differed between high and low salience trials (Figure 7). Even though saliency-based models (Itti et al., 1998) predict slightly faster deployment of attention to more salient than to less salient targets, the effect is likely too small to explain the size of the observed reaction time difference in no-choice trials. Allocation of attention can then not be the main reason for the onset differences in the accumulation process.

An alternative hypothesis is that the onset difference is caused by differences in the visual processing time required for computing the value of high and low salience targets (Ratcliff et al., 2007; Ratcliff and Smith, 2011). Low salience targets might need more time to be identified than high salience targets. This hypothesis is consistent with our behavioral data, since the salience effect on reaction time is similar for choice and no-choice trials. It is also supported by neurophysiological findings of clear effects of contrast, but not of attention, on visual response latencies in primates (Lee et al., 2007).Our results suggest therefore that the onset time of accumulation is time-locked to the end of the visual processing. This implies a sequential form of information processing, similar to a recent model of target selection in frontal eye fields (Purcell et al., 2010). What might keep the accumulators from integrating evidence earlier? One possibility is that a specific gating mechanism blocks accumulation until a certain degree of difference has developed in the input sources. Alternatively, in our model information about the location of potential targets drives the accumulators equally well and the two accumulators inhibit each other sufficiently to suppress any activity increase. Only when

value information is added, the symmetry is broken and the differentiated accumulation process can start.

2.3.2 Functional architecture of value-based decision-making in primates

Our analysis using stochastic accumulator models aimed at investigating the neuronal mechanisms underlying behavior. Obviously, simple modeling studies can only provide indirect evidence about mechanisms implemented in the brain. Nevertheless, the fact that our models show qualitative differences in their ability to explain behavioral data allows us to rule out entire families of functional architectures. The failure of Model 1, the independent model, shows that mutual inhibition between choices is required for the decision mechanism. The comparison between the two feed-forward inhibition models, speed and onset model, shows that increased visual salience leads to an earlier start of accumulation rather than an increased rate of accumulation. That the rate of accumulation plays a minor role, if any, is underscored by the fact that including it in addition to the change in onset time (Model 4) does not improve performance significantly. These findings allow us to formulate a strong hypothesis about the type of decision architecture that underlies the effects of visual salience and value information on choice behavior.

One hypothesis is that value and salience independently drive action selection and compete for access to the motor system. Indeed, we observed that early choices reflected more strongly visual salience, while later choices were more driven by value, consistent with previous findings by Markowitz et al. (2011). These authors suggested that the reaction time difference is due to the time-varying balance between stimulus- and reward-driven selections. This was reasonable, since in their study salience influenced both location and value-related information simultaneously. Information about target location

influences the preparation of motor acts directed towards these locations (Schiller and Tehovnik, 2005). Information about target identity, on the other hand, is crucial for the generation of value information, which in turn affects competition between different value options (Padoa-Schioppa, 2011). However, in our study, we designed stimuli whose salience influenced only the discrimination of target identity, but did not affect the ability to locate a target. Therefore, automatic selection processes driven by stimulus location were equally strong for all targets as confirmed by our second pilot study (singleton task; see Figure 2.4 & 2.7). If value and salience were competing during the decision process, the choice behavior should show a joint dependence on sensory and goal-directed processes. In contrast, our behavioral results do not show an interaction between visual salience and value.

This suggests a second hypothesis that there is a combined value and salience map within the visuomotor system (Navalpakkam et al., 2010; Schutz et al., 2012). Under this hypothesis, the salience map formed is first influenced by bottom-up factors (in our case luminance contrast with the background) and is only later modified by value information. This implies that bottom-up salience alone can influence behavior independent of value information, in particular during early responses. However, in our study we were interested in dissociating the effect of salience on value-based decision-making from the one on motor generation in general. Indeed, the salience manipulation that we used does not seem to have influenced motor behavior very much, since the reaction time for both high and low salience targets is the same in the singleton task (Figure 2.4 & 2.7). Moreover, if the salience map is modulated by the attention captured by the objects associated with reward (Anderson et al., 2011), we would expect to see a

joint dependence between reward and salience, which is not shown in the result. Therefore, the salience effect in our experiment is less likely to be the result of early activation in the salience map driven by bottom up factors.

Instead, these findings support a third alternative hypothesis about the interaction of salience and value in decision-making; namely that value-based action selection is a serial iterative decision process. First, lower sensory areas process the stimuli and derive value and location information from them. The salience of the relevant visual feature influences how long this process takes, but has no influence on the output of this stage. The processed information is then sent to accumulators in a higher comparative area that selects the final (and motor) response. At this point the value input has been stripped of other content, such as saliency. This serial processing hypothesis contains the predictions of the combined saliency map hypothesis as a special case. When the sensory features carrying both target location and identity information are of varying salience, the targets with more salient features will influence the decision-making stage earlier and there will be a higher likelihood that the subject will choose the more salient target (in particular, if the accumulation process was fast and there was less time for the less salient target to reach the accumulation stage). Behavior will appear as if bottom-up salience of the targets alone can influence choice independent of value information. Thus, for this set of experimental conditions, both hypotheses explain the behavior equally well. In contrast, our present experimental findings can only be explained by the serial processing hypothesis, but not the combined saliency map hypothesis. This attribute of the serial processing hypothesis is attractive. Nevertheless, at this point we do not know, if this

conjecture is indeed correct, since we have not tested subjects in both conditions and determined if our model can really explain data across both situations.

The higher order areas involved in the final decision likely include structures representing subjective value, such as orbitofrontal (Padoa-Schioppa and Assad, 2006) and ventromedial prefrontal cortex (Kim et al., 2008; Lim et al., 2011), and/or visual-motor association structures, such as the lateral intraparietal area (Platt and Glimcher, 1999; Sugrue et al., 2004), supplementary eye field (So and Stuphorn, 2010), or the supplementary motor area (Scangos and Stuphorn, 2010). Given our results, it is worth investigating whether and how these areas integrate both visual salience and value information during value-based decision- making when salience influences selectively the value perception of an object, but not awareness of its presence.

Chapter 3

General Methods

This chapter is a methods chapter. In the chapter, the main behavior paradigm will be introduced. This paradigm together with its modified versions will be used throughout the whole dissertation work. The chapter will also discuss the basic techniques used in the dissertation project, including monkey neurophysiology set up, the general methods for recording and basic analysis methods. This will provide background knowledge for the following chapters.

3.1 Experimental Set-Up and Surgery

Two rhesus monkeys (both male; monkey A: 7.5 kg, monkey I: 7.2 kg) were trained to perform the tasks used in this study. All animal care and experimental procedures were approved by Johns Hopkins University Animal Care and Use Committee. During the experimental sessions, each monkeys was seated in a primate chair, with its head restrained, facing a video screen. Eye position was monitored with an infrared corneal reflection system (Eye link,SR Research ltd., Ottawa, Canada) and recorded with the Plexon system (Plexon Inc., Dalls,TX) at a sampling rate of 1000 Hz.

The monkeys were water restricted, and we use steamed water as reward to motivate the monkeys' participation. We used a newly developed fluid delivery system to deliver the water. The system was based on the two syringe pumps connected to a fluid container that was controlled by a stepper motor. This delivery system made sure the accuracy of the fluid amounts which is critical for our experiment design.

All surgical procedures were done under sterile conditions and also accordance with the rules and regulations of the Johns Hopkins Animal Care and Use Committee.

3.2 Behavior Paradigm --- a gambling task

In the gambling task, the monkeys had to make saccades to peripheral targets that were associated with different amounts of reward (Figure 3.1A). The targets were squares of various colors, 2.25×2.25° in size. They were always presented 10° away from the central fixation point at a 45, 135, 225, or 315° angle. There were 7 different targets (Figure 3.1B), and each gamble target consisted of two colors corresponding to the two possible reward amounts. The portion of a color within the target corresponded to the probability of receiving that reward amount. Four different colors indicated four different reward amounts (increasing from 1, 3, 5 to 9 units of water, where 1 unit equaled 30 μl). The minimum reward amount for the gamble option was always 1 unit of water, while the maximum reward amount ranged from 3, 5 to 9 units, with three different probabilities of receiving the maximum (20, 40, and 80%). This resulted in a set of gambles, as shown in the matrix (Figure 3.1B), whose expected value on the diagonal axis was the same.

The task consisted of two types of trials- choice trials and no-choice trials. All the trials started with the appearance of a fixation point at the center of the screen (Figure

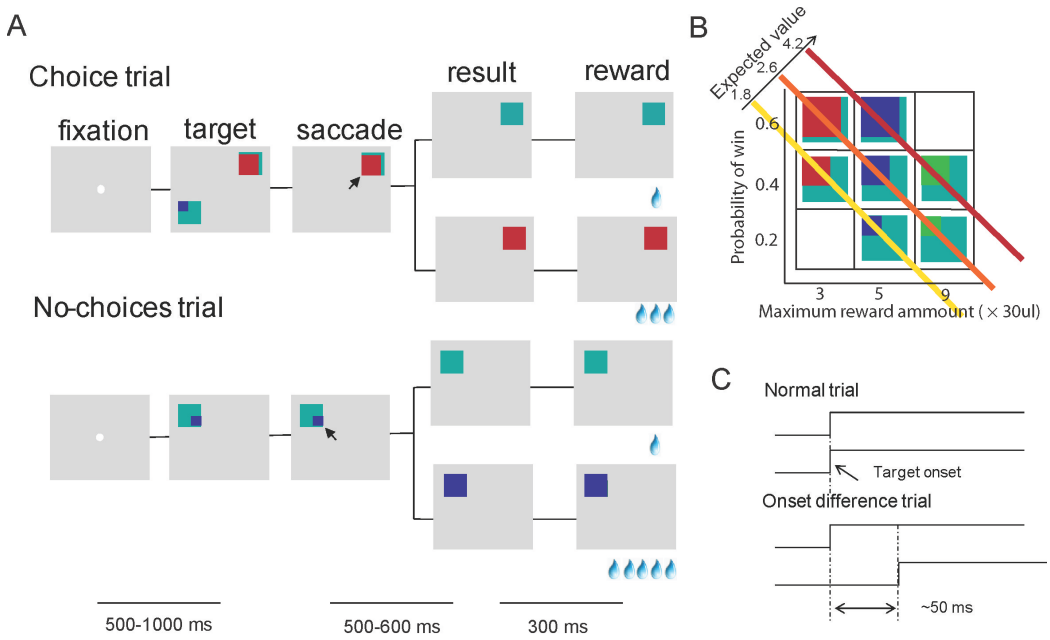

Figure 3.1 Gambling task. A: Sequence of events during choice trials (top) and no-choice trials (bottom). The lines below indicate the duration of various time periods in the gambling task. The black arrow is not part of the stimuli; it symbolizes the monkeys' choices which then lead to the next stimulus shown. B: Visual cues used in the gambling task. Four different colors indicated four different reward amounts (increasing from 1, 3, 5 to 9 units of water, where 1 unit equaled 30 µl). The expected value of the gamble targets along the diagonal axis was the same. C: Target set for the new gamble experiment.

3.1A), on which the monkeys were required to fixate for 500-1000 ms. In choice trials, two targets appeared on two locations that were randomly chosen among the four quadrants. Simultaneously, the fixation point disappeared and within 1000 ms the monkeys had to choose between the gambles by making a saccade toward one of the targets. Following the choice, the non-chosen target disappeared from the screen. The monkeys were required to keep fixating on the chosen target for 500-600ms, after which the target changed color. The two-colored square then changed into a single-colored square associated with the final reward amount. This indicated the result of the gamble to the monkeys. The monkeys were required to continue to fixate on the target for another 300 ms until the reward was delivered. In the choice trial, each gamble option was paired with all other six gamble options. This resulted in 21 different combinations of options that were offered in choice trials. The sequence of events in the no-choice trials was the same as in the choice trials except that only one target was presented. In those trials, the monkeys were forced to make a saccade to the given target. All 7 gamble options were presented during no-choice trials. A subset (22%) of choice trials were onset-difference trials, in which one target appeared three video frames (~50ms) earlier than the second target (Figure 3.1C). The onset-difference trials consisted of four specific comparisons of gamble options with varying degrees of difference in subjective value. Each option could be either the early or late onset target, resulting in 8 different types of onset-difference trials.

We presented no-choice and choice trials mixed together in blocks of trials that consisted of all twenty one different choice trials and eight onset different trials and seven different no-choice trials. Within a block, the order of trials was randomized. The

locations of the targets in each trial were also randomized, which prevented the monkeys from preparing a movement toward a certain direction before the target appearance.

3.3 Estimation of subjective value

We used Maximum Likelihood Difference Scaling (MLDS) (Maloney and Yang, 2003; Kingdom and Prins, 2010) to estimate the subjective value of different targets. The algorithm is an optimization algorithm which gives the best estimation of the subjective value and internal noise based on the maximum across-trial. The maximum across-trial likelihood is defined as:

$$LL(\psi(1),\psi(2),...\psi(N),\sigma_d \,|\, r) = \sum_{k=1}^{T} \log_e p(r_k \,|\, D_k;\psi(1),\psi(2),...\psi(N),\sigma_d) \qquad (3.1)$$

where $\psi(i)$ are the subjective value for all the targets, σ_d is the internal noise, r_k is the response (chosen:1 or non-chosen:0) on the kth trial, and D_k is the estimated subjective value difference between two targets in the kth trial given the set of subjective value and internal noise, r the full set of responses across all trials and T the number of trials. We performed the MLDS using Matlab based toolbox "Palamedes " developed by Prins and Kindom (Prins and Kingdom, 2009).

3.4 Electrophysiology recording

3.4.1 Single unit recording

After training, we placed a hexagon chamber (29 mm in diameter) centered over the midline, 28 mm (monkey A) and 27 mm (monkey I) anterior of the interaural line. . Then after a minimum six week healing period, we performed a craniotomy within this

chamber under ketamine anesthesia. The site of the craniotomy was cleaned daily with sterile saline (0.9% sodium chloride), Betadine Solution (10% povidine iodine), and Nolvasan (0.5% chlorhexidine gluconate). When recording within the opened region was complete, the craniotomy was enlarged to expose a new area for sampling. After each recording session, the craniotomy and surrounding area were thoroughly cleaned, the recording chamber was filled with sterile saline, and a titanium cover was screwed onto the chamber in order to keep the area clean and isolated from the external environment.

During each recording session, single units were recorded using 1-4 tungsten microelectrodes with an impedance of 2-4 MΩs (Frederick Haer, Bowdoinham, ME). The microelectrodes were advanced using a self-built microdrive system. .A hexagonal chamber system enabled us to position the electrode over the brain within a grid framework of 0.25 mm spacing.

Data were collected using the PLEXON system. Up to four template spikes were identified using principal component analysis and the time stamps and local field potential were then collected at a sampling rate of 1,000 Hz. Data were subsequently analyzed off-line to ensure only single units were included in consequent analyses.

3.4.2 Cortical location

To determine the location of the SEF, we obtained magnetic resonance images (MRI) for monkey A and monkey I. A three-dimensional (3-D) model of the brain was constructed using MIPAV (BIRSS, NIH). As an anatomical landmark, we used the location of the branch of the arcuate sulcus. The locations of neuronal recording sites are shown in (Figure 3.2). In monkey A, we found neurons during the saccade preparation

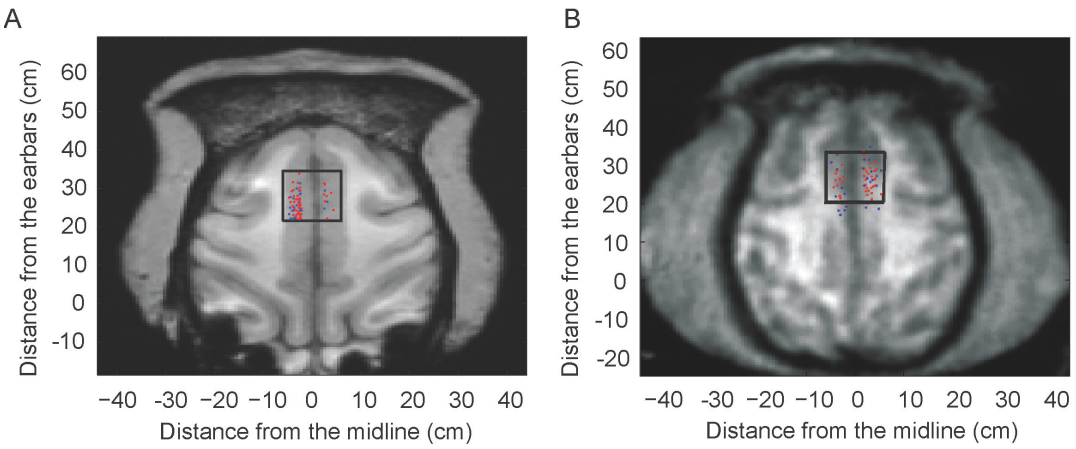

Figure 3.2 Recording locations in SEF. Red dots indicate the locations in which neurons showed task related activity before saccade onset. Blue dots indicate the locations in which neurons were not modulated by task before saccade onset. Black squares indicate the position of the cooling plate. A: Recording sites in monkey A. B: Recording sites in monkey I.

period in the region from 0 to 11 mm anterior to the genu of the arcuate branch and within 5 mm to 2mm of the longitudinal fissure (Figure 3.2A). We designated these neurons as belonging to the SEF, consistant with previous studies from our lab and existing literature (Tehovnik et al., 2000; So and Stuphorn, 2011). In monkey I, neurons from 0 to 11 mm anterior to the genu of the arcuate branch and within 5 mm to 2mm of the longitudinal fissure formed a cluster of neurons with saccade-related activity and were designated as belonging to the SEF (Figure 3.2B).

3.5 Neurophysiology data analysis

3.5.1 Spike density functions

To represent neural activity as a continuous function, we calculated spike density functions by convolving the spike train with a growth-decay exponential function that resembled a post-synaptic potential. Each spike therefore exerts influence only forward in time. The equation describes rate (R) as a function of time (t):

$$R(t) = (1 - exp(-t/\tau_g)) \cdot exp(-t/\tau_d) \quad (3.2)$$

, where τ_g is the time constant for the growth phase of the potential, and τ_d, is the time constant for the decay phase. Based on physiological data from excitatory synapses, we used 1 ms for the value of τ_g and 20 ms for the value of τ_d(Sayer et al., 1990).

3.5.2 Task-related neurons

We used several criterions to determine whether neurons were task related. To test whether a neuron was active while the monkey generated saccades to the targets, we analyzed the neuronal activity in the time period between target onset to saccade

initiation. We performed a t-test on the spike rate in 50 ms intervals throughout the saccade preparation time period (150 ms to 0 ms before saccade onset or 50ms to 200 ms after target onset) to compare against the baseline period (200 ms to 150ms prior to target onset). If p value were ≤ 0.05 for any of the intervals, the cell was deemed to have activity significantly different form baseline.

Furthermore, we used a more stringent way to define the task related neuron by fitting a family of regression models to the neuronal activity and determining the best-fitting model (So and Stuphorn, 2011).

The influence of value (V) on neuronal activity was described using a sigmoid function

$$f(V) = \frac{b_1}{1+e^{-s(V-t)}} \tag{3.3}$$

where b_1 is the weight coefficient, s ($s \in (0,1)$) is the steepness, and t ($t \in (0,1)$)is the threshold value.

The influence of saccade direction (D) on neuronal activity was described using a circular Gaussian function

$$g(D) = b_2 \times e^{\{w \times [\cos(D-p)]^{-1}\}} \tag{3.4}$$

where $b_2$is the weight coefficient, w ($w \in (0, 4\pi]$)is the turning width, p ($p \in [0,2\pi]$) is the preferred direction of the neuron.

The interaction of value and direction was described using the product of $f(V)$ and $g(D)$

$$h(V,D) = f(V) \times g(D) = b_3 \times \frac{1}{1+e^{-s(V-t)}} \times e^{\{w \times [\cos(D-p)]^{-1}\}} \quad (3.5)$$

where b_3 is the weight coefficient.

For each neuron, we fitted the average neuronal activity before saccade (50ms before saccade onset to 20 ms after saccade onset) on each no-choice trial with all possible linear combinations of the three terms $f(V)$, $g(D)$, $h(V,D)$ as well as with a simple constant model (b_0) . We identified the best fitting model for each neuron by finding the model with the minimum Bayesian information criterion (Burnham and Anderson, 2002; Busemeyer and Diederich, 2010)

$$BIC = n \times \log(\frac{RSS}{n}) + k \times \log(n) \quad (3.6)$$

where n is the number of trials (a constant in our case), and RSS the residual sum of squares after fitting. We used a loosely defined BIC in order to include more neurons into analysis, where k is the number of independent variables in the equation. A lower numerical BIC value indicates better fit of a model, with a lower residual sum of squares indicating better predictive power, and a larger k penalizes less parsimonious models. All neurons with lower BIC value than the baseline model were considered stringently task related and were included in the following chapters.

Chapter 4

Competition between Choice Options

After the animal training as described in the previous chapter, we did recording in SEF to look at the correlation between neuronal activity and monkeys' choice behavior. In this chapter, we will discuss in detail whether and how the action value signals for both choice options compete with each other, and contribute to the decision process.

4.1 Specific Methods

4.1.1 Population analysis

The normalized time-direction maps for population analysis were generated from the neuronal activity in no-choice trial and in choice trial when two options were 180° apart. The colors indicate the magnitude of firing rate which was normalized by setting the baseline activity (mean activity between 50 to 0 before target onset for all trials) as 0 and maximum activity (the maximum mean activity across all the trial type) as 1. For each cell, we first estimated its preferred direction by fitting the directional tuning with circular Gaussian term as described in BIC analysis (section **3.4.2**). After that, we calculated the relative angular distance between its preferred direction and the target

location for every trial. We then sorted the relative angular distance from small to large and rotated the matrix to let the chosen target position to always be 90° (except the analysis of the error trial in which we let the larger value targets instead of the chosen target to be in 90°). By doing this, we could average across all the trials since the target position is always the same. Population data were finally displayed as 2D pseudo-color plot, with each horizontal row representing the location of the selected target with respect to each cell's preferred direction (interpolated at an angle of 7.2°) and each column representing the target with respect to either target onset or movement onset.

4.1.2 Leaky integrator model

A mean-rate leaky-integrator neuronal model with two layers of 200 neurons each was implemented as a dynamical system describing the neuronal activity in SEF. In this model, the first layer is an input layer, which receives action value input for different target options VD_j and send the activity to the second layer through a feed forward network. The second layer is an decision layer where the each neuron is activated not only by the output from the first layer but also by the direction information of the target as described by D_i. Each neuron in the decision layer is governed by the following non-linear differential equation:

$$\frac{dX_i}{dt} = f(E_i - I_i + \Theta - \alpha(X_i)) \tag{4.1}$$

where E_i is the excitory input into the decision layer:

$$E_i = D_i + \sum_j w_{ij} \cdot VD_j \tag{4.2}$$

and I_i is the inhibitory input from the first layer:

$$I_i = \sum_j v_{ij} \cdot X_j + \beta \sum_j D_j \quad (4.3)$$

The first term in the function describes the mutual inhibition between different neurons, and the second term describes the global inhibition or activation from the first layer to the second layer. In function 4.1, α is a decay rate and α is the Gaussian noise. f is a sigmoid transfer function, which implements the quenching dynamics. This transfer function contains a faster than linear portion for large value of x. It allows the neuron to exert more inhibition to other neurons when its activity gets large while reduce the neuron's sensitivity to noisy input.

4.2 Results

4.2.1 Subjects' choice behavior in the gamble task

As discussed in Chapter 3 (section **3.2**), two monkeys (A and I) were trained to perform a gambling task (Figure 3.1), in which they chose between two different gamble options with different maximum reward and reward probability. The maximum and minimum amounts of reward they can get were indicated by the color of the target. The portion of a color within the target corresponded to the probability of receiving the reward amount. We used the Maximum Likelihood Difference Scaling to estimate the subjective value for each targets based on the choice probability of the monkeys for all combinations of options (section **3.3**). The subjective value of the targets increased as the expected value of the target increased (Figure 4.1A), since both animals chose the targets more often as their expected amount of reward increased. However, two monkeys showed different risk attitude. While, monkey I was always risk seeking, Monkey A was risk seeking when the reward probability was low and maximum reward was high and

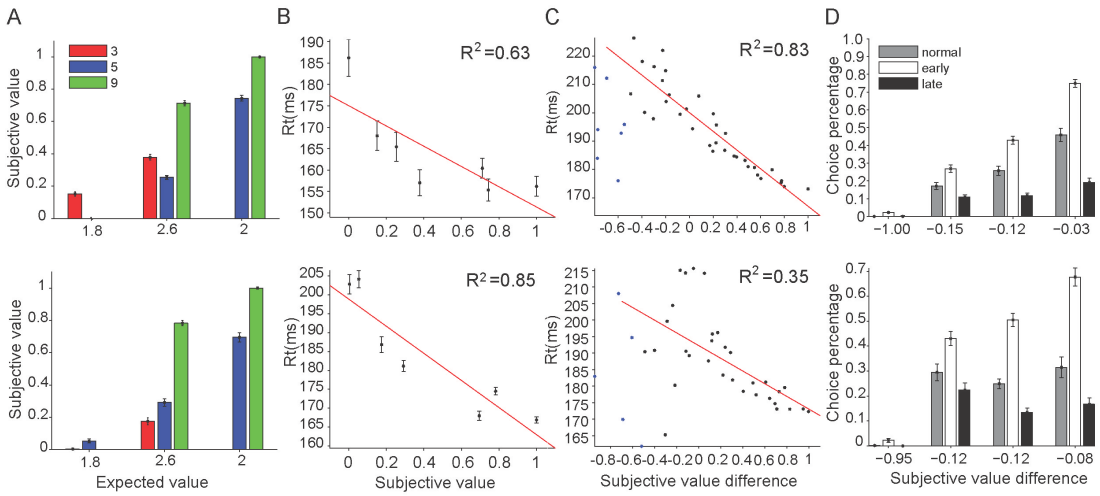

Figure 4.1 Behavior results for monkeys A (top) and monkey I (bottom). A: The mean subjective value of the 7 gamble options is plotted as a function of expected value. Different colors indicate different amounts of maximum reward. B: The mean reaction times in no-choice trial as a function of subjective value. C: The mean reaction times in choice trial as a function of subjective value differences. D: The influence of onset time on choice probability.

risk aversive when the reward probability was high and maximum reward was low. The value referred in following analysis is the subjective value rather than the expected value.

Consistent with the human study as described in chapter 2, the mean saccade reaction times during no-choice trials were significantly negatively correlated with subjective value of the target (Figure 4.1B, monkey B: $p=0.03$ and monkey I: $p=0.003$, respectively). On the two choice trials, the reaction times were significantly correlated with the subjective value difference between the two targets (Figure 4.1C, monkey B: $p<10^{-14}$ and monkey I: $p<10^{-4}$, respectively). On the onset difference trial (Figure 4.1D), the probabilities of both monkeys choosing the early onset target were larger than normal condition, while the probability of them choosing the late onset target was smaller than normal condition. The effect of onset difference was larger as the subjective value difference between two targets was larger.

4.2.2 Non-divisive normalized firing pattern in SEF

To understand the neuronal mechanisms underlying the choice behavior, we collected 516 neurons in SEF (290 from monkey A, 187 from monkey I, Figure 3.2). Of these, 362 neurons (70.16%) showed significant activities (t-test, $p<0.05$) during the saccade preparation period (210 from monkey B, 152 from monkey A). 128 neurons form 362 neurons (35.36%) were considered as stringently task related by BIC criteria and were used in the following analysis (see Methods).

Comparing choice and no-choice trial, SEF neurons either increased (Figure 4.2A) or decreased (Figure 4.2B) their activity when adding the second target in the choice trial. Over all, compared with the no-choice trial, the mean activity for the preferred direction

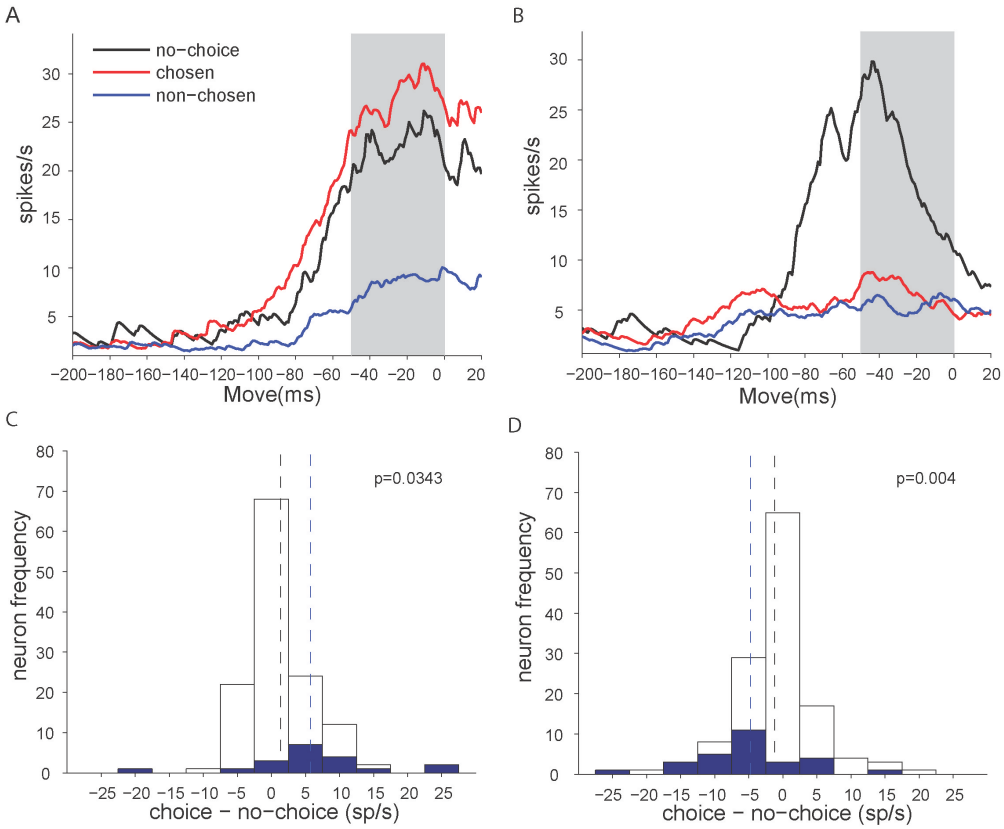

Figure 4.2 Comparison of neuronal activity in choice and no-choice trials. A: A representative neuron which shows higher activity when the target in the receptive field was chosen and lower activity when it was non-chosen comparing to that in the no-choice trial. Shaded areas show the time period (50 ms before movement onset) used for the statistic test. B: A representative neuron which shows lower activity in choice trial than in no-choice trial. C: Distribution of activity differences between the choice trail when the target in receptive field was chosen and the no-choice trial. D: Distribution of activity difference between the choice trial when the target was not chosen and the no-choice trial.

was significantly larger in choice trial when the target was chosen (Wilcoxon signed-rank test, p=0.03; mean difference: 1.38 spike/second for all neurons and 6.38 spike/second for the significant different ones, Figure 4.2C). Meanwhile, the mean activity for the preferred direction was significantly reduced in choice trial than in no-choice trial when the target was not chosen (Figure 4.2D; Wilcoxon signed-rank test, $p<10^{-3}$; mean difference: -1.43 spike/second for all neurons and -4.73 spike/second for the significant different ones). It is worthwhile to note that, in order to have a fair comparison, we controlled the value of chosen target, value of non-chosen target in choice trial and value of the chosen target in no-choice trial to be the same. Therefore, the difference shown here cannot be explained by the average value difference between the chosen targets and non-chosen targets.

That this neuronal activity pattern in SEF is very different from the divisive normalization effect. Under such condition as divisive normalization, the neurons always show less activity when the number of options increase. Here, in the presence of an attractor/non-chosen target, the neuronal activity for the chosen targets was stronger than the activity in the no-choice trial.

4.2.3 Competition between value of the choice options

In order to visualize the competition between chosen and non-chosen value, we systematically varied either the chosen value or the non-chosen value while maintain the other to be the same. Figure 4.3 shows a representative SEF neuron. The neuronal activity was grouped by whether saccade was directed towards (preferred direction trials, PD trials) or opposite (non-preferred direction trials, NPD trials) to the preferred direction of the neuron. In the no-choice trials (Figure 4.3A), the neuron was modulated

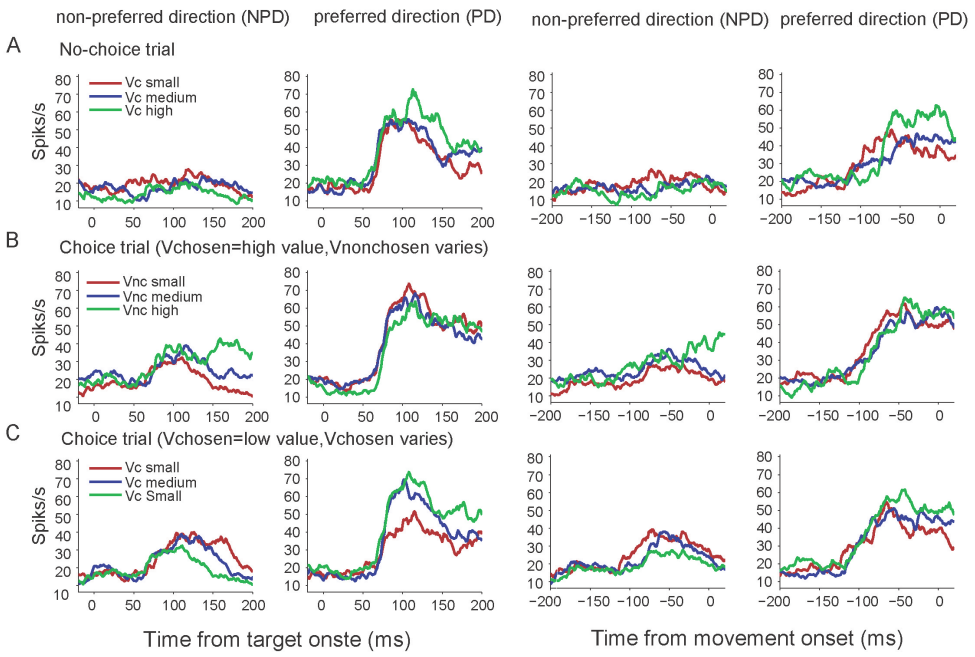

Figure 4.3 An representative neuron showing different degrees of chosen and non-chosen values aligning on target onset (left) and movement onset (right). A: The neuronal activity in the no-choice trial. Colors indicate the chosen value. B: The neuronal activity in the choice trial when the chosen value was controlled. Colors indicate the non-chosen value of the choice. C: The neuronal activity in the choice trial when the non-chosen value was controlled. Colors indicate the chosen value of the choice.

by the chosen value of the targets in PD trials but was not activated by targets in NPD trials. Contrasting with the choice trials (Figure 4.3A, B), this neuron showed increased activity in both PD trials and NPD trials, and its activity was modulated by both chosen value and non-chosen value. Since each neuron represented the target information within its receptive field, the activity in PD trials then represented the activity to the target in receptive field which had been chosen, while the activity in the NPD trials represented the activity of the target in the receptive which was not chosen.

Figure 4.3B shows the effect of non-chosen value on neuronal activity. In the figure, the chosen value was controlled to be the highest amount while the non-chosen value was grouped into high, medium and small. As in the figure, the neuronal activity in the NPD trials which represent the activity for the non-chosen target was positively correlated with the value of non-chosen target. Meanwhile, the neuronal activity in PD trials, which represent the neuronal activity for the chosen target, was also modulated by the non-chosen value in a negative way especially when aligned on the target onset. The smaller the non-chosen value was, the earlier the neuronal activity for the chosen target peaked. Figure 4.3 C shows the effect of chosen value on neuronal activity in the choice trial. When controlling the non-chosen value to be lowest, the neuronal activity in PD trials for the chosen target was strongly positively correlated with the chosen value, while neuronal activity for the non-chosen target was negatively correlated with the chosen value in the NPD trials. This negative correlation was led by the inhibition from the chosen target to the non-chosen target, while the negative correlation in Figure 4.3 B PD trials was led by the inhibition from the non-chosen target to the chosen target. In summary, the results suggest that both chosen value and non-chosen value contributed to

the neuronal activity in SEF. The neuronal activity was positively contributed by the target in its receptive field, and was inhibited by the targets outside of its receptive field. More importantly, the contribution of chosen value and non-chosen value is asymmetric. The chosen value had larger effect in terms of both activation and inhibition than the non-chosen target. This effect is closely linked with the competition process between the two options, and will be quantified and discussed further in Chapter 5.

Figure 4.4 shows the neuronal population activity in no-choice trials and choice trials averaging across all 128 task related neurons. The mean average across all the neurons shows similar pattern of neuronal activity as comparing to the representative neuron. It suggests that the competition in the value space is a general phenomenon in SEF rather than occurring only in several representative neurons.

4.2.4 Competition between direction of the choice options

In order to visualize the competition between different direction combinations, we also systematically varied the non-chosen direction while maintain the chosen direction to be the same. Figure 4.5A shows the representative neuronal activity. The neuronal activity for both preferred direction and non-preferred direction was the strongest when the non-chosen targets were in the contra-lateral hemisphere 180° away (light grey line); was medium when the non-chosen targets were in the contralateral hemisphere 90° away (grey line); and was lowest when the chosen targets were in the ipsilateral hemisphere and 90° away. Although this result is less consistent across population as the effect of target value, considering that the directional effect always confounds with the width of the receptive field of different neurons (Figure 4.5B). However, the mean activity across all the neurons demonstrated the same trend. This result suggests the mutual inhibition is

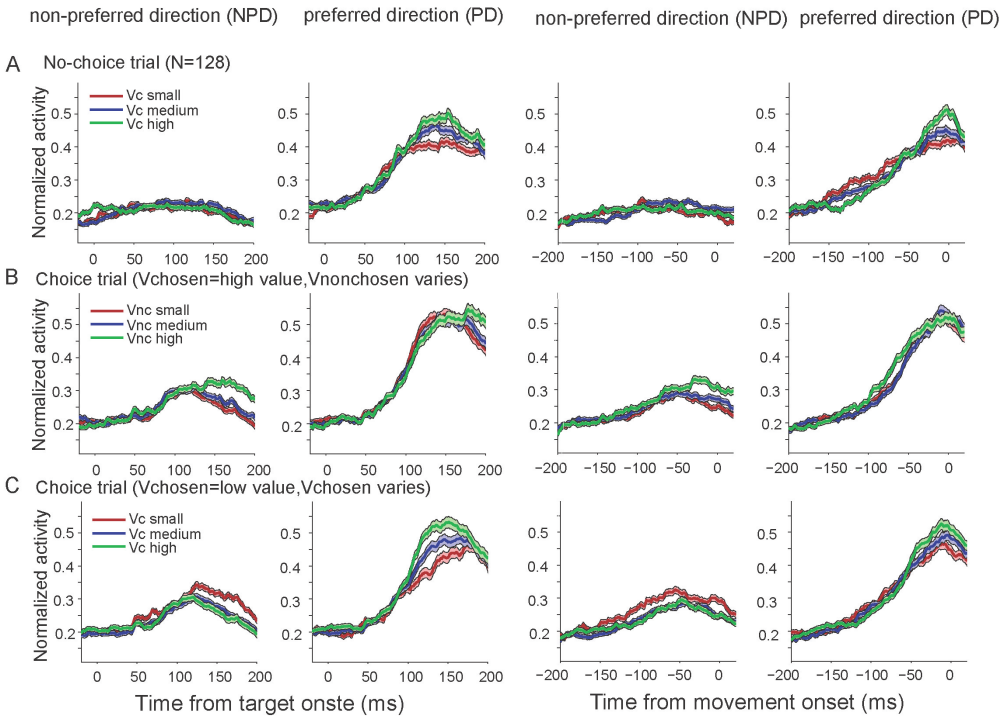

Figure 4.4 Average neuronal activity across 128 neurons representing different degrees of chosen and non-chosen values. Conversion is the same as Figure 4.3.

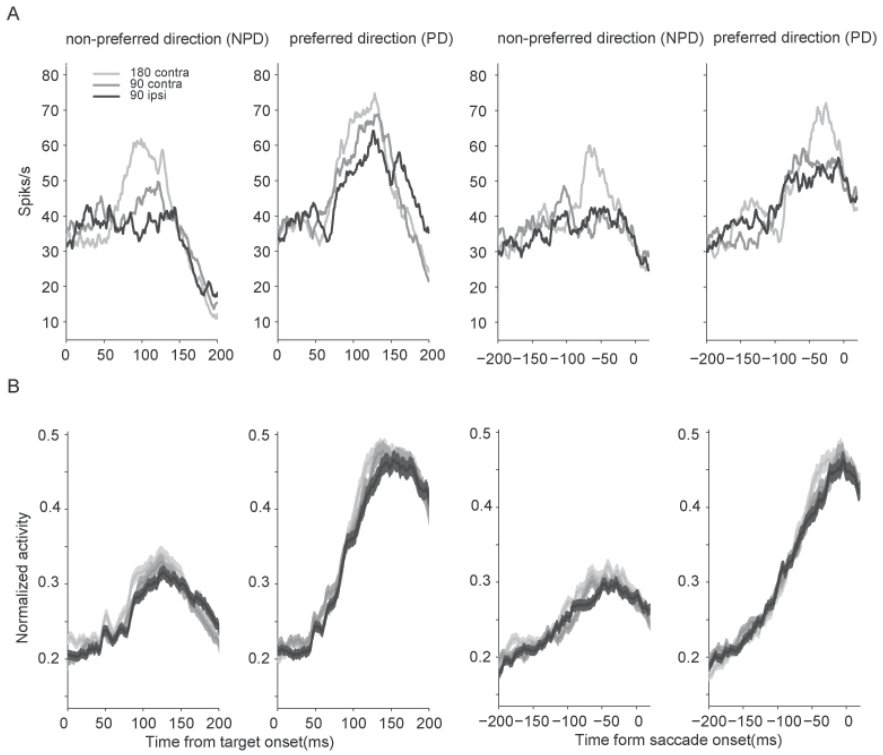

Figure 4.5 Directional effect. SEF neuronal activity is modulated by the angular position between two targets. The darkness of the line indicate different direction combination: when two targets were 180° apart in the different hemisphere (light grey), when two targets were 90° apart in the different hemisphere (medium grey), and when two targets were 90° apart in the same hemisphere of visual field (black). A: A representative neuron. B: Mean average across 128 neurons. The shade indicates the standard error.

the weakest when the targets were 180 degrees away, and strongest when the targets were90 degrees away in the same hemisphere. Overall, the results suggest that there is mutual competition not only between the value representation, but it also occurs between the directional representation. In another words, in addition to the value information competing with each other, the direction information was also in competition with each other. Second, the mutual inhibition between neurons has certain directional tuning. The further the targets are apart the less inhibition between targets. This result is very important since it helps in determining the turning function of mutual inhibition for the simulation (section 4.2.7).

4.2.5 The competition between two options in action value map in SEF

We next looked at the population activity for all 128 neurons using time-direction maps to investigate the temporal dynamics of neuronal activity for each neuron during the decision process. In the map, we sorted the neurons according to their preferred direction from 0° to 360°(see section 4.1.1). The colors indicate the strength of the normalized activity. Assuming that each neuron represented the action value of saccades directed towards its preferred direction, the whole activity distribution across the entire distribution encodes the combined estimation of the relative value of various saccades that the monkey can make. Each vertical line in the map represented the state of this activity distribution in the action value map at one moment in time. In our experiment, since all targets were presented with the same distance from the center of the screen, we then can presume that our spatial map here is one-dimensional (direction). Thus, the time-direction map represented the development of action value-related activity over the course of decision-making SEF.

The map to the left (Figure 4.6A) shows the simple no-choice case with one target presented. In response to the target presentation, activity in a broad set of neurons increased. Activity centered on the target direction reached a maximum around the time of saccade initiation. The map to the right shows the more complex case in which two targets were presented. Compared with the time-direction map in the no-choice case, there are several differences. First, activity started to rise in two parts of the map. One was centered on the target that would be chosen, while the other one was centered on the non-chosen target. The initial rise in activity relative to saccade onset started earlier when aligned on movement onset, in keeping with the fact that reaction times were longer when the monkey had to choose between two response options. At the beginning, the activity associated with both possible targets was of similar strength, but around 50 ms before saccade onset, a difference developed between these two different groups of cells. The activity centered on the chosen target became much stronger than the one centered on the non-chosen target and increased until saccade onset.

Figure4.7 further compares the competition between two targets when the value difference between them differed. The chosen value in both conditions was controlled to be the same, while the non-chosen value differed. Comparing between two time-direction maps, the neuronal activity for the non-chosen target was stronger and lasted longer in the small value difference trials than the large value difference trials. The stronger neuronal activity for the non-chosen target was due to the larger non-chosen value in the small value difference trial, and the longer lasting activity was because of the weaker competition. The long lasting activity in the small value difference trial was consistent with the behavior results of longer reaction time for the smaller value difference trial

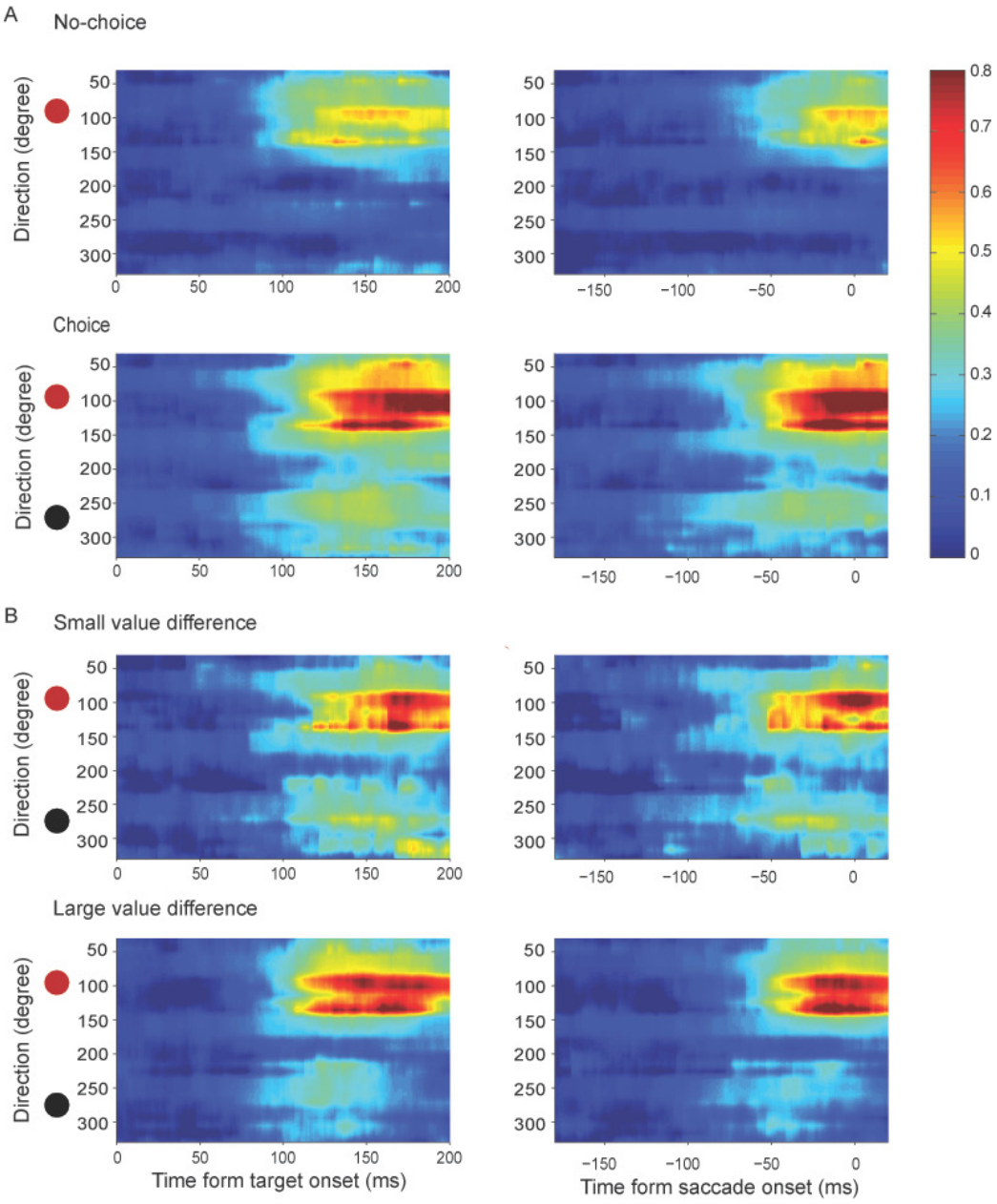

Figure 4.6 Time-direction maps showing population activity in SEF. A: Time-direction maps for population activity in SEF in no-choice (one-target , up row) and choice (two target, bottom row) aligning on both target onset (left) and saccade onset (right). Each horizontal row within the plot represents the average activity of cells with preferred direction located at the corresponding direction on direction axis. Colors indicate the average change in firing rate relative to the background firing rate. Red circles indicate the position for the chosen targets and the black circles indicate the position for the non-chosen targets. B: Comparison between the large value difference trial and small value difference trial.

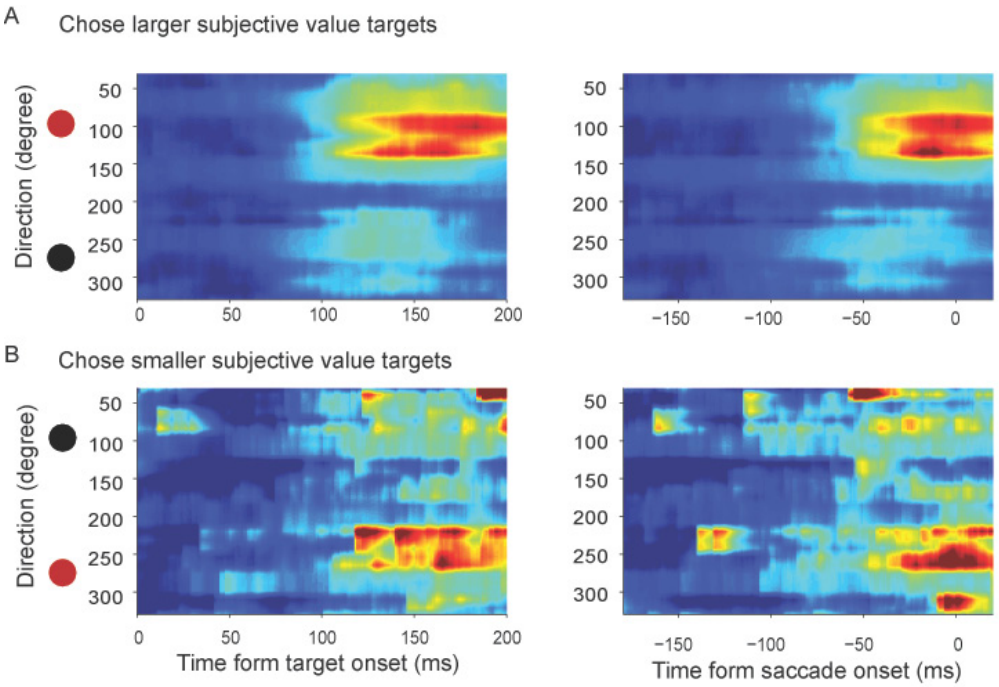

Figure 4.7 Time-direction maps for comparison between correct and error trials. Up row shows the neuronal activity in correct trials. The red circle indicates the position for the chosen targets, which were the higher value targets. And the black circle indicates the position for the non-chosen targets, which were the lower value targets. Bottom row shows the activity in error trials. The red circle indicates the position for the chosen targets, which were the lower value targets, and the black circle indicates the position for the non-chosen targets, which were the higher value targets.

(Figure 4.1C). Moreover, the activity for the chosen target was also weaker in the small value difference trial especially early in the time period (100-150 ms after target onset). These results deliberate the competition between neuronal representations of the two targets in a large population of SEF neurons.

However, it is still unclear that whether the neuronal activity here represents the average subjective value which was retrieved each time during the decision process, or the trial by trial subjective value used for decision. In order to answer this question, we also compared the neuronal activity in the trials when the monkeys chose the large subjective value target and small subjective value target (Figure 4.7). In the trial when the monkeys chose the larger value target, the time-direction map is similar to the choice case (left figure). However, when the monkeys chose smaller value target, the neurons activity for the chosen target also increased its firing rate in regardless of the chosen target is a low value target. Therefore, the neuronal activity in SEF is more correlated with choice or trial based subjective value rather than the average subjective value estimated across the recording section (see section 3.2.2).

The analysis so far is more concerned with the competition between value information and/ or competition between directions in a uniform inhibition manner without directional tuning. In order to visualize the mutual inhibition in the action space with directional tuning, similar analysis can also be performed by comparing different direction combinations of the targets. Unfortunately, only a subset of neurons was tested with full direction combination. Therefore, there were not enough neurons with different preferred direction to create the time-direction maps.

Overall, the results suggest that SEF participates or at least represents the competition between two options during the value-based decision process.

4.2.6 The onset manipulation of the competition process

In order to perturb the decision process, we manipulated the onset difference between two targets in a subset of choice trials. As described in section **4.2.1** (Figure 4.1D), behaviorally and comparing to the normal trial, both monkeys were more likely to choose the early onset target while less likely to choose the late onset target. The early onset target showed behavior advantages than the late onset target. Therefore, if the competition did happen in SEF, we would expect to see similar advantages in neuronal activity representing the early onset target relative to those representing the late onset target. This was exactly what we found in the SEF.

Figure 4.8A shows the comparison of a representative neuron's activity in the trials when the monkey picked early onset target (early onset trial) and the trials when the monkey picked late onset target (late onset trial). The color of the spike density function shows whether the chosen target (red) or the non-chosen target (black) was in the receptive field. As shown in the carton on the left of the figures, in the trials when the monkeys chose the early onset trial, the red line indicates the neuronal activity for the chosen target which was the early onset target (as demonstrated in the red block). The black line indicates the neuronal activity in the trial when the non-chosen target which was the late onset target was in the receptive field (as demonstrated in the red block). If assuming the neuronal activity represents the choice option within its receptive field, we could consider the neuronal activity in two trial types act as two counter neurons representing two different choice options in the same trial type. The neuronal activity for

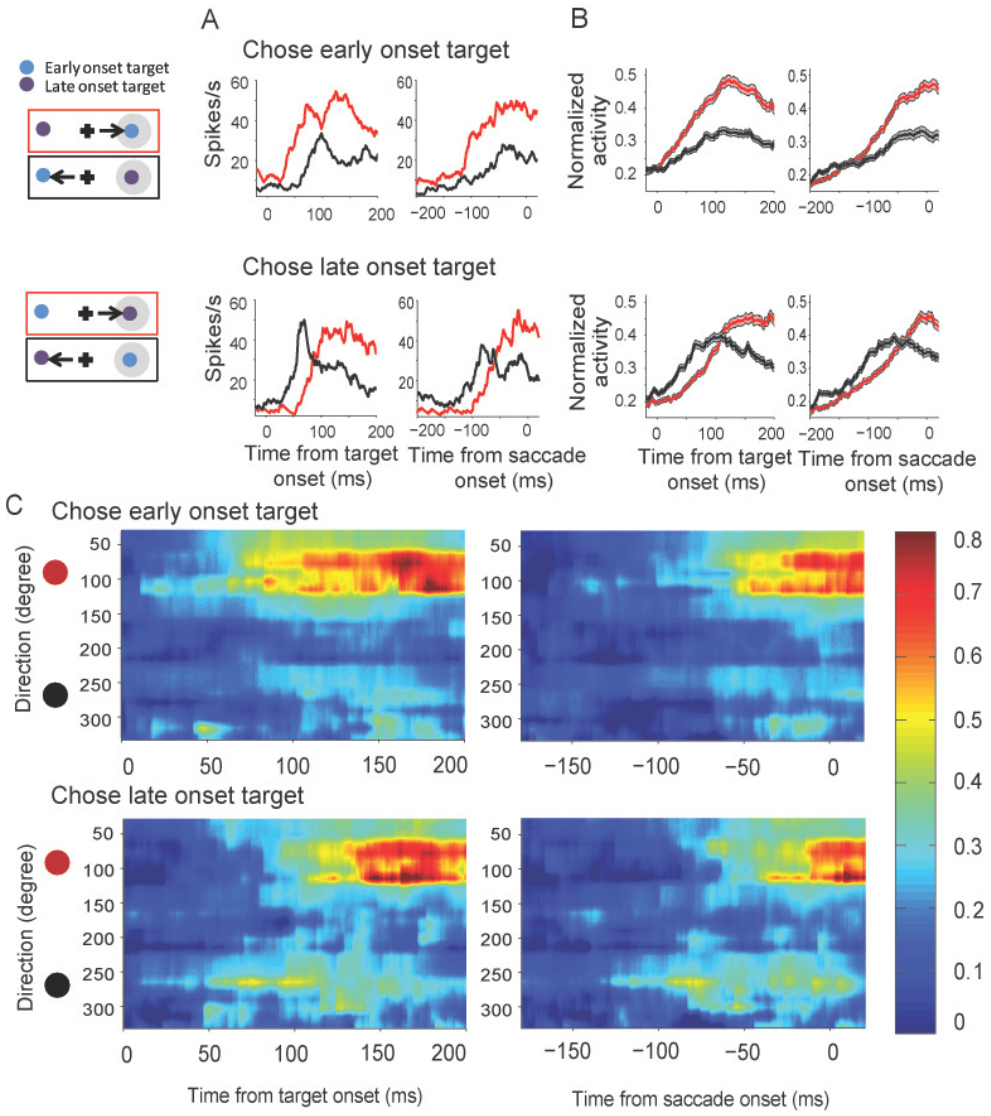

Figure 4.8 SEF activity in onset difference trials. A: A representative neuron. Top row shows the neuronal activity in early onset trial. Red line shows the neuronal activity for the early onset target which was the chosen target. Black line shows the activity to the late onset target which was the non-chosen target. Bottom row shows the activity in late onset trial. Red line shows the activity for the late onset target which was chosen and black line shows the activity to the early onset target which was not chosen. B: The average neuronal activity across all neurons. Symbols are same as A. C: Time-direction map for the onset difference trials. Up row shows the neuronal activity in early onset trial. Bottom row shows the activity in late onset trial.

the early onset target therefore increases at the beginning and then was depressed as the late onset target increases its activity. The neuronal activity for the early onset target later won the competition and the monkey therefore chose the early onset target. Similarly, in the trials when the monkey chose the late onset targets, the red line indicates the neuronal activity for the late onset target and the black line shows the activity for the early onset target. The neuronal activity for the early onset target began to increase early on in the trial, however got depressed as the late onset target increased its firing rate. The neuronal activity for the late onset target continued to increase across time and won the competition for the decision process. The monkey then chose the late onset target. The subplots on the left within each figure show the same comparison but now aligned on the movement onset. They show that all the activity difference between chosen and non-chosen target happen before the saccade onset when the monkey indicate their choice by eye movements.

To visualize the activity for the whole action value map in SEF, we did the population analysis for the onset different trials and formed the time-direction maps for each comparison. As shown in Figure 4.8C, in the trail monkey chose the early onset target, the neurons representing the early onset target activated earlier in time and continued to increase firing till the movement onset if the early onset target was chosen (up row). In contrary, in the trial when monkey chosen the late onset targets, the neuronal activity for the early onset target increased first and then decreased as the activity for the late onset target increased if the late onset target was chosen (bottom row). These results again demonstrate that the competition indeed happened between chosen

and non-chosen targets in a mutual inhibit way. Moreover, we could manipulate this competition or decision process by changing the presenting time of the visual stimulus.

4.2.7 Simulation of neurophysiologic data

To prove what we saw in the neuronal activity represent the mutual inhibition process for competition, we further used a mean-rate leaky-integrator model (Grossberg, 1973; Cisek, 2006) to simulate the competition process. The simulated network contained 200 neurons which were inhibited against each other through lateral inhibition as described in the method. The simulation results exhibited many similar phenomena as shown in the recordings (Figure 4.9): In the no-choice condition, the simulated neurons increased its firing rate as the value of the targets increased. In addition, in the two-choice condition, the simulated firing rate correlated with both chosen and non-chosen values in both preferred and non-preferred direction of the neuron (Figure 4.9A), which is very similar to the real neuronal activity (Figure 4.3 and 4.4). Furthermore, we looked at the activity for the whole simulated population. Similar to the real neurophysiological recording, the simulated time-direction map shows that neurons with the preferred direction near the target direction got activated in the no-choice trial. In the choice-trial, the simulated neurons with preferred directions consistent with both the chosen target direction and non-chosen target direction got activated (Figure 4.9B). In the simulated time-direction map, the activity for both target were equally activated at the early stage. Later on, while the activity for the chosen target increased, the activity for the non-chosen target became gradually depressed. To further look at the competition process, we also did the simulation for small value difference and large value difference trial. As shown in Figure 4.9C, consistent with Figure 4.7, the length of the competition process was

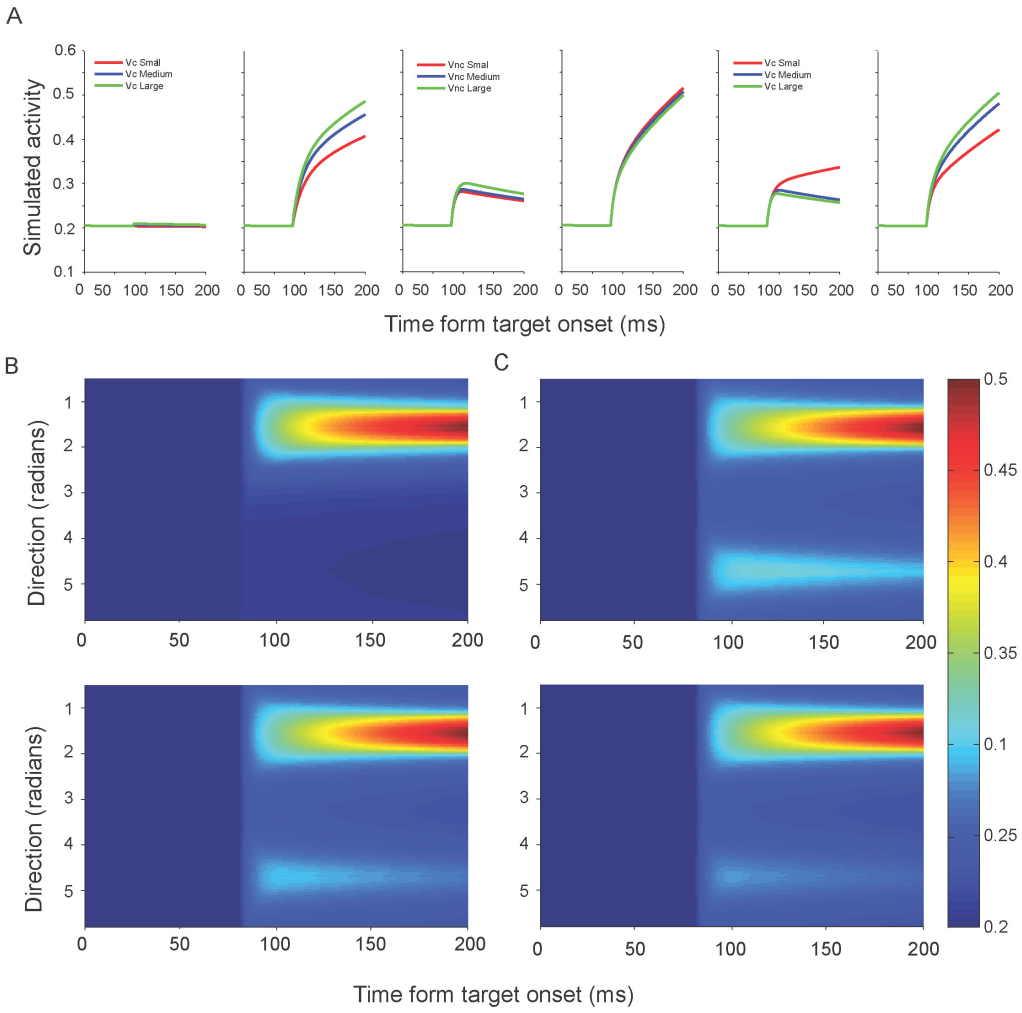

Figure 4.9 Simulation results. A. Simulated neuronal activity in no-choice trial (left two columns), choice trial when controlling chosen value to be the same (middle two columns) or controlling non-chosen value to be the same (left two columns). B. Simulated time-direction maps for no-choice trial (top row) and choice trial (bottom row).Colors indicate the strength of activity. C. Simulated time-direction maps for small value difference trial (top row) and large value difference trial (bottom row).

determined by value difference between two targets. The smaller the value difference was the longer the competition process lasted. The similarity between the simulated results and real recording suggests competition process with mutual inhibition happened in SEF.

4.3 Discussion

4.3.1 Non divisive normalization in SEF

This chapter focuses on describing the competitive process between choice options. We observed a non-divisive normalization pattern of neuronal activity in SEF when comparing the neuronal activity in choice trials with that from the no-choice trials. This result suggests that coding mechanism in SEF is different from many other cortical areas in the sensory systems (Shapley and Victor, 1978; Bonin et al., 2005), the motor systems (Basso and Wurtz, 1998), and higher order processes such as multisensory integration (Ohshiro et al., 2011), visual attention (Reynolds and Heeger, 2009) or even decision-making (Louie et al., 2011; Louie et al., 2013). The non-divisive normalization may suggest that SEF is functionally important during decision-making process, which frees the cortical area from the general efficient encoding mechanism of information in the cortical maps (Louie et al., 2013). This non-devisive normalization pattern may contribute to better signal to noise ratio for neuronal coding during the decision-making process, and preserve the chosen value information in a "transitive" way.

4.3.2 Competition between two choice options in SEF

Action-value signal is of central importance in selecting an appropriate action during value base decision-making (Rangel et al., 2008; Kable and Glimcher, 2009). It links value representation to action representation. Action-value signal have been

reported in DLPF (Kobayashi et al., 2002; Kennerley and Wallis, 2009), SEF (Wunderlich et al., 2009, So and Stuphorn, 2010) and caudate (Lau and Glimcher, 2008). However the action value in different cortical area may serve different functions during value based decision process. Whether and how the action value signal in SEF dynamically contributes to the value based decision process is still unknown.

The results from this chapter suggest that action value in SEF represents the competition between two options in a mutual inhibition way. To visualize the competition in value representation and direction representation separately, we looked at the value competition and direction competition by controlling either value or direction of one target to be constant, and let the value or direction of the other target varies. We found that not only did the value representation of the targets exhibit mutual inhibition on each other, the directional information also competed with each other in a directional way. Ideally, a rational value based choice should not be influenced by directional information. However consistent with previous research in pre-motor cortex (Pastor-Bernier and Cisek, 2011), we did find the spatial distance between two options exerting an effect on the decision process. Specifically, the mutual inhibition between different neurons has directional tuning. The mutual inhibition is weaker if the distance between the targets is larger. These results suggest that the competition process during decision-making process occurs both in value space and in direction space. Therefore, SEF is less likely to be a path way which is merely modulated by the input value information in the decision-making process. These observations together support the idea that rather than being a downstream motor area which simply is in charge of motor control, SEF participates or at least represents the decision-making process.

The competition processes in both value space and action space will be further quantified in the next chapter. The causal role of SEF rather than correlation will be tested by a series of perturbation experiments which will be described in chapter 6.

Chapter 5

Cascade Process between Value and Direction Representation

After discussing the competition process between two targets in the previous chapter, this chapter will focus on the investigation of the temporal dynamics of the transition process between value information and direction information. We dissociated the competition of value and of direction embedded in the same neuronal activity using different analysis techniques. The results from different methods support the same idea that in SEF, competition between option values occurs earlier than competition between directions in our behavior paradigm.

5.1 Specific Methods

5.1.1 Classification analysis

Binary linear classification was performed using Matlab toolboxes and custom codes. The analysis was performed using neuronal activity 200ms before movement onset till 20ms after neuron onset at 1ms time resolution. For each neuron at given time bin, we

used the neuronal activity in part of the choice trials to train the classifier, and then used the trained classifier to predict either the direction of the chosen target or the value of the chosen target for each trial. Specifically, when predicting the chosen direction, we first determined the two targets' location in a choice trial. We then used the neuronal activity in all choice trials where the monkey chose one of the target locations regardless of the non-chosen location and its value, to train the classifier. This optimized classifier was then used to predict which of the target position was chosen based on the observed neuronal activity in each trial. Similarly when predicting the chosen value, we trained the classifier using the neuronal activity from all chosen trial where the monkey chose one of the target value regardless of the non-chosen value and the direction positions .This trained classifier was then used to predict which target was chosen among the two possible options. We performed the classification for every 1 ms time bin during the trial. The classification accuracy was calculated by averaging across all trials for each neuron. Next, a permutation test which shuffled the chosen and the non-chosen direction or value of all trials for 100 times, was used to test whether the classification accuracy was significant ($p<0.05$). If the classification result is better than the 5^{th} highest classification accuracy in the permutation test, we consider the result to be significant.

5.1.2 Mutual information analysis

In order to compare the relative strength of saccade value and direction, we calculated separately for each neuron the mutual information between neuronal activity and value/direction.

To reduce bias in estimating the mutual information, we discretized the neuronal activities so that each bin could hold equal number of trials. We set the number of bins

for neuronal activity (N_F) as four. The boundaries between the bins were fixed across all time windows. At each particular time window, we collected the mean neuronal firing rates (F) from every trial. Neuronal activity below first quartile (Q_1) was classified as F_1, between Q_1 and Q_2 as F_2, between Q_2 and Q_3 as F_3, and lastly the neuronal activity above Q_3 was classified as F_4.

The mutual information between the neuronal activity F and the variable X, which could be of either value or direction, was by the following:

$$I(F,X)=\left(\sum_{i=1}^{N_F}\sum_{j=1}^{N_X}\frac{M_{ij}}{M}\log\frac{M_{ij}M}{M_{i\cdot}M_{\cdot j}}\right)-Bias \tag{3.4}$$

where M_{ij} was the number of trials having both F_i and X_j ; $M_{i\cdot}$ was the number of trials having F_i; and $M_{\cdot j}$ was the number of trials having X_j. M was the number of total trials. As mentioned before, we set N_F, the number of distinct states of neuronal activity, to four. In the case of direction, we set N_x, the number of distinct states of the relevant variable, to four, because we tested four different saccade directions. For value, we tested 7 different values. However, distinguishing 7 different value levels would have resulted in different maximum amounts of mutual information for the two variables (direction: 2 bits; value: $\leq$ 2.8 bits). This would have led to an overestimation of value information relative to directional information. In order to make the value and direction information estimations directly comparable, we also set N_x for value to be four as well. In grouping the 7 different values into four bins, we followed the same binning procedure as we did for the neuronal activities. So that each bin held approximately equal number of trials. We computed a first approximation of the bias as follows:

$$Bias = \frac{1}{2M \log 2}\left(U_{FX} - U_F - U_X + 1\right) \tag{3.5}$$

where U_{FX} was the number of nonzero M_{ij}'s for all i and j, U_F was the number of nonzero $M_{.i}$ for all i, and U_X was the number of nonzero $M_{i.}$ for all j. This procedure followed the approach described in Ito and Doya (2009).

Finally, we performed a permutation procedure to test whether the amount of mutual information was significant, and to further reduce any remaining bias. We generated a random set of F_i and X_j pairs, by permuting both F and X arrays respectively. We calculated the mutual information between F and X, using the same method described above, and repeated this process for 100 times. The mean of the mutual information obtained from these 100 random processes represented remaining bias and was subtracted from I(F,X). To test whether the final estimated mutual information was significant ($p < 0.05$), we compared it with the 6th highest information obtained from the 100 random processes. If it was non-significant, we set the mutual information to zero. The bias reductions sometimes led to negative estimates of mutual information. In that case, we also set the final estimated information to be zero.

5.1.3 Regression analysis

A linear regression was used to determine the temporal contribution of chosen target and non-chosen target to the neuronal firing rate in choice trials. First, for each neuron, we calculated the mean firing rate on no-choice trials for each direction and chosen values ($\overline{S_{no-chocie}}(V_{chosen}, D_{chosen}, t)$). Then, in the regression analysis, we tested three descriptive models:

$$\text{Model1: } S_{choice}(t) = b_0 \tag{7}$$

$$\text{Model2: } \mathrm{S_{choice}}\ (\mathrm{t}) = \mathrm{b_1}\overline{\mathrm{S_{no-chocie}}}\,(\mathrm{V_{chosen}}\,, \mathrm{D_{chosen}}\,, \mathrm{t}) \tag{8}$$

$$\text{Model3: } S_{choice}(t) = b_1\overline{S_{no-chocie}}\,(V_{chosen}\,, D_{chosen}\,, t)$$

$$+b_2\overline{S_{no-chocie}}\,(V_{nonc\ hosen}\,, D_{nonc\ hosen}\,, t) \tag{9}$$

Model 1 is a simple baseline model, where b_0 is a constant. Model 2 evaluates the contribution of the chosen target to the firing rate. Model 3 evaluates the contribution of both chosen target and non-chosen target to the firing rate based on neuron's firing rate in the no-choice trial. The data were fitted with linear least-squares fitting routine implemented in Matlab (The Math Works, Natick, MA) to minimize the sum of squared deviation between observed and predicted values. BIC was used to determine the best model for each neuron. After the BIC test, a permutation procedure was performed to test whether the coefficient for the chosen and non-chosen target were significant. In the permutation test, neuronal activity was assigned in each trial with permutated chosen value and permutated non-chosen value. The difference between the chosen and non-chosen coefficient was calculated using the same method described above for 1000 times. To compare whether the estimated difference between chosen and non-chosen coefficient was significant, a two-tailed test was used, by comparing it with the 25 highest differences and 25 lowest differences from the 1000 permutation process. The first differential time, onset time, was defined as the first time when the chosen coefficients for all the neurons was significant larger than non-chosen coefficients (t-test).

5.2 Results

5.2.1 Temporal sequence between chosen value and chosen direction

To answer whether there are any temporal differences between the development of chosen value and chosen direction information, we performed a trial by trial analysis using linear classification to decode the monkeys' chosen direction and chosen value from the firing rate with 1 ms temporal resolution. This method allowed us to ask the question of whether and when did one type of chosen target information appear in the neuronal activity and how it develop over time. Figure 5.1A shows the average classification accuracy which was significantly better than random averaging across all 128 task-related neurons (see method). The red line indicates the significant classification accuracy for the chosen value. The black line is for the chosen direction. The results demonstrate that neuronal activity in SEF predict both chosen value and chosen direction better than chance. When aligned with saccade onset, the time point where the activity allowed us to predict chosen value better than random (around 160 ms before saccade onset) was much earlier than the time for predicting saccade direction (around 60 ms before saccade onset). After the early peak for chosen value prediction, the classification accuracy for chosen value gradually decreased while the accuracy of prediction for direction increased over time. Figure 5.1B further explicates the number of neurons showing significant classification accuracy as a function of time. Consistent with the temporal dynamic of the classification accuracy, there was larger proportion of neurons showing significantly better prediction accuracy than random for chosen value than direction early in the trial.

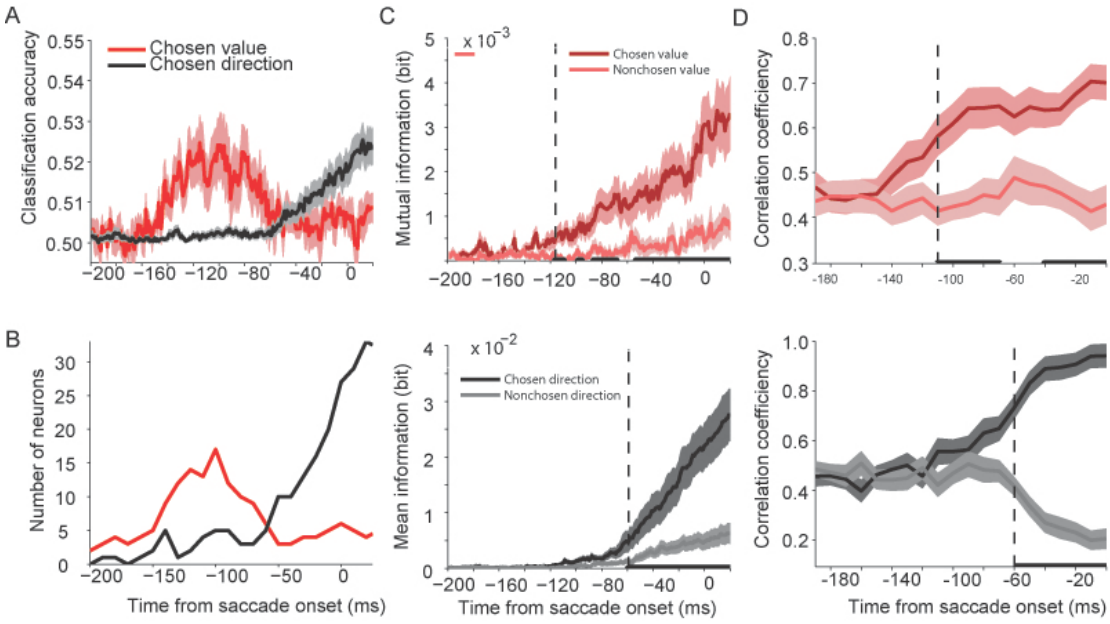

Figure 5.1 Temporal sequence between value and direction information. A: Time course of classification accuracy for both value (red) and direction (black) aligned on and saccade onset. B: The number of neurons showing significant classification for both value and direction. C: Comparison between chosen and non-chosen information for both value (up row) and direction (bottom row). D: Comparison between chosen and non-chosen correlation coefficients in the regression analysis for both value (up row) and direction (bottom row).

The similar analysis can also be done in the high dimension space, in which the neuronal activity for each neuron represents one feature dimension. The trajectory of the population activity, determined by the neurons recorded simultaneously, changed as the neuronal activity developed. Figure 5.2A shows the principle component of the neuronal activity for four different trajectories representing four different chosen directions. Figure 5.2 B shows the mean average of classification results from all the recording assemblies. Consistent with the single neuronal analysis, the decoding result from neuron assembles using support vector machine (SVM) shows similar temporal sequence between value information and direction information. However, the prediction accuracy using the neuronal assembles is much higher than using the single unit, (see figure 5.2B and figure 5.1A).

5.2.2 Mutual value and direction information

The classification results suggest there is temporal difference between the appearance of chosen direction and chosen value information. However, this analysis is more about the temporal difference between the result of competition for value and direction, rather than the dynamic difference between competition process in value space and direction space. Therefore, we also performed mutual information analysis to compare the value and direction information for both chosen and non-chosen targets. We focused on the difference between the chosen and non-chosen information, which is directly correlated with the competition process between chosen and non-chosen options. We used 106 neurons (26 from monkey A and 80 from monkey I) out of the 128 neurons for this analysis. These 106 neurons are those we tested with 8-12 direction combinations in the experiment. For early recording (the other 22 neurons), we only used 4 direction

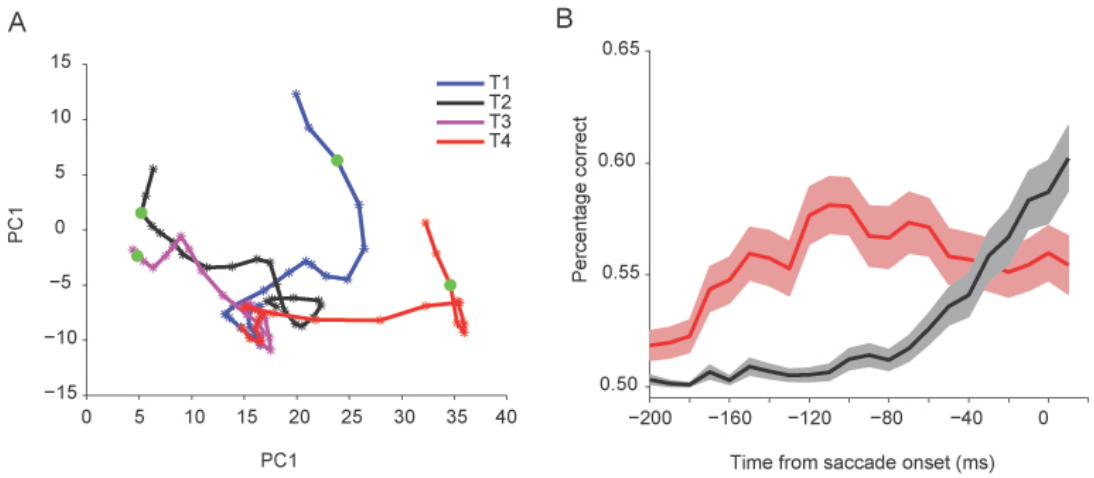

Figure 5.2 Neuronal dynamics within a neuronal state space and results of SVM classifier. A. The activity of the simultaneously recorded neurons defined a 10-dimensional state space. A projection of this state space onto a 2-dimensional subspace is shown. The subspace is defined by the first two principal components (PC1, PC2) explaining variance in the neuronal state vector distribution. The temporal succession of the mean state vector location between target and saccade onset is shown separately for trials in which one of four saccade directions was chosen by the monkey. The mean state vector locations form a trajectory (T1: blue, T2: black, T3: violet, T4: red line). The green dot on the trajectories indicates the moment of saccade initiation. B. SVM analysis of the distribution of state vectors for all combination of saccade directions and value was performed. The percentage of correctly predicted choices based on this analysis is plotted as a function of the time bin during which the state vectors were defined, showing the mean classification accuracy of all recording sections. The shaded color indicates the standard error.

combination, where the two target were exactly opposite to each other. Therefore, the chosen direction and non-chosen direction information for these 22 neurons could be confounded and these neurons were excluded from the analysis.

The mutual information analysis (Figure 5.1 B) shows that, first, value and direction information for both chosen target and non-chosen target were represented in the neuronal activity. Second, the chosen target information was significantly stronger than non-chosen target information later on in the decision process. Third, consistent with the classification analysis, the onset time when chosen value information significantly differed from non-chosen value information (-116 ms before saccade onset) was 57ms earlier than the onset time when different chosen direction information significantly differed from non-chosen direction information (-59 ms). These results suggest that SEF not only represented the result of the competition as quantified by the classification, it also reflected the two choice options and the competition process between them in both value and direction domain. While the chosen direction and value information grew stronger across time, the non-chosen direction and value information gradually decreased.

Note that the result profiles differed between two different analyses. This is possibly because of the different questions asked in each analysis. In the classification analysis, we wanted to know whether we can successfully predict which target the monkey chose (target value or target direction) other than the other target based on the chosen value/direction information embedded in neuronal activity. In the mutual information analysis, we sought to determine which of the four different values (see method) or directions was for either chosen or non-chosen targets. Moreover, the sensitivity to different type of information also differs for different techniques. For

example, for the classification analysis, it has only one decision threshold for binary classification. But the threshold can be placed in the optimal place according to the training sample. This analysis is easier to pick up option value information than action value information. For the information analysis, it divides the data into more parts, However, the way for data division is predetermined (Wallisch et al., 2010), rather than being in the most proper place as in the classification analysis. Therefore, the information analysis can be more sensitive in some cases (such as detecting action value), but less sensitive in other cases (such as detecting option value).

5.3 Competition process in both value representation and direction representation in SEF

We used regression analysis to further quantify the mutual inhibition process between the chosen and non-chosen target. In the analysis, we used the neuronal activity in the no-choice trial with targets of both chosen and non-chosen targets (same value and direction) as the independent variables, and the neuron activity in the choice trial as the dependent variable. Compare with previous literatures (Cai et al., 2011; So and Stuphorn, 2011), this method allows us to estimate the turning of direction and value based on the neuronal activity in no-choice trial rather than assuming the tuning function empirically in the regression analysis. It reduces the chance of incorrectly predetermine the type of turning function, as well as the number of parameters needed to be estimated in the regression model.

Figure 5.1D shows the comparison between the correlation coefficient of both chosen target and non-chosen target for both value and direction. Consistent with

previous results, as the competition continued, the correlation coefficient for the chosen value gradually rise above the average, while the correlation coefficient for the non-chosen value gradually dropped below the average. Although the decrease in correlation coefficient for non-chosen target was less pronounced for value than for direction, the mutual inhibition between the two options is still visible. The regression analysis again confirms that difference between chosen and non-chosen value (-116ms) appear earlier than difference between chosen and non-chosen direction (-59 ms).

5.4 Discussion

This chapter focuses on the temporal difference between the competition in value representation and in direction representation. The classification results demonstrate that the chosen value information appears earlier than the chosen target information in SEF during value based decision-making process. Mutual information analysis and regression analysis further elaborate the competition process between chosen target and non-chosen target by comparing the relative strength for both targets. All together, the results suggest two important aspects as discussed in following.

First, the results suggest that the competition process occurs in both value space and direction space. In chapter 4, we did observe strong mutual competition in value domain and weak competition with directional tuning in direction domain. However even though the competition process can be represented in SEF, it is still possible that the neuronal activity in SEF was merely driven or modulated by the competition process from the input in value space. That is, SEF only serves as a relay point mapping the value information to the corresponding target direction. If this is true, we should observe that both value space and direction space competition occurring simultaneously, or value

space competition occurring earlier but with similar profile as in direction space. However the results showed temporal difference between these two competitions and difference in their profile arguing against this possibility. It is very likely that the competition in the value domain can occur in OFC, vmPFC, or ACC (Padoa-Schioppa, 2011), and then project onto SEF. The neuronal activity in SEF with directional tuning compete with each other, and then biases the competition process in motor domain which can take place in frontal or parietal cortical area or through cortical-basal ganglia loop (Cisek, 2007; Kable and Glimcher, 2009).

Second, these results argue against the action based hypothesis in its pure form (Cisek, 2007, 2012). If the action based hypothesis in its pure form is true, we should see the chosen direction information appearing earlier than the chosen value information since the competition in the action space is the only precursor before choice. However, the results from all three different analyses suggest that the competition in value space occurs earlier than the competition in the action space. Therefore, it is less likely that the competition process only takes place within motor representation.

Based on these results, we suggest a cascade hypothesis of decision-making, in which competitions in both the value space and the direction space take plac. The competition in the value space can bias the competition process in the action space. In our experiment paradigm, the competition in the direction representation was balanced at the beginning after targets were presented, since the information for all the targets were equally strong without value information. As shown in the Figure 5.1D, the regression correlation coefficients for both chosen and non-chosen target increase equally at the beginning of the competition. However, the competition in the value representation was

imbalanced, since the value of different options differed. This imbalanced competition in the value space then led to the generation of chosen value information, and biases the competition process in the action space. The cascade hypothesis will be discussed further in Chapter 7.

Chapter 6

Causal Relation between SEF and Value based Choice Behavior

In the previous two chapters, we have discussed the correlation between SEF neuronal activity and choice behavior exhibited by monkeys. In this chapter, we seek to test if there is causal relation between the neuronal activity and the monkeys' behavior through perturbing SEF using cryogenic deactivation.

6.1 Specific Methods

6.1.1 The cryogenic deactivation

The cooling or cryogenic deactivation technique of cortical area can be traced back to 1960 (Dondey et al., 1962). Cryotips (Skinner and Lindsley, 1968; Zhang et al., 1986), cooling plates (Schiller and Malpeli, 1977; Sandell and Schiller, 1982; Michalski et al., 1993) and cryoloops (Salsbury and Horel, 1983; Lomber et al., 1999; Long and Fee, 2008; Koval et al., 2011) have been used in different cooling experiments. SEF is a surface cortical structure that is relatively large and smooth in area. Therefore, cooling plate is the ideal method for deactivating this cortical area.

Two most common forms of reversible inactivation techniques are pharmacological and cryogenic or cooling. Compared to pharmaco-chemical deactivation, cooling has several advantages (Lomber, 1999). First, cooling can simultaneously deactivate a relatively larger area, which often requires multiple injections to achieve the same effect using chemical deactivation. Second, repeated chemical inactivation of a particular region in brain often results in permanent damage that cannot be reversed. Thirdly, the size of the inactivation locus is easier to replicate between different deactivating agents. Considering these advantages, we employed the cooling technique instead of pharmacology to perturb the activity in SEF.

In this experiment, cooling plates were used to inactivate the SEF bilaterally or unilaterally. The location of SEF was determined by the electrophysiological recording where saccade related activity was recorded (Figure 3.2). The size of the cooling plate is 10mm from anterior to posterior, and 12mm from left to right. For unilateral cooling, in which either left or right hemisphere SEF was cooled, the plate is 10 mm from anterior to posterior and 6mm from medial to lateral. In those experiments, the left or right hemisphere was alternately cooled across experiment sections.

Room temperature methanol was pumped through Teflon tubing that passed through a dry ice bath, in which methanol was reduced to subzero temperature. Chilled methanol was then pumped through a cryoloop. The cryoloop was attached to a stainless steel plate (Figure 6.1A), the surface of which was used to cool down the corresponding

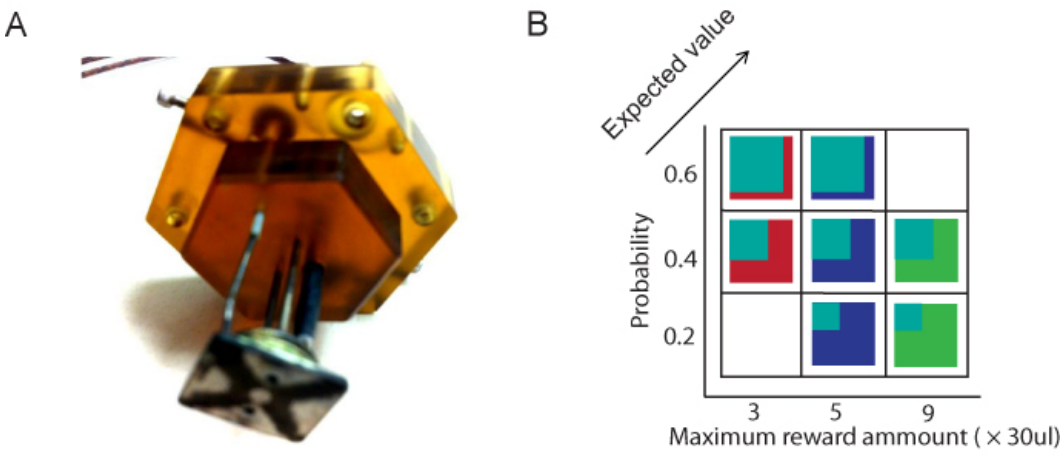

Figure 6.1 The cryogenic deactivation. A: Cooling plate used to deactivate SEF. B: Target set for the new gamble experiment.

cortical area. The methanol was returned to the same reservoir from which it came to form a closed loop. The cortical temperature on the dura was monitored by an attached micro-thermocouple. At the same time, two electrodes were recording simultaneously inboth left and right hemispheres SEF to monitor the neuronal activity. A total of over 30 blocks of data in each section were obtained. During each session, monkeys initially performed the task for 10-15 min in normal state, and then the SEF region was deactivated bilaterally for 10-15 min by pumping chilled methanol through the cryoloop while the task continued. After that, the cortical temperature returned to normal for another 10-15 min as the cooling device was turned off. This whole process was then repeated at least 3 times over 900 trials.

6.1.2 Time frequency analysis

Time-frequency analysis was performed using the matching pursuit (MP) algorithm (Mallat and Zhang, 1993). Matching pursuit has been used previously to analyze LFPs (Ray et al., 2008a; Chen et al., 2010). It is a procedure for computing adaptive signal representations and can eliminate all cross terms of the Wigner distribution of the signal. The Gabor function dictionaries used in MP provide the best time-frequency resolution possible in agreement with the uncertainty principle. The multi-scale decomposition of MP allows sharp transients in the LFP signal to be represented by functions that have narrow temporal support, rather than oscillatory functions with a temporal support of hundreds of milliseconds (such as in Short Time Fourier Transform in time-frequency analysis, multi-tapering for spectrum analysis) (Ray et al., 2008a; Ray et al., 2008b).

The algorithm is an iterative procedure that selects a set of Gabor functions (atoms) from a redundant dictionary of functions that constitute the best possible description of the original signal. Time-frequency plots were then obtained by calculating the Wigner distribution of every atom and taking the weighted sum. All computations were performed using MATLAB (Mathworks, Natick, MA). We performed the MP computation using custom MATLAB scripts and the free software toolbox 'LastWave' [http://www.cmap.polytechnique.fr/~bacry/LastWave/], developed by Emmanuel Bacry.

The LFP signal was sampled at 1 kHz and was analyzed in 900 separate 1 ms time bins. For stimulus-related activity, we examined the LFP signal in the 900 ms time interval starting at 300ms before target onset. For movement related activity, we examined the 900 ms time interval starting at 500 ms before movement onset. Matching pursuit yields a 430×615 array of time-frequency values (with a time resolution of ~1.5 ms, frequency resolution of ~0.35 Hz).

6.1.3 The new target gamble task

In a subset of the inactivation experiment, we performed new gamble experiments using seven different gamble cues which the monkeys had never seen before (Figure 6.1B). This was done to differentiate the cooling effect between the habituate system and the goal-direct system. In those sections, we reversed the position for the maximum reward and the minimum reward, while maintaining the rule in the same way. The colors cyan, red, blue, and green represent 1, 3, 5, and 9 units of water respectively. The percentage of area covered by color indicated the probability to receive the reward.

6.2 Results

6.2.1 Neuronal response to cool temperature: Action potentials

By cooling down the temperature in SEF, we temporarily and reversibly deactivated this cortical area by slowing down its metabolism. Figure 6.2 shows a representative recording in one section. In the experiment, the cooling sections were interleaved with normal temperature sections. The cooling sections lasted around 15-20mins each time. As the cooling device turned on (first row), cortical temperature on the dura above SEF gradually went down within 1-2 minutes. The neuron in both hemisphere (forth row: left hemisphere; fifth row: right hemisphere) decreased their firing rates as the temperature dropped and were almost diminished at around 5°C. Throughout the experiment, the neuronal activity returned to normal level every time after the temperature returned to normal temperature range (37-38 °C). This is despite the fact that reversible deactivation occurred 14 times and lasted around 4 hours. Note that the deactivation of the right hemisphere was weaker than the left hemisphere in this recording section. This is because the recording position in right hemisphere was deeper than that in the left hemisphere. Figure 6.3 summarize the neuronal activity as a function of both the depth of recording position and the temperature above dura. As shown in the figure, neuronal activity always decreased with decreasing temperature or shallow recording position. In all of the behavior analysis, we only included the data when the dura temperature was below 15 Celsius which is considered as the cooling condition. As shown in the figure, at this temperature range, even the neurons in the infra-granular layer reduced their firing rate to approximately 30% of their normal firing rate. Therefore, the majority of the neurons in SEF were inactivated under the cooling condition.

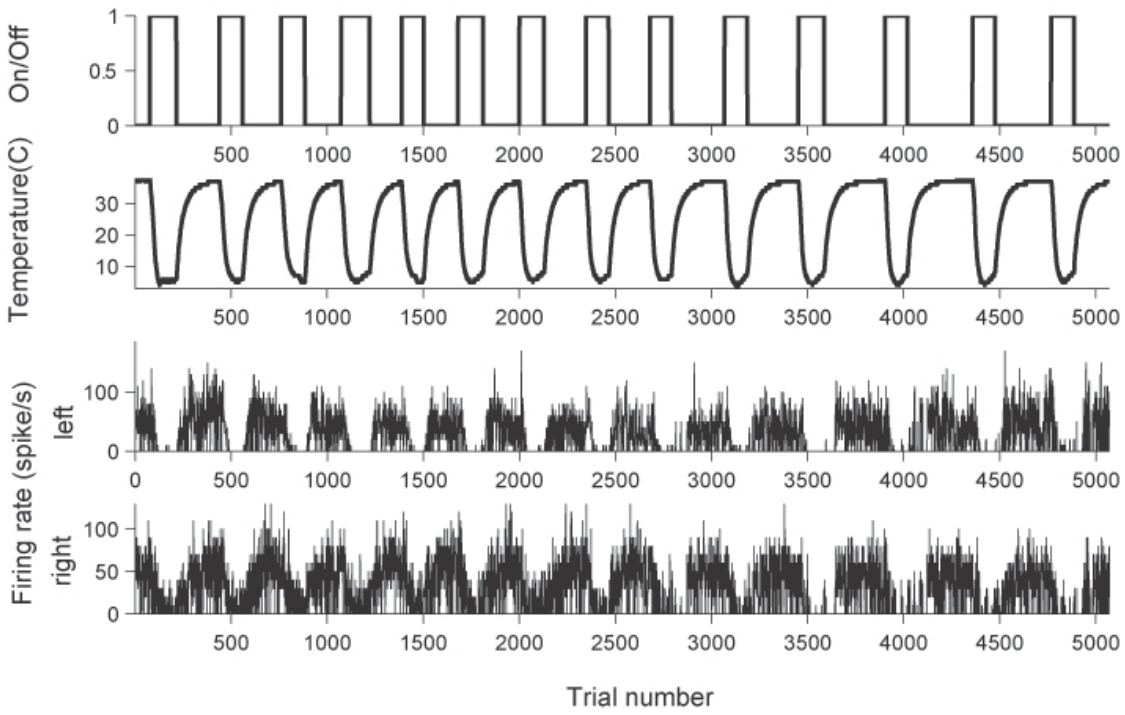

Figure 6.2 A representative cooling section. The first row shows the turning on and off of the cooling device. The second row shows the cortical temperature recorded above durra. The third and forth rows show the neuronal activity recorded simultaneously in both left (third row) and right (forth row) SEF.

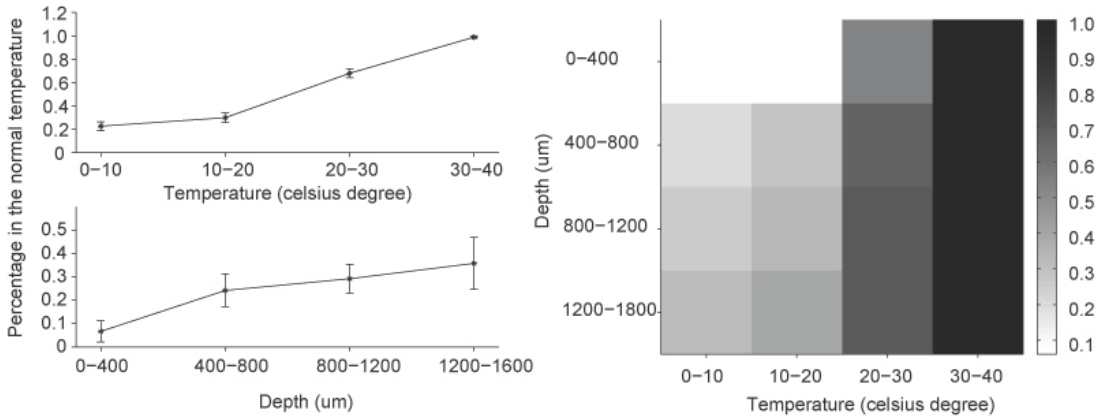

Figure 6.3 Neuronal activity as a function of temperature above the dura and depth of recording. Color in the right plot indicates the strength of the activity compared to the normal temperature condition. The darker the color, the closer the activity is to normal firing.

6.2.2 Neuronal response to cool temperature: Local field potential

In addition to action potential, we also measured the local field potential during cooling situation. Currently the origin of LFP is still under debate. Different literatures have different hypotheses about the local field potential in different frequency band (Buzsaki et al., 2012; Reimann et al., 2013). The cooling technique provides us with an ideal perturbation technique to probe how the energy distribution across different bands will change when the frequency of action potentials is modulated.

Figure 6.4 shows a representative recording. The color maps in both subplots represent the energy distribution of LFP as a function of both time and energy. The black line overlaid indicates the neuronal activity recorded simultaneously. In the normal condition, after target onset, the firing rate increased and peaked around the time before the saccade movements. The cooling condition, in contrary, showed no such pattern in firing rate, and even the baseline firing rate was greatly reduced as shown in figure 6.4B. The energy distribution of LFP, on the other hand, did not show any difference between the two conditions. After the target onset, energy in the gamma and high gamma range began to increase together with the increasing firing rate of action potential. The beta band activity also increased from negative to zero. The fact that cooling had a bigger impact on action potential rather than LFP suggest that the energy distribution of LFP is more related to the synaptic input to the neuron rather than the action potential output. The action potential output is more closely linked to the metabolism of neurons, which can be modulated by temperature.

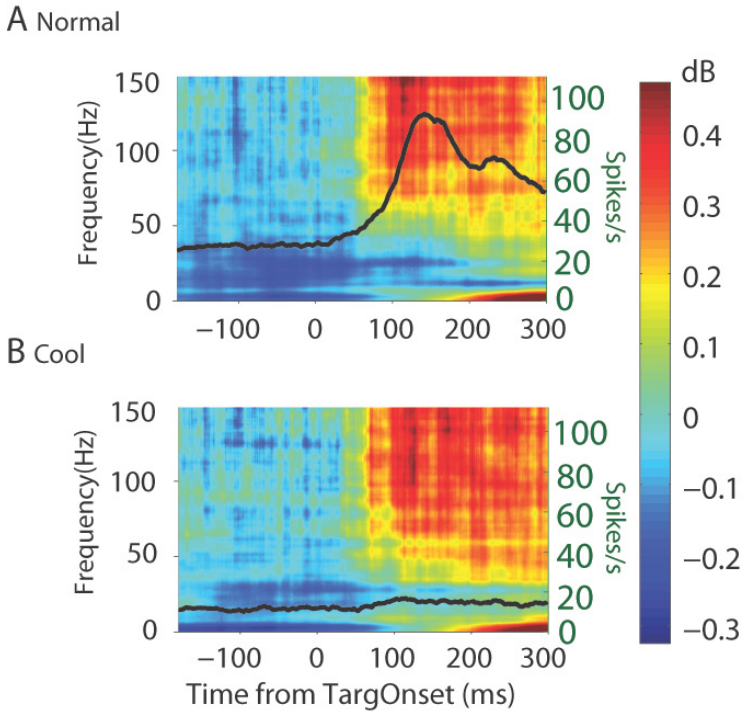

Figure 6.4 Comparison of LFP energy distribution in normal (A) and cooling (B) conditions. The LFP energy distribution was plotted as a function a time and frequency. The overlaid black lines show the multi-unit activity recorded simultaneously.

6.2.3 The effect of SEF deactivation on choice probability

In order to test the causal relation between monkeys' choice and neuronal activity, we further compared monkeys' choice function in cooling situation and normal situation. Figure 6.5 (top row) shows both Monkey A's and Monkey I's choice performances in gamble paradigm when their SEF were bilaterally cooled down in the cooling sections. Comparing the normal condition (blue bars) with the cooling condition (red bars), both monkeys made significantly more mistakes (Monkey A: paired t-test, df=99, p=0.002; Monkey I: paired t-test, df=99, p=0.01) during the cooling sections. The increase of error was largest for intermediate value difference. This is probably due to the fact that there is a ceiling effect for very small value-difference comparisons. Whereas for very large value differences, the decision is so easy that other brain regions besides the SEF are sufficient to select the better option.

We did observe a significant difference between normal condition and cooling condition. However, as shown in the figures, the monkeys were still able to made reasonable choices most of the time. Considering that both monkeys were trained on the tasks for approximately a year, we reasoned that the habitual system can also participate in the task, and therefore compensate for the perturbation effect on the goal directed system. In order to weaken the participation of habitual system during the decision process, we created a gamble experiments with a new set of target cues which the monkeys were never trained with (Figure 6.1B). As expected, the effect of cooling in the new gamble experiments was more pronounced. Both monkeys (Monkey A: paired t-test, df=49, p=0.003; Monkey I: paired t-test, df=59, p=0.002) showed more mistakes in cooling condition than in normal condition (Figure. 6.5A bottom row). Moreover, not

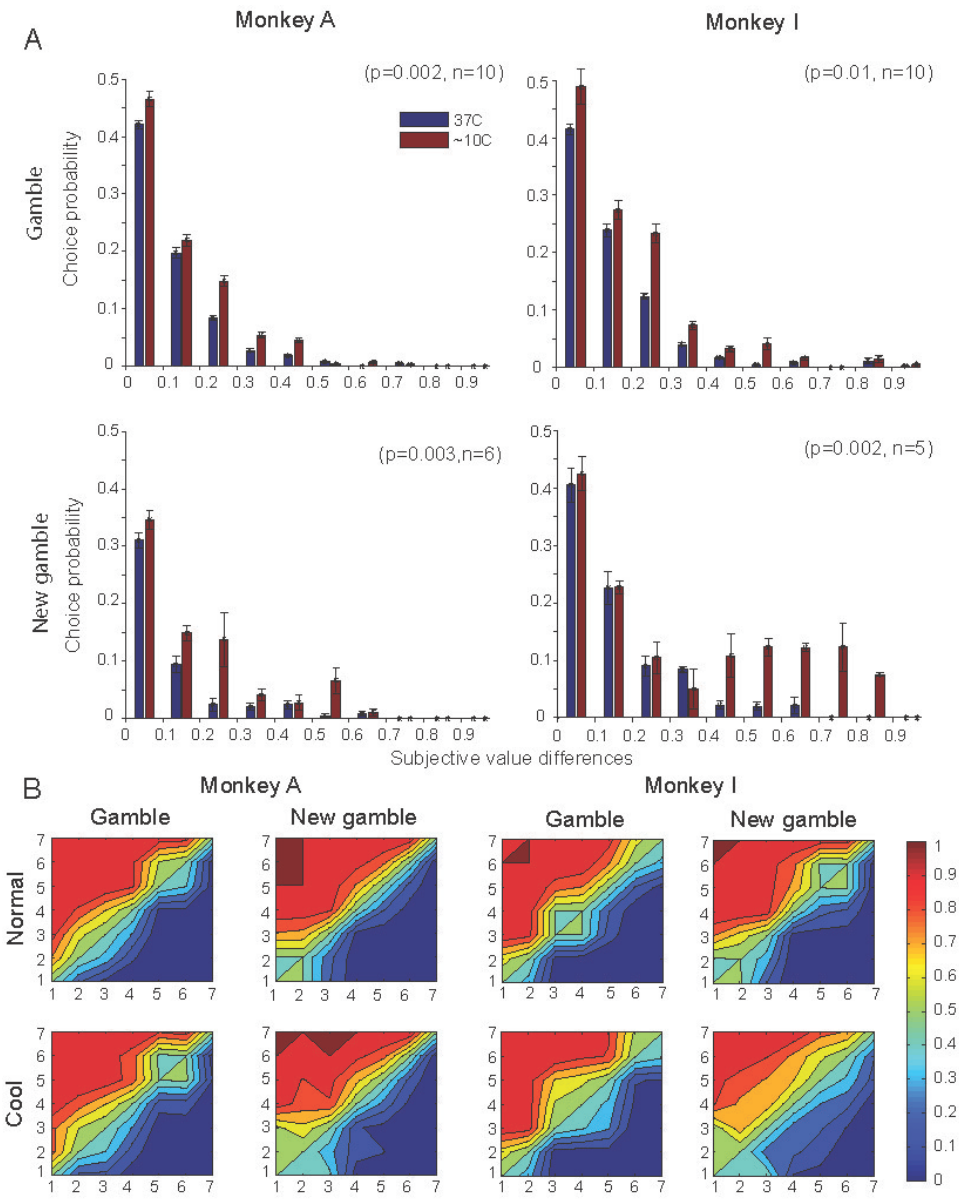

Figure 6.5 Choice probability affected by cooling. A. The probability of choosing the smaller value target in choice trial was plotted as a function of subjective value differences of two options for both monkeys. The behavior under normal conditions is shown by the blue bars (normal temperature; 37 ºC). The behavior when SEF is inactivated in both hemispheres is shown by the red bars (~10 ºC). B. Contour plot of choice probability between any two of the target pairs. The targets' numbers were sorted by their subjective values in the normal temperature condition. The colors indicate the choice probability. The top row shows the choice probability in both gamble tasks for both monkeys in the normal condition. The bottom row shows the monkeys' choices probability when the SEFs were bilaterally deactivated.

only did the monkeys make more mistakes in small value difference trials, they also tended to make more mistakes in relatively large value difference trials. Figure 6.5B shows the choice probability contour comparing each pair among 7 targets in both gamble and new gamble experiments. The order of the target was sorted by the subjective value in the normal condition, and therefore was the same for both normal and cooling conditions. The result further confirms the monkeys' tendency to show more randomness in choices selection instead of changing their preference when SEF was inactivated. As shown in the figure, the preference of the targets was almost consistent between the normal and cooling situation. However, the border area along the diagonal axis is much wider in the cooling condition than in the normal condition. This indicates that the mean subjective value of the targets were consistent across both conditions. However, the standard deviations of the subjective values were larger in cooling condition than that in normal condition.

6.2.4 Unilateral deactivation

In order to test whether the cooling effect is local, we carried out a set of unilateral cooling experiments. In these experiments, only SEF on one hemisphere (Monkey A: 3 sections on left side and 2 sections on right side; Monkey B: 3 sections on left side and 4 sections on right side) was inactivated while the other SEF on the opposite hemisphere maintained its normal function. The unilateral cooling experiments were also done using the new target gamble experiment.

To quantify the imbalance effect led by unilateral cooling, we divided the trials into incongruent trials and congruent trials based on whether or not the high value target was on the contra lateral side of inactivation: In the congruent trial, the high value target

was on the unaffected side of visual field. Therefore, the low value targets had weaker neuronal representation and the value competition was congruent with the inactivation effect. Conversely in the incongruent trial, the higher value target was on the affected side of visual field. Consequently, the higher value target had weaker neuronal representation. The value competition is incongruent with the inactivation effect. Both monkeys showed significantly more errors in the incongruent trials than in the congruent trials (Monkey A: paired t-test, df=49, p=0.005; Monkey I: paired t-test, df=69, p=0.036, Figure 6.6). The error rates for normal temperature condition always fell in between the congruent condition and incongruent condition. These results reflect the imbalance in contribution to the competition process by the affected and the unaffected SEF due to the unilateral inactivation. Therefore, the results support a local effect from cooling.

6.3 Discussion

6.3.1 Dissociation between action potential and LFP

Any excitable membrane, whether it is a spine dendrite, soma, axon or axon terminal, and any type of transmembrane current can contribute to the extracellular field. However, it is less clear which are the most important factors. While some researches consider cooperative postsynaptic activity (Mitzdorf, 1985; Linden et al., 2011), cellular-synaptic architectural organization of the network and synchrony of the current source (Buzsaki et al., 2012) as the most important factors of LFP, others argue that the active currents and not synaptic input dominate the generation of LFPs (Reimann et al., 2013). Many researches haves also shown spike "contamination" of the LFP (Rasch et al., 2008; Zanos et al., 2011). However, by deactivating SEF, our results demonstrate that even as the action potential was diminished, the energy distribution across different frequency

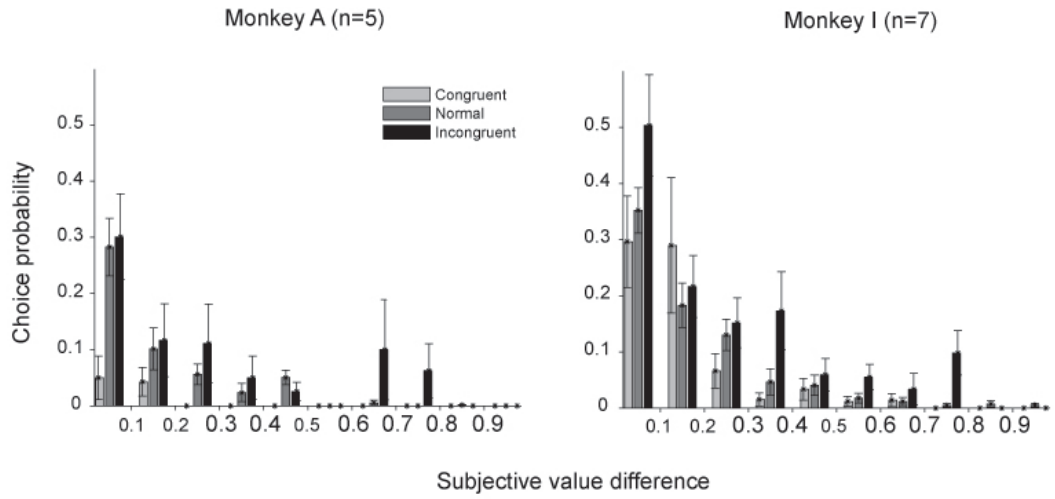

Figure 6.6 Choice probability affected by unilateral cooling for two monkeys. The probability of choosing the smaller value target in the choice trial was plotted as a function of subjective value differences of two options for both monkeys. The behavior in congruent trial, in which the unaffected side is congruent with the higher value target side, is shown by the grey. The behavior in incongruent trial, in which the unaffected side is on the opposite side to the higher value target side is shown by the black.

bands is still similar to the distribution from when the action potential was present. This suggests that, spike "contamination" cannot be a major influence on LFP energy distribution, at least in SEF. LFP including the high frequency band is largely determined by the synaptic input or postsynaptic potentials and other non-spike-related membrane voltage fluctuations (Nicholson and Freeman, 1975; Ray and Maunsell, 2010; Belluscio et al., 2012).

The fact that LFP is more dependent on synaptic input rather than the action potential output from SEF as suggested by the cooling results, highlight the importance of LFP analysis. In this way, LFP analysis provided a possible way to investigate the information flow rather than information repetition of a certain cortical area. LFP analysis could potentially dissociate the information of synaptic input from other cortical areas and the information led by local computation.

6.3.2 Causal role of SEF in value based decision-making

Action value neurons have been found in SEF during no-choice trials in a experiment similar to this dissertation study (So and Stuphorn, 2010). As reported, the neuronal activity was not only tuned by saccade direction, but also modulated by the reward amount of the targets. The human imaging literature also supports this finding. Specifically, the imaging research found action value signal in medium frontal area in general, whereas saccade related action value was coded in SEF and arm movement related action value was coded in SMA (Wunderlich et al., 2009). The dissertation research in Chapter 4 and Chapter 5 also demonstrated how the action value can correlate with the decision process. However, these findings which correlate neuronal activity with decision process could not determine if there is causal relationship between the function

role of SEF and choice behavior (Teller, 1984). Therefore, in this chapter, by using a perturbation experiment, we were testing the causal role of SEF in decision-making.

The result shows that inactivation of neuronal activity in SEF leads to increase of monkeys' error rate in choice behavior. Moreover, several reasons make it unlikely that this increase of error rate can explained by a deficiency in the movement generation. First, previous research shows that, unlike FEF, SEF lesion usually produced a mild impairment on the contra-lateral side or even no impairment in visually guided or single memory-guided saccades (Gaymard et al., 1990; Schiller and Chou, 1998). Second, in the no-choice trial, during cooling, the monkeys never showed any directional difficulty choosing any targets. This suggests that the monkeys did not have motor difficulties in a simple visual triggered task. Third, if the deficiency is due to the generation of the movement, we should see the error rate increase equally strong for both easy choice comparison and difficult choice comparison. Therefore, a motor deficit should lead to a global increase of the error rate rather than a change of the slope of the choice function (Figure 6.5). Considering all these reasons, we conclude that the increase of error rate during cooling was due to difficulties in making a choice rather than in the generation of movements.

The results of the new targets gamble show that, when the monkeys were less familiar with the targets, their choice selection became more inconsistent once SEF was inactivated. This is in line with the idea that SEF plays a causal role in goal-directed decision-making. In the new gamble task, the decision depended more on the goal directed system than on the habitual system. Therefore, cooling down SEF had a larger effect on choice behavior. Nevertheless, although the influence of inactivation on choice

behavior were significant, we still observed that both monkeys could make relatively rational choices in the new gamble experiment instead of just random decisions. This phenomenon can be explained in several ways. One possibility is that, even though the new target gamble task required more involvement of the goal directed system, the habituate system still participated to some degree. For example, in the new gamble experiment, the monkey can still use color cues without estimating the subjective value of all the targets. For instance they can always choose a green-containing target with larger maximum value rather than a blue-containing target. Since both monkeys showed strong risk seeking behavior under normal condition, the choice behavior would be similar under the cooling condition even if the monkeys used simple color mapping rules to make choices. In order to rule out this possibility, future experiment should use completely different target cues (such as different pictures) to train the monkey shortly and then test the cooling effect. Doing this can possibly prevent the simple mapping between certain feature dimension to specific choice. Another possible explanation would be that SEF is only part of a larger network participating in coding action value. There are other cortical areas such as DLPFC (Kobayashi et al., 2002; Wallis and Miller, 2003; Kim et al., 2008) and striatum (Samejima et al., 2005; Lau and Glimcher, 2008) that participate in coding action value in parallel. Therefore, deactivating SEF would only weaken the overall action value representation within this network, rather than completely out take action value information. Currently, it is still not clear what the specific roles of DLPFC, caudate, and putamen are in coding action value. It is very possible that DLPFC and SEF interact cooperatively in transforming option into action-value representation considering the reciprocally connection between them. Both DLPFC

and SEF project to FEF and SC, and share overlapping regions of the caudate (Huerta and Kaas, 1990; Wang et al., 2005). It is also possible that SEF may receive action value input information from DLPFC (Kennerley and Wallis, 2009). In order to test the possible interaction between SEF and DLPFC, it would be interesting to record these cortical areas simultaneously while perturbing the activity of one of them. This would allow testing the influence of activity in one area on activity in the other area.

Although cooling did not completely eliminate rational choice behavior in our gambling task, the effect of the SEF inactivation as discussed is comparable to the effect of permanent lesions of the orbitofrontal cortex through ablation (Noonan et al., 2010). Overall, the fact that inactivation of SEF has an immediate effect on value-based decisions establishes a causal link between SEF single unit activity and choice based on subjective preferences (at least in regards to eye movements).

Chapter 7

General Discussion

In previous chapters, we elucidated in detail on how our current findings are related to previous researches in specific aspects. In this chapter, we will discuss in general how value representation interacts with action selection during decision process, and how SEF might work in concert with other brain areas in value based decision-making.

7.1 Comparison between different value based decision- making hypotheses

As discussed in chapter 1, currently there are two major hypotheses about value based decision-making (Cisek, 2012): the goods-based hypothesis and the action-based hypothesis.

In the goods-based hypothesis, all the relevant decision factors can be integrated into a single variable capturing the subjective value of each offer. The decision is made in this subjective value representation and the option with the highest value is chosen. The

appropriate action plan then is computed to produce the requirement movement for the offer. Good-based hypothesis is more consistent with the traditional cognitive theories (Marr, 1982) which propose that "what to do " was selected before specifying "how to do it". Neurophysiological and imaging studies have suggested that the variables contributing to the decision in value space are encoded in the orbitofrontal cortex (Plassmann et al., 2007; Wallis, 2007; Padoa-Schioppa, 2011) and ventromedial prefrontal cortex (Kable and Glimcher, 2007; Kennerley and Walton, 2011). In orbitofrontal cortex, offer value neurons and chosen value neurons were found. The firing of offer value neuron has been identified to be linearly correlated with the subjective value of one of the offered rewards, regardless of what the other rewards are. Chosen value neuron has been shown to track the subjective value of the chosen reward in a single common currency independent of the juice type. Although the precise location for the occurrence of competition in the value space is still under debate (Padoa-Schioppa, 2011), the existence of subjective value or expected utility provides a foundation of possible competition or choice selection in the value space. The good-based hypothesis in its pure form states that only action plan corresponding to the chosen target is represented in the motor related area. Moreover, there should be no competition between the two targets in the motor actions. The findings from this dissertation study argue against the goods-based hypothesis in its pure form for two reasons. First, SEF a motor related cortical area (Schlag and Schlag-Rey, 1987; Lynch and Tian, 2006) reflects both chosen and non-chosen targets in its action value map. Second, in addition to the competition in the value space, we also observed competition in the motor space with directional tuning. Therefore, though our result support value-based hypothesis in a general sense that

competition do occur in the value space, they argue against the good-based hypothesis in its pure form and its prediction of competition only presenting in the value space.

Action-based hypothesis (Glimcher et al., 2005; Cisek, 2007; Rangel and Hare, 2010) suggests that decision is made through biased competition between action representations. Thus, the other decision factors such as subjective value, effect of actions, only biases the competition process in action space, rather than directly competing with each other. The existence of action value related activity has challenged the good-based hypothesis. Numerous cortical regions have been found to code action value or are modulated by relative value information. These regions include the dosolateral prefrontal cortex (Leon and Shadlen, 1999; Kim et al., 2008), the anterior cingulate cortex (Shidara and Richmond, 2002; Seo and Lee, 2007), the lateral intraparietal area (Sugrue et al., 2004; Louie and Glimcher, 2010), supplementary eye fields (Amador et al., 2000; So and Stuphorn, 2010), the superior colliculus (Ikeda and Hikosaka, 2003), and the striatum (Samejima et al., 2005; Lau and Glimcher, 2008). Chosen action value information was also found among these area including ACC (Kennerley and Wallis, 2009) and caudate (Lau and Glimcher, 2008). It is still under debate as to why option value and action value coexist in brain, and their functional specialties in value based decision process. The action-based hypothesis in its pure form would suggest that chosen action information appear earlier in brain than chosen value information. In contrary, our result argues against this hypothesis in its pure form. Our study shows that chosen value information or competition between value spaces occurs earlier than chosen direction information in motor space.

Based on these results, we propose a cascade hypothesis of decision-making. This hypothesis argues that competition in value space and action space happen simultaneous in time. The competition in the value space can bias the competition in the action space. In the current experiment paradigm, the competition in the action space was balanced at the beginning. Therefore, imbalances appear in the value space competition earlier than those in the action space. This hypothesis is consistent with the hieratical control of the frontal lobe (Fuster, 2001; Badre, 2008; O'Reilly, 2010). It is very likely that good-based hypothesis and action-based hypothesis are two extreme cases of decision-making. For decision based on visual trigger, such as perceptual decision-making (Shadlen and Newsome, 2001) or in situation of unbalanced visual cues (Markowitz et al., 2011) as discussed in chapter 2, the competition occurs mainly in action space, and is very weak or equilibrated in value space. For the decision purely based on abstract component such subjective value which integrates different decision effectors in different contact, the competition is more likely to appear early in the value space than in the action space.

7.2 The functional role of SEF in value based decision- making ---- executive control of saccade selection

Decision-making and action selection are likely a distributed process that takes place within a larger network of areas, including SEF (Ledberg et al., 2007; Hernandez et al., 2010). As suggested by affordance hypothesis, the competition in the action space is likely to happen within an interconnected network of parietal and frontal areas, such as FEF and LIP (Cisek, 2007; Cisek and Kalaska, 2010), and sub-cortical areas (Gurney et al., 2001). This competition among the potential motor responses can be strongly influenced and controlled by executive signals depending on different cognitive demands.

This executive control signal can come from the prefrontal cortex and medial frontal cortex, including the SEF (Stuphorn and Schall, 2006; Isoda and Hikosaka, 2007; Johnston et al., 2007).

Previous researches have shown that SEF does not directly participate in movement generation. Similar to the neuronal activity in other medial frontal cortex (Scangos and Stuphorn, 2010), the neuronal activity in SEF also does not reach a fixed level of activity just before movement generation (Figure 4.4) (Schall et al., 2002; Stuphorn et al., 2010). SEF also does not show divisive normalization which is widely observed in many other motor related area, such as LIP (Louie et al., 2011), and SC (Basso and Wurtz, 1998). These facts support the notion that there is a fundamental difference in the functional role of SEF comparing to other oculomotor areas in motor control. In accordance with the idea that SEF participates in self-generated saccade movement, in this dissertation study, we found that SEF participates in coding action value based on internal representation of subjective value in the decision- making process. SEF can serve as a transition area bridging higher cognitive process within the value space and motor control in the action space. This is supported by the fact that the value information in SEF behave as if in between OFC and motor area. Unlike the neuronal activity in LIP or SC, SEF shows no divisive normalization in the neuronal representation. Therefore SEF can still faithfully represent the value in a monotonic way as OFC does. However, unlike the neuronal activity in OFC, the value signal in SEF has directional tuning and is also influenced by the value of other options. Therefore, it reflects the action value for each option and the mutual inhibition between them. The action value map in SEF can further provides a basic drive to bias the movement generation process in

downstream motor area as a form of executive control. Previous research found SEF influencing neuronal activity in oculomotor areas (Huerta and Kaas, 1990), such as FEF and SC, which directly control gaze (Hanes and Schall, 1996; Pare and Hanes, 2003). SEF's influence on motor competition could be exerted either directly through connection with FEF and SC, or indirectly through projection to the caudate nucleus, with which it forms a cortical-basal ganglia loop. In order to test this executive control hypothesis, it would be very interesting to record simultaneously in SEF and FEF, and observe how stimulation or inactivation of SEF can influence the neuronal pattern in FEF.

The inactivation experiment in this dissertation study further suggests a causal role of SEF in value based decision-making. Previous studies showed that in humans, lesions in SEF and SMA disrupt the automatic inhibitory control of motor plans that are evoked by external stimuli (Goldberg and Bloom, 1990; Sumner et al., 2007). Here, in our experiment paradigm, when inactivating the neuronal activity in SEF, the monkeys show less consistency and more randomness when making value based decisions. This inactivation is akin to taking out the executive control signal based on the value information, Although both monkeys could still make decision in a relatively rational way due to several possible reasons as discussed in section 6.3.2 , the magnitude of the SEF inactivation effect is comparable to the effect of permanent lesions of the orbitofrontal cortex through ablation (Noonan et al., 2010).

7.3 Concluding remarks

This dissertation study focuses on the neuronal mechanism underlying value based decision-making. Together with modeling, psychophysics research, neurophysiology recording, and perturbation technique, this study investigated the

functional role of SEF during value based decision making. Further it studied how value representation and action representation can interact with each other during the decision-making process. Specifically, the pilot psychophysics research suggests how visual salience can influence the onset time of value representation and can influence action selection. After that, the main body of the research focused on neurophysiology recording in SEF, a value-action association area linking the value representation and motor control. The recording in SEF suggests that the action value information represented in SEF participate in choice selection process. The perturbation experiment produced further evidence supporting the causal role of SEF in value based decision-making. As an association area, SEF provides us a special opportunity in the study of the relation between value representation and action representation. Different from both of the currently prevalent theories of decision-making, we suggest a cascade hypothesis, in which competition occurs in both value space and motor space during value based decision-making. If the motor competition is balanced, such as in our experiment design, the imbalanced competition in value space which happens earlier can bias the competition process in the motor space.

Bibliography

Amador N, Schlag-Rey M, Schlag J (1998) Primate antisaccades. I. Behavioral characteristics. J Neurophysiol 80:1775-1786.

Amador N, Schlag-Rey M, Schlag J (2000) Reward-predicting and reward-detecting neuronal activity in the primate supplementary eye field. J Neurophysiol 84:2166-2170.

Amador N, Schlag-Rey M, Schlag J (2004) Primate antisaccade. II. Supplementary eye field neuronal activity predicts correct performance. J Neurophysiol 91:1672-1689.

Anderson BA, Laurent PA, Yantis S (2011) Value-driven attentional capture. Proc Natl Acad Sci U S A 108:10367-10371.

Badre D (2008) Cognitive control, hierarchy, and the rostro-caudal organization of the frontal lobes. Trends Cogn Sci 12:193-200.

Basso MA, Wurtz RH (1998) Modulation of neuronal activity in superior colliculus by changes in target probability. J Neurosci 18:7519-7534.

Belluscio MA, Mizuseki K, Schmidt R, Kempter R, Buzsaki G (2012) Cross-frequency phase-phase coupling between theta and gamma oscillations in the hippocampus. J Neurosci 32:423-435.

Bendiksby MS, Platt ML (2006) Neural correlates of reward and attention in macaque area LIP. Neuropsychologia 44:2411-2420.

Berg DJ, Boehnke SE, Marino RA, Munoz DP, Itti L (2009) Free viewing of dynamic stimuli by humans and monkeys. J Vis 9:19 11-15.

Bizzi E (1967) Discharge of frontal eye field neurons during eye movements in unanesthetized monkeys. Science 157:1588-1590.

Bizzi E, Schiller PH (1970) Single unit activity in the frontal eye fields of unanesthetized monkeys during eye and head movement. Exp Brain Res 10:150-158.

Bogacz R, Brown E, Moehlis J, Holmes P, Cohen JD (2006) The physics of optimal decision making: a formal analysis of models of performance in two-alternative forced-choice tasks. Psychol Rev 113:700-765.

Bon L, Lucchetti C (1990) Neurons signalling the maintenance of attentive fixation in frontal area 6a beta of macaque monkey. Exp Brain Res 82:231-233.

Bon L, Lucchetti C (1992) The dorsomedial frontal cortex of the macaca monkey: fixation and saccade-related activity. Exp Brain Res 89:571-580.

Bonin V, Mante V, Carandini M (2005) The suppressive field of neurons in lateral geniculate nucleus. J Neurosci 25:10844-10856.

Britten KH, Shadlen MN, Newsome WT, Movshon JA (1992) The analysis of visual motion: a comparison of neuronal and psychophysical performance. J Neurosci 12:4745-4765.

Bruce CJ, Goldberg ME (1985) Primate frontal eye fields. I. Single neurons discharging before saccades. J Neurophysiol 53:603-635.

Bruce CJ, Goldberg ME, Bushnell MC, Stanton GB (1985) Primate frontal eye fields. II. Physiological and anatomical correlates of electrically evoked eye movements. J Neurophysiol 54:714-734.

Burnham KP, Anderson DR (2002) Model selection and multimodel inference: a practical information-theoretic approach. New York: Springer.

Busemeyer JR, Diederich A (2010) Cognitive modeling. Thousand Oaks, CA: Sage.

Buzsaki G, Anastassiou CA, Koch C (2012) The origin of extracellular fields and currents--EEG, ECoG, LFP and spikes. Nat Rev Neurosci 13:407-420.

Cai X, Kim S, Lee D (2011) Heterogeneous coding of temporally discounted values in the dorsal and ventral striatum during intertemporal choice. Neuron 69:170-182.

Carello CD, Krauzlis RJ (2004) Manipulating intent: evidence for a causal role of the superior colliculus in target selection. Neuron 43:575-583.

Chen LL, Wise SP (1995) Supplementary eye field contrasted with the frontal eye field during acquisition of conditional oculomotor associations. J Neurophysiol 73:1122-1134.

Chen X, Scangos KW, Stuphorn V (2010) Supplementary motor area exerts proactive and reactive control of arm movements. J Neurosci 30:14657-14675.

Cisek P (2006) Integrated neural processes for defining potential actions and deciding between them: a computational model. J Neurosci 26:9761-9770.

Cisek P (2007) Cortical mechanisms of action selection: the affordance competition hypothesis. Philos Trans R Soc Lond B Biol Sci 362:1585-1599.

Cisek P (2012) Making decisions through a distributed consensus. Curr Opin Neurobiol 22:927-936.

Cisek P, Kalaska JF (2010) Neural mechanisms for interacting with a world full of action choices. Annu Rev Neurosci 33:269-298.

Cisek P, Puskas GA, El-Murr S (2009) Decisions in changing conditions: the urgency-gating model. J Neurosci 29:11560-11571.

Coe B, Tomihara K, Matsuzawa M, Hikosaka O (2002) Visual and anticipatory bias in three cortical eye fields of the monkey during an adaptive decision-making task. J Neurosci 22:5081-5090.

Ding L, Gold JI (2013) The Basal Ganglia's Contributions to Perceptual Decision Making. Neuron 79:640-649.

Dondey M, Albe-Fessard D, Le Beau J (1962) [First neurophysiologic applications of a method permitting reversible elective block of central structures by localized refrigeration]. Electroencephalogr Clin Neurophysiol 14:758-763.

Egeth HE, Yantis S (1997) Visual attention: control, representation, and time course. Annu Rev Psychol 48:269-297.

Ferrier D (1875) Experiments on the brains of monkeys. Proc R Soc Lond 23:409-430.

Ferrier D, ed (1886) The functions of the brain. London: Elder.

Fuster JM (2001) The prefrontal cortex--an update: time is of the essence. Neuron 30:319-333.

Gaymard B, Pierrot-Deseilligny C, Rivaud S (1990) Impairment of sequences of memory-guided saccades after supplementary motor area lesions. Ann Neurol 28:622-626.

Ghashghaei HT, Hilgetag CC, Barbas H (2007) Sequence of information processing for emotions based on the anatomic dialogue between prefrontal cortex and amygdala. Neuroimage 34:905-923.

Glimcher PW (2005) Indeterminacy in brain and behavior. Annu Rev Psychol 56:25-56.

Glimcher PW, Dorris MC, Bayer HM (2005) Physiological utility theory and the neuroeconomics of choice. Games Econ Behav 52:213-256.

Gold JI, Shadlen MN (2007) The neural basis of decision making. Annu Rev Neurosci 30:535-574.

Goldberg G, Bloom KK (1990) The alien hand sign. Localization, lateralization and recovery. Am J Phys Med Rehabil 69:228-238.

Goldberg ME, Bushnell MC (1981) Behavioral enhancement of visual responses in monkey cerebral cortex. II. Modulation in frontal eye fields specifically related to saccades. J Neurophysiol 46:773-787.

Grossberg S (1973) Contour enhancement, shourt term memory, and constancies in reverberateing neural networks. Studies Appl Math 52:213-257.

Gurney K, Prescott TJ, Redgrave P (2001) A computational model of action selection in the basal ganglia. I. A new functional anatomy. Biol Cybern 84:401-410.

Hanes DP, Schall JD (1996) Neural control of voluntary movement initiation. Science 274:427-430.

Hanks TD, Mazurek ME, Kiani R, Hopp E, Shadlen MN (2011) Elapsed decision time affects the weighting of prior probability in a perceptual decision task. J Neurosci 31:6339-6352.

Heinen SJ (1995) Single neuron activity in the dorsomedial frontal cortex during smooth pursuit eye movements. Exp Brain Res 104:357-361.

Heinen SJ, Liu M (1997) Single-neuron activity in the dorsomedial frontal cortex during smooth-pursuit eye movements to predictable target motion. Vis Neurosci 14:853-865.

Hernandez A, Nacher V, Luna R, Zainos A, Lemus L, Alvarez M, Vazquez Y, Camarillo L, Romo R (2010) Decoding a perceptual decision process across cortex. Neuron 66:300-314.

Horwitz GD, Newsome WT (1999) Separate signals for target selection and movement specification in the superior colliculus. Science 284:1158-1161.

Horwitz GD, Newsome WT (2001) Target selection for saccadic eye movements: prelude activity in the superior colliculus during a direction-discrimination task. J Neurophysiol 86:2543-2558.

Huerta MF, Kaas JH (1990) Supplementary eye field as defined by intracortical microstimulation: connections in macaques. J Comp Neurol 293:299-330.

Ikeda T, Hikosaka O (2003) Reward-dependent gain and bias of visual responses in primate superior colliculus. Neuron 39:693-700.

Isoda M, Hikosaka O (2007) Switching from automatic to controlled action by monkey medial frontal cortex. Nat Neurosci 10:240-248.

Itti L, Koch C, Niebur E (1998) A model of saliency-based visual attention for rapid scene analysis. IEEE Transactions on Pattern Analysis and Machine Intelligence 20:1254-1259.

Johnston K, Levin HM, Koval MJ, Everling S (2007) Top-down control-signal dynamics in anterior cingulate and prefrontal cortex neurons following task switching. Neuron 53:453-462.

Kable JW, Glimcher PW (2007) The neural correlates of subjective value during intertemporal choice. Nat Neurosci 10:1625-1633.

Kable JW, Glimcher PW (2009) The neurobiology of decision: consensus and controversy. Neuron 63:733-745.

Kennerley SW, Wallis JD (2009) Reward-dependent modulation of working memory in lateral prefrontal cortex. J Neurosci 29:3259-3270.

Kennerley SW, Walton ME (2011) Decision making and reward in frontal cortex: complementary evidence from neurophysiological and neuropsychological studies. Behav Neurosci 125:297-317.

Kim JN, Shadlen MN (1999) Neural correlates of a decision in the dorsolateral prefrontal cortex of the macaque. Nat Neurosci 2:176-185.

Kim S, Hwang J, Lee D (2008) Prefrontal coding of temporally discounted values during intertemporal choice. Neuron 59:161-172.

Kingdom FAA, Prins N (2010) Psychophysics: A prctical introduction. London: Academic Press: an imprint of Elsevier.

Kobayashi S, Lauwereyns J, Koizumi M, Sakagami M, Hikosaka O (2002) Influence of reward expectation on visuospatial processing in macaque lateral prefrontal cortex. J Neurophysiol 87:1488-1498.

Koval MJ, Lomber SG, Everling S (2011) Prefrontal cortex deactivation in macaques alters activity in the superior colliculus and impairs voluntary control of saccades. J Neurosci 31:8659-8668.

Krajbich I, Rangel A (2011) Multialternative drift-diffusion model predicts the relationship between visual fixations and choice in value-based decisions. Proc Natl Acad Sci U S A 108:13852-13857.

Lau B, Glimcher PW (2008) Value representations in the primate striatum during matching behavior. Neuron 58:451-463.

Ledberg A, Bressler SL, Ding M, Coppola R, Nakamura R (2007) Large-scale visuomotor integration in the cerebral cortex. Cereb Cortex 17:44-62.

Lee J, Williford T, Maunsell JH (2007) Spatial attention and the latency of neuronal responses in macaque area V4. J Neurosci 27:9632-9637.

Lee K, Tehovnik EJ (1995) Topographic distribution of fixation-related units in the dorsomedial frontal cortex of the rhesus monkey. Eur J Neurosci 7:1005-1011.

Leon MI, Shadlen MN (1999) Effect of expected reward magnitude on the response of neurons in the dorsolateral prefrontal cortex of the macaque. Neuron 24:415-425.

Lim SL, O'Doherty JP, Rangel A (2011) The decision value computations in the vmPFC and striatum use a relative value code that is guided by visual attention. J Neurosci 31:13214-13223.

Linden H, Tetzlaff T, Potjans TC, Pettersen KH, Grun S, Diesmann M, Einevoll GT (2011) Modeling the spatial reach of the LFP. Neuron 72:859-872.

Lomber SG (1999) The advantages and limitations of permanent or reversible deactivation techniques in the assessment of neural function. J Neurosci Methods 86:109-117.

Lomber SG, Payne BR, Horel JA (1999) The cryoloop: an adaptable reversible cooling deactivation method for behavioral or electrophysiological assessment of neural function. J Neurosci Methods 86:179-194.

Long MA, Fee MS (2008) Using temperature to analyse temporal dynamics in the songbird motor pathway. Nature 456:189-194.

Louie K, Glimcher PW (2010) Separating value from choice: delay discounting activity in the lateral intraparietal area. J Neurosci 30:5498-5507.

Louie K, Grattan LE, Glimcher PW (2011) Reward value-based gain control: divisive normalization in parietal cortex. J Neurosci 31:10627-10639.

Louie K, Khaw MW, Glimcher PW (2013) Normalization is a general neural mechanism for context-dependent decision making. Proc Natl Acad Sci U S A 110:6139-6144.

Lynch JC, Tian JR (2006) Cortico-cortical networks and cortico-subcortical loops for the higher control of eye movements. Prog Brain Res 151:461-501.

Mallat S, Zhang Z (1993) Matching pursuit with time-frequency dictionaries. IEEE Transactions on Signal Processing 41:3397-3415.

Maloney LT, Yang JN (2003) Maximum likelihood difference scaling. Journal of vision 3:573-585.

Mann SE, Thau R, Schiller PH (1988) Conditional task-related responses in monkey dorsomedial frontal cortex. Exp Brain Res 69:460-468.

Markowitz DA, Shewcraft RA, Wong YT, Pesaran B (2011) Competition for visual selection in the oculomotor system. J Neurosci 31:9298-9306.

Marr DC, ed (1982) Vision. San Francisco, CA.

Masciocchi CM, Mihalas S, Parkhurst D, Niebur E (2009) Everyone knows what is interesting: salient locations which should be fixated. J Vis 9:25 21-22.

McPeek RM, Keller EL (2004) Deficits in saccade target selection after inactivation of superior colliculus. Nat Neurosci 7:757-763.

Michalski A, Wimborne BM, Henry GH (1993) The effect of reversible cooling of cat's primary visual cortex on the responses of area 21a neurons. J Physiol 466:133-156.

Milosavljevic M, Malmaud J, Huth A, Koch C, Ratcliff R (2010) The drift diffusion model can account for the accuracy and reaction time of value-based choices under high and low time pressure. Judgment and Decision Making 5:437-449.

Milstein DM, Dorris MC (2007) The influence of expected value on saccadic preparation. J Neurosci 27:4810-4818.

Mitzdorf U (1985) Current source-density method and application in cat cerebral cortex: investigation of evoked potentials and EEG phenomena. Physiol Rev 65:37-100.

Mushiake H, Fujii N, Tanji J (1996) Visually guided saccade versus eye-hand reach: contrasting neuronal activity in the cortical supplementary and frontal eye fields. J Neurophysiol 75:2187-2191.

Navalpakkam V, Koch C, Rangel A, Perona P (2010) Optimal reward harvesting in complex perceptual environments. Proc Natl Acad Sci U S A 107:5232-5237.

Nicholson C, Freeman JA (1975) Theory of current source-density analysis and determination of conductivity tensor for anuran cerebellum. J Neurophysiol 38:356-368.

Nishijo H, Ono T, Nishino H (1988a) Topographic distribution of modality-specific amygdalar neurons in alert monkey. J Neurosci 8:3556-3569.

Nishijo H, Ono T, Nishino H (1988b) Single neuron responses in amygdala of alert monkey during complex sensory stimulation with affective significance. J Neurosci 8:3570-3583.

Noonan MP, Walton ME, Behrens TE, Sallet J, Buckley MJ, Rushworth MF (2010) Separate value comparison and learning mechanisms in macaque medial and lateral orbitofrontal cortex. P Natl Acad Sci USA 107:20547-20552.

O'Reilly RC (2010) The What and How of prefrontal cortical organization. Trends Neurosci 33:355-361.

Ohshiro T, Angelaki DE, DeAngelis GC (2011) A normalization model of multisensory integration. Nat Neurosci 14:775-782.

Padoa-Schioppa C (2009) Range-adapting representation of economic value in the orbitofrontal cortex. J Neurosci 29:14004-14014.

Padoa-Schioppa C (2011) Neurobiology of economic choice: a good-based model. Annu Rev Neurosci 34:333-359.

Padoa-Schioppa C, Assad JA (2006) Neurons in the orbitofrontal cortex encode economic value. Nature 441:223-226.

Padoa-Schioppa C, Assad JA (2008) The representation of economic value in the orbitofrontal cortex is invariant for changes of menu. Nat Neurosci 11:95-102.

Pare M, Hanes DP (2003) Controlled movement processing: superior colliculus activity associated with countermanded saccades. J Neurosci 23:6480-6489.

Parkhurst DJ, Niebur E (2003) Scene content selected by active vision. Spat Vis 16:125-154.

Parkhurst DJ, Law K, Niebur E (2002) Modeling the role of salience in the allocation of overt visual attention. Vision Res 42:107-123.

Pastor-Bernier A, Cisek P (2011) Neural correlates of biased competition in premotor cortex. J Neurosci 31:7083-7088.

Paton JJ, Belova MA, Morrison SE, Salzman CD (2006) The primate amygdala represents the positive and negative value of visual stimuli during learning. Nature 439:865-870.

Plassmann H, O'Doherty J, Rangel A (2007) Orbitofrontal cortex encodes willingness to pay in everyday economic transactions. J Neurosci 27:9984-9988.

Platt ML, Glimcher PW (1999) Neural correlates of decision variables in parietal cortex. Nature 400:233-238.

Prins N, Kingdom FA (2009) Palamedes: Matlab routines for analyzing psychophysical data. In.

Purcell BA, Heitz RP, Cohen JY, Schall JD, Logan GD, Palmeri TJ (2010) Neurally constrained modeling of perceptual decision making. Psychol Rev 117:1113-1143.

Pylyshyn ZW (1984) Computation and Cognition: Toward a Foundation for Cognitive Science. Massachusetts: The MIT Press.

Rangel A, Hare T (2010) Neural computations associated with goal-directed choice. Curr Opin Neurobiol 20:262-270.

Rangel A, Camerer C, Montague PR (2008) A framework for studying the neurobiology of value-based decision making. Nat Rev Neurosci 9:545-556.

Rasch MJ, Gretton A, Murayama Y, Maass W, Logothetis NK (2008) Inferring spike trains from local field potentials. J Neurophysiol 99:1461-1476.

Ratcliff R, Smith PL (2011) Perceptual discrimination in static and dynamic noise: the temporal relation between perceptual encoding and decision making. J Exp Psychol Gen 139:70-94.

Ratcliff R, Hasegawa YT, Hasegawa RP, Smith PL, Segraves MA (2007) Dual diffusion model for single-cell recording data from the superior colliculus in a brightness-discrimination task. J Neurophysiol 97:1756-1774.

Ray S, Maunsell JH (2010) Differences in gamma frequencies across visual cortex restrict their possible use in computation. Neuron 67:885-896.

Ray S, Crone NE, Niebur E, Franaszczuk PJ, Hsiao SS (2008a) Neural correlates of high-gamma oscillations (60-200 Hz) in macaque local field potentials and their potential implications in electrocorticography. J Neurosci 28:11526-11536.

Ray S, Hsiao SS, Crone NE, Franaszczuk PJ, Niebur E (2008b) Effect of stimulus intensity on the spike-local field potential relationship in the secondary somatosensory cortex. J Neurosci 28:7334-7343.

Reimann MW, Anastassiou CA, Perin R, Hill SL, Markram H, Koch C (2013) A biophysically detailed model of neocortical local field potentials predicts the critical role of active membrane currents. Neuron 79:375-390.

Reynolds JH, Heeger DJ (2009) The normalization model of attention. Neuron 61:168-185.

Russo GS, Bruce CJ (1996) Neurons in the supplementary eye field of rhesus monkeys code visual targets and saccadic eye movements in an oculocentric coordinate system. J Neurophysiol 76:825-848.

Salsbury KG, Horel JA (1983) A cryogenic implant for producing reversible functional brain lesions. Behav Brain Res Methods Instrum 15.

Samejima K, Ueda Y, Doya K, Kimura M (2005) Representation of action-specific reward values in the striatum. Science 310:1337-1340.

Sandell JH, Schiller PH (1982) Effect of cooling area 18 on striate cortex cells in the squirrel monkey. J Neurophysiol 48:38-48.

Scangos KW, Stuphorn V (2010) Medial frontal cortex motivates but does not control movement initiation in the countermanding task. J Neurosci 30:1968-1982.

Schall JD (1991) Neuronal activity related to visually guided saccadic eye movements in the supplementary motor area of rhesus monkeys. J Neurophysiol 66:530-558.

Schall JD, Stuphorn V, Brown JW (2002) Monitoring and control of action by the frontal lobes. Neuron 36:309-322.

Schiller PH, Malpeli JG (1977) The effect of striate cortex cooling on area 18 cells in the monkey. Brain Res 126:366-369.

Schiller PH, Chou IH (1998) The effects of frontal eye field and dorsomedial frontal cortex lesions on visually guided eye movements. Nat Neurosci 1:248-253.

Schiller PH, Tehovnik EJ (2005) Neural mechanisms underlying target selection with saccadic eye movements. Prog Brain Res 149:157-171.

Schlag-Rey M, Amador N, Sanchez H, Schlag J (1997) Antisaccade performance predicted by neuronal activity in the supplementary eye field. Nature 390:398-401.

Schlag J, Schlag-Rey M (1985) Unit activity related to spontaneous saccades in frontal dorsomedial cortex of monkey. Exp Brain Res 58:208-211.

Schlag J, Schlag-Rey M (1987) Evidence for a supplementary eye field. J Neurophysiol 57:179-200.

Schutz AC, Trommershauser J, Gegenfurtner KR (2012) Dynamic integration of information about salience and value for saccadic eye movements. Proc Natl Acad Sci U S A 109:7547-7552.

Seo H, Lee D (2007) Temporal filtering of reward signals in the dorsal anterior cingulate cortex during a mixed-strategy game. J Neurosci 27:8366-8377.

Shadlen MN, Newsome WT (1996) Motion perception: seeing and deciding. Proc Natl Acad Sci U S A 93:628-633.

Shadlen MN, Newsome WT (2001) Neural basis of a perceptual decision in the parietal cortex (area LIP) of the rhesus monkey. J Neurophysiol 86:1916-1936.

Shapley RM, Victor JD (1978) The effect of contrast on the transfer properties of cat retinal ganglion cells. J Physiol 285:275-298.

Shidara M, Richmond BJ (2002) Anterior cingulate: single neuronal signals related to degree of reward expectancy. Science 296:1709-1711.

Skinner JE, Lindsley DB (1968) Reversible cryogenic blockade of neural function in the brain of unrestrained animals. Science 161:595-597.

So N, Stuphorn V (2012) Supplementary eye field encodes reward prediction error. J Neurosci 32:2950-2963.

So NY, Stuphorn V (2010) Supplementary eye field encodes option and action value for saccades with variable reward. J Neurophysiol 104:2634-2653.

So NY, Stuphorn V (2011) Supplementary eye field encodes option and action value for saccades with variable reward. J Neurophysiol 104:2634-2653.

Stuphorn V, Schall JD (2006) Executive control of countermanding saccades by the supplementary eye field. Nat Neurosci 9:925-931.

Stuphorn V, Taylor TL, Schall JD (2000a) Performance monitoring by the supplementary eye field. Nature 408:857-860.

Stuphorn V, Bauswein E, Hoffmann KP (2000b) Neurons in the primate superior colliculus coding for arm movements in gaze-related coordinates. J Neurophysiol 83:1283-1299.

Stuphorn V, Brown JW, Schall JD (2010) Role of supplementary eye field in saccade initiation: executive, not direct, control. J Neurophysiol 103:801-816.

Sugrue LP, Corrado GS, Newsome WT (2004) Matching behavior and the representation of value in the parietal cortex. Science 304:1782-1787.

Sugrue LP, Corrado GS, Newsome WT (2005) Choosing the greater of two goods: neural currencies for valuation and decision making. Nat Rev Neurosci 6:363-375.

Sumner P, Nachev P, Morris P, Peters AM, Jackson SR, Kennard C, Husain M (2007) Human medial frontal cortex mediates unconscious inhibition of voluntary action. Neuron 54:697-711.

Tehovnik EJ (1995) The dorsomedial frontal cortex: eye and forelimb fields. Behav Brain Res 67:147-163.

Tehovnik EJ, Lee K (1993) The dorsomedial frontal cortex of the rhesus monkey: topographic representation of saccades evoked by electrical stimulation. Exp Brain Res 96:430-442.

Tehovnik EJ, Slocum WM, Schiller PH (1999) Behavioural conditions affecting saccadic eye movements elicited electrically from the frontal lobes of primates. Eur J Neurosci 11:2431-2443.

Tehovnik EJ, Sommer MA, Chou IH, Slocum WM, Schiller PH (2000) Eye fields in the frontal lobes of primates. Brain Res Brain Res Rev 32:413-448.

Teller DY (1984) Linking propositions. Vision Res 24:1233-1246.

Van Zandt T, Colonius H, Proctor RW (2000) A comparison of two response time models applied to perceptual matching. Psychon Bull Rev 7:208-256.

Wallis JD (2007) Orbitofrontal cortex and its contribution to decision-making. Annu Rev Neurosci 30:31-56.

Wallis JD, Miller EK (2003) Neuronal activity in primate dorsolateral and orbital prefrontal cortex during performance of a reward preference task. Eur J Neurosci 18:2069-2081.

Wallisch P, Lusignan ME, Benayoun MD, Baker TI, Dickey AS, Hatsopoulos NG (2010) MATLAB for Neuroscientists: An Introduction to Scientific Computing in MATLAB: Elsevier Science.

Wang Y, Isoda M, Matsuzaka Y, Shima K, Tanji J (2005) Prefrontal cortical cells projecting to the supplementary eye field and presupplementary motor area in the monkey. Neurosci Res 53:1-7.

White BJ, Munoz DP (2011) Separate visual signals for saccade initiation during target selection in the primate superior colliculus. J Neurosci 31:1570-1578.

Wolfe JM (1998) Visual search. In: Attention (Pashler H, ed), pp 17-73: London UK: University College London Press.

Woolsey CN, Settlage PH, Meyer DR, Sencer W, Pinto Hamuy T, Travis AM (1952) Patterns of localization in precentral and "supplementary" motor areas and their relation to the concept of a premotor area. Res Publ Assoc Res Nerv Ment Dis 30:238-264.

Wunderlich K, Rangel A, O'Doherty JP (2009) Neural computations underlying action-based decision making in the human brain. Proc Natl Acad Sci U S A 106:17199-17204.

Zanos TP, Mineault PJ, Pack CC (2011) Removal of spurious correlations between spikes and local field potentials. J Neurophysiol 105:474-486.

Zhang JX, Ni H, Harper RM (1986) A miniaturized cryoprobe for functional neuronal blockade in freely moving animals. J Neurosci Methods 16:79-87.

Xiaomo Chen

Education

Ph.D.	2013	Psychology and Brain Sciences Advisor: Veit Stuphorn	Johns Hopkins University
M.A.	2010	Psychology and Brain Sciences Advisor: Veit Stuphorn	Johns Hopkins University
M.E.	2008	Biomedical Engineering Advisor: Shangkai Gao	Tsinghua University
B.E.	2005	Biomedical Engineering Advisor: Jiarui Lin	Huazhong University of Science and Technology

Honors and Rewards

Teaching assistant fellowship, Johns Hopkins University	2008-2013
Professional scholarship, Tsinghua University	2005-2008
Best paper awards for young scientist, China BME Joint Annual Conference	2007
Guanghua scholarship, Tsinghua University	2007
Best undergraduate thesis, Hubei, China	2005
Summa cum Laude, Huazhong Univ. of Sci. and Tech.	2005
Distinguished Chinese Students, Hewlett-Packard Scholarship	2004

Publications

Peer-review publications:

Chen X., Stuphorn V. "Neural dynamics in supplementary eye field underlying value based decision making" (in preparation).
Chen X., Mihalas S., Neibur E., Stuphorn V. (2013) "Influence of salience on value-based decision-making."J. Vision, 13(12): 1-23
Chen X., Scangos K.W., Stuphron V. (2010) "Supplementary motor area exerts proactiveand reactive control of arm movements."J Neurosci, 30(44): 14657-14675.

Chen X., Qiao Z., Gao S., Hong. B. (2007) "Extracellular recording for the study of cortical plasticity in vivo. " Acta Physiologica Sinica, 59(6): 851-857. (main text in Chinese)
Chen X., Hong B., Gao S. (2007) "Neural population decoding and its application in brain-computer Interfaces. " Beijing Biomedical Engineering, 26(3): 330-333. (main text in Chinese)
Chen X., Lin J. (2006). "The research on imitations and modeling of a micro controller based magnetic stimulation system. " Beijing Biomedical Engineering, 25(5): 503-506. (main text in Chinese)
Chen X., Lin J. (2005). "The research advances on wearable biosensors system. " Biomedical engineering (foreign medical sciences), 28(3): 138:142. (main text in Chinese)

Book and book chapter

Stuphorn V., **Chen X.** (forthcoming) "An introduction to neuroscientic methods: single-cell recordings."In: An introduction to model-based cognitive neuroscience, Springer Publications, New York, NY.
Lin J., Xu B., **Chen X.** "Biomedical digital signal processing workbook "(reference manual of Biomedical Digital Signal Processing written by Willis J. Tompkins), 2007, Huazhong Univ. of Sci. and Tech. Pulications, Wuhan, China. (in Chinese)

Conference presentation

Chen, X., Mihalas S., Stuphorn V., "The non-divisive normalization in supplementary eye field." Poster will bepresented at 2013 SFN, SD. USA
Chen, X., Mihalas S., Stuphorn V., "Competition between different action value signals in supplementary eye field during value-based decision making." Poster presented at 2012 SFN, New Orleans. USA
Chen, X., Mihalas S., Neibur E., Stuphorn V., "Influence of salience on value-based decision-making." Poster presented at 2011 SFN, DC. USA
Chen, X., Mihalas S., Scangos K.W., Stuphorn V., "Supplementary motor area exerts proactive and reactive control of arm movements." Poster presented at 2010 SFN, SD. USA